Copyright 2010 Amy Lynn Nicely

CHARGE AND TEMPERATURE EFFECTS ON BIOMOLECULE HYDRATION: AN EXPERIMENTAL AND COMPUTATIONAL INVESTIGATION

BY

AMY LYNN NICELY

DISSERTATION

Submitted in partial fulfillment of the requirements
for the degree of Doctor of Philosophy in Chemistry
in the Graduate College of the
University of Illinois at Urbana-Champaign, 2010

Urbana, Illinois

Doctoral Committee:

Professor James M. Lisy, Chair
Professor Zaida Luthey-Schulten
Assistant Professor Benjamin J. McCall
Professor James Gary Eden

Abstract

The focus of this dissertation is on the role of charge and temperature on the structure of hydrated cluster ions. This is investigated using a combination of infrared photodissociation (IRPD) spectra and geometry and frequency calculations.

The particular cluster ions examined here include hydrated rubidium cluster ions and hydrated sodium- and potassium-containing tryptamine, 2-amino-1-phenylethanol and ephedrine. In every case, there are significant differences between spectra obtained at different temperatures as well as those containing different metal ions.

The argon tagging method, which was used to facilitate the temperature comparisons, had an unintended consequence: the cluster formation process trapped high-energy isomers in the experiments performed at lower temperatures. In addition, thermodynamic calculations showed the important role of entropy in determining the structures formed at warm temperatures. Both of these observations make it clear that the identification of one or two minimum-energy isomers based on zero-point energy calculations is not sufficient to mimic the isomer populations which are present during the experiments.

A summary of the methods used to explore the potential energy surfaces of the various cluster ions is also given. An in-house Monte Carlo simulation program was originally written to aid the discovery of $M^+(H_2O)_n$ structures and was later expanded to include additional ligands in the clusters. More recent efforts have focused on using molecular dynamics to explore the conformations of the more complex $M^+(Biomolecue)(H_2O)_n$ cluster ions.

Table of Contents

Chapter 1: Introduction

Dissertation Overview

The focus of this dissertation is on the role of charge and temperature on the structure of hydrated cluster ions. This is investigated using a combination of infrared photodissociation (IRPD) spectra and geometry and frequency calculations. This first chapter will provide the details of both the experimental and calculation methods.

In Chapter 2, hydrated cluster ions containing rubidium will be examined and compared with those containing other alkali metal ions, particularly potassium and cesium. The IRPD spectra of $M^+(H_2O)_{n=2-5}$ and $M^+(H_2O)_{n=1-5}Ar$ with M = Li, Na, K and Cs have previously been reported.[1-6] In many cases, there were notable differences between the potassium- and cesium-containing spectra, attributed to a shift in the balance between noncovalent interactions (electrostatic versus water-water). Because rubidium has a charge density between that of potassium and cesium, it makes an inviting target for comparison with the previous studies.

The balance of noncovalent interactions becomes more complicated as additional components are added into the system. Chapter 3-5 examine the structure of various biomolecules in the presence of either a sodium or potassium cation. As discussed in further detail in these chapters, the neutral structures of both the bare and hydrated biomolecules have been studied extensively.[7-27] What these studies have not taken into account however, is the large concentration of ions present in biological systems. Many recent studies have probed the role of protons and metal ions in directing amino acid structure.[28-33] The M^+(amino acid) systems often have different structures than the bare

amino acids,[28, 29, 33] and the structures can be metal-ion dependent.[28-31] This provides the motivation to examine the structures of various biomolecules in the presence of several different metal ions. Specifically, this dissertation examines the structure of tryptamine (Chapter 3), 2-amino-1-phenylethanol (Chapter 4) and ephedrine (Chapter 5).

Chapter 6 provides a summary of the methods used to explore the potential energy surfaces of the various cluster ions. An in-house Monte Carlo simulation program was originally written to aid the discovery of $M^+(H_2O)_n$ structures and was later expanded to include additional ligands in the clusters. More recent efforts have focused on using molecular dynamics to explore the conformations of the more complex $M^+(Biomolecue)(H_2O)_n$ cluster ions.

Experimental Details

The data provided in the following chapters was obtained through a series of experiments using a combination of mass spectrometry and infrared vibrational spectroscopy. Although the systems studied vary from chapter to chapter, the basic experimental techniques remained the same. A schematic of the apparatus is shown in Figure 1.1.

Neutral clusters were formed via a supersonic expansion through a 30° conical nozzle. The expansion included argon atoms and water molecules, and for many of the experiments described here, an additional ligand. When present, the additional ligand was housed in a heated sample holder located just prior to the nozzle. The temperature of the sample holder was generally close to the melting point of the ligand. Specifically,

temperatures near 115 °C were used for tryptamine, 85 °C for APE and 50 °C for ephedrine.

Alkali metal cations were produced via thermionic emission and collided perpendicularly with the fully-expanded neutral clusters. The nascent cluster ions contained an excess of internal energy (~10 eV) that was dissipated through evaporative cooling of the most labile ligands. The internal energy of resulting cluster ions depended on the composition of the initial expansion – by increasing the Ar:H_2O ratio, the cluster ions were stabilized primarily through the loss of argon atoms and had a lower internal energy (or effective temperature) compared to cluster ions formed primarily through the loss of water.[6]

The quasi-stable cluster ions (with unimolecular dissociation lifetimes longer than the flight time through the apparatus) were imaged through a skimmer into a differential pumping chamber and then into the entrance of a triple quadrupole mass spectrometer. The first quadrupole mass-selected the parent ion of interest. In the second, RF-only quadrupole, the cluster ions could interact with the photons from a tunable IR. The laser used was a custom-built LaserVision OPO/OPA pumped by the 1064 nm output from a 10 Hz Continuum Surelite II YAG. The laser scanned through the infrared region, typically at the rate of 3000 shots/frequency. When the laser frequency was resonant with a vibrational mode of the cluster ions, the cluster ions could absorb the photons and subsequently undergo dissociation. The third quadrupole was used to mass-select for fragment ions. The infrared photodissociation spectrum (IRPD) was recorded as a function of laser frequency and linearly corrected for fluctuations in laser fluence. The

spectra reported in the following chapters were smoothed using a three-point averaging algorithm and scaled for comparative purposes.

Calculation Details

Calculations were used to aid interpretation of the experimental spectra. Initial structures generated using Spartan[34] were optimized using the Gaussian 03 software package[35]. For the rubidium cluster ions (Chapter 2), geometry optimizations and harmonic frequency calculations were performed at the second-order Møller–Plesset (MP2) level. An aug-cc-pvdz basis was used for hydrogen, oxygen and argon, while the lanl2dz effective core potential was used for the rubidium cation. The calculated frequencies were scaled uniformly by a factor of 0.96 to facilitate agreement between the calculated and experimental values. For cluster ions involving tryptamine (Tryp), 2-amino-1-phenylethanol (APE) and ephedrine (Eph), density functional theory (DFT) calculations were performed at the B3LYP/6-31+G* level of theory. Harmonic frequencies were scaled by 0.976 (OH – Tryp and APE), 0.9734 (OH – Eph), 0.959 (NH) and 0.961 (CH). These local scaling factors were chosen to facilitate agreement between calculated frequencies at this level of theory and experimental frequencies of neutral H_2O[36], Tryp[14] and APE[23] molecules. Although global scaling factors for all XH (X=O, H, C) stretches have generally been used in the past, recent literature suggests using localized scaling factors to provide better agreement between experiment and theory.[37-39]

The SWizard program[40] was used to generate theoretical spectra by applying Gaussian lineshapes to the scaled, calculated frequencies. Thermodynamic properties

such as entropy and free energy were calculated as a function of temperature using the Thermo.pl script.[41]

Figures

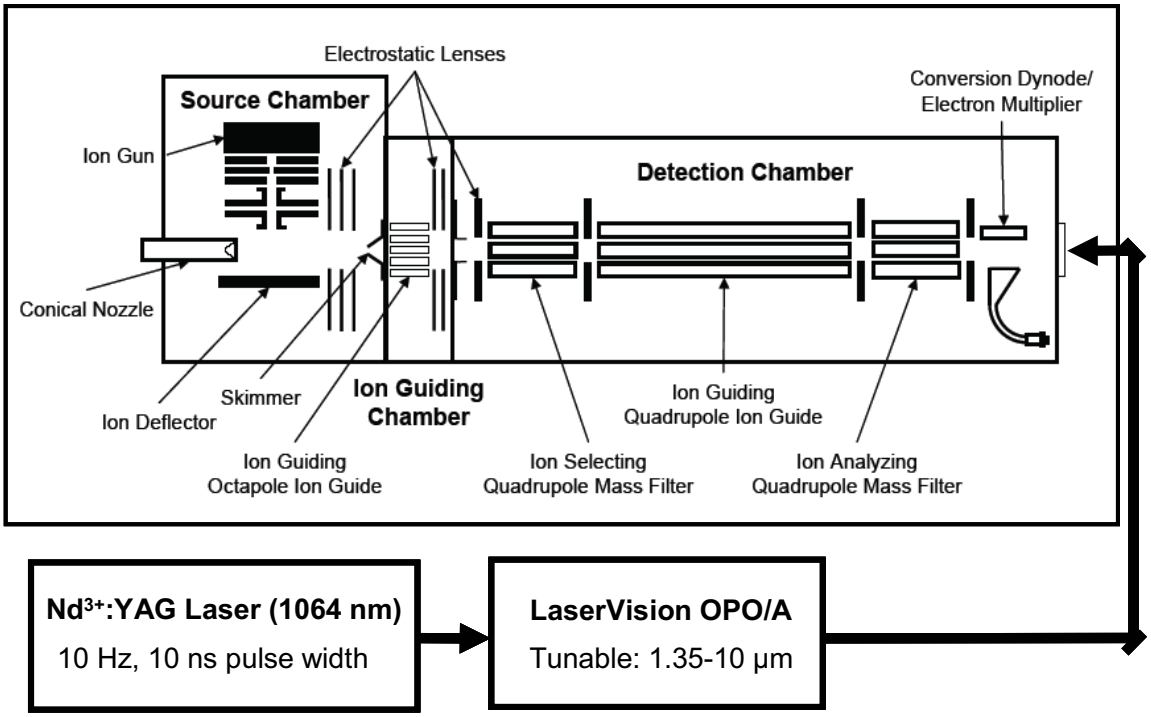

Figure 1.1: Schematic of the experimental apparatus used to obtain infrared photodissociation (IRPD) spectra

References

1. Kolaski, M.; Lee, H. M.; Choi, Y. C.; Kim, K. S.; Tarakeshwar, P.; Miller, D. J.; Lisy, J. M., J. Chem. Phys. 2007, 126, (7), 074302.
2. Miller, D. J.; Lisy, J. M., J. Chem. Phys. 2006, 124, (2), 024319.
3. Miller, D. J.; Lisy, J. M., J. Am. Chem. Soc. 2008, 130, (46), 15393-15404.
4. Miller, D. J.; Lisy, J. M., J. Am. Chem. Soc. 2008, 130, (46), 15381-15392.
5. Vaden, T. D.; Forinash, B.; Lisy, J. M., J. Chem. Phys. 2002, 117, (10), 4628.
6. Vaden, T. D.; Weinheimer, C. J.; Lisy, J. M., J. Chem. Phys. 2004, 121, (7), 3102.
7. Alonso, J. L.; Sanz, M. E.; Lopez, J. C.; Cortijo, V., J. Am. Chem. Soc. 2009, 131, (12), 4320.
8. Butz, P.; Kroemer, R. T.; Macleod, N. A.; Simons, J. P., J. Phys. Chem. A 2001, 105, (3), 544.
9. Park, Y. D.; Rizzo, T. R.; Peteanu, L. A.; Levy, D. H., J. Chem. Phys. 1986, 84, (12), 6539.
10. Philips, L. A.; Levy, D. H., J. Phys. Chem. 1986, 90, (21), 4921.
11. Philips, L. A.; Levy, D. H., J. Chem. Phys. 1988, 89, (1), 85-90.
12. Sipior, J.; Sulkes, M., J. Chem. Phys. 1988, 88, (10), 6146.
13. Carney, J. R.; Dian, B. C.; Florio, G. M.; Zwier, T. S., J. Am. Chem. Soc. 2001, 123, (23), 5596.
14. Carney, J. R.; Zwier, T. S., J. Phys. Chem. A 2000, 104, (38), 8677-8688.
15. Carney, J. R.; Zwier, T. S., Chem. Phys. Lett. 2001, 341, (1-2), 77.
16. Clarkson, J. R.; Herbert, J. M.; Zwier, T. S., J. Chem. Phys. 2007, 126, (13), 134306.
17. Dian, B. C.; Clarkson, J. R.; Zwier, T. S., Science 2004, 303, (5661), 1169-1173.
18. Nguyen, T. V.; Korter, T. M.; Pratt, D. W., Mol. Phys. 2005, 103, (11), 1603 - 1613.
19. Peteanu, L. A.; Levy, D. H., J. Phys. Chem. 1988, 92, (23), 6554-6561.
20. Schmitt, M.; Bohm, M.; Ratzer, C.; Vu, C.; Kalkman, I.; Meerts, W. L., J. Am. Chem. Soc. 2005, 127, (29), 10356-10364.
21. Zwier, T. S., J. Phys. Chem. A 2001, 105, (39), 8827-8839.
22. Baker, C. M.; Grant, G. H., J. Phys. Chem. B 2007, 111, (33), 9940.
23. Graham, R. J.; Kroemer, R. T.; Mons, M.; Robertson, E. G.; Snoek, L. C.; Simons, J. P., J. Phys. Chem. A 1999, 103, (48), 9706.
24. Macleod, N. A.; Robertson, E. G.; Simons, J. P., Mol. Phys. 2003, 101, (14), 2199.
25. Macleod, N. A.; Simons, J. P., Mol. Phys. 2006, 104, (20/21), 3317.
26. Miller III, T. F.; Clary, D. C., J. Phys. Chem. B 2004, 108, (7), 2484.
27. Miller III, T. F.; Clary, D. C., J. Phys. Chem. A 2006, 110, (2), 731.
28. Armentrout, P. B.; Rodgers, M. T.; Oomens, J.; Steill, J. D., J. Phys. Chem. A 2008, 112, (11), 2248.
29. Rodgers, M. T.; Armentrout, P. B.; Oomens, J.; Steill, J. D., J. Phys. Chem. A 2008, 112, (11), 2258.
30. Bush, M. F.; Oomens, J.; Saykally, R. J.; Williams, E. R., J. Phys. Chem. A 2008, 112, (37), 8578-8584.

31. Bush, M. F.; Forbes, M. W.; Jockusch, R. A.; Oomens, J.; Polfer, N. C.; Saykally, R. J.; Williams, E. R., J. Phys. Chem. A 2007, 111, (32), 7753-7760.
32. Remko, M.; Fitz, D.; Rode, B. M., J. Phys. Chem. A 2008, 112, (33), 7652.
33. Kamariotis, A.; Boyarkin, O. V.; Mercier, S. R.; Beck, R. D.; Bush, M. F.; Williams, E. R.; Rizzo, T. R., J. Am. Chem. Soc. 2006, 128, (3), 905-916.
34. Deppmeier, B. J., et al. SPARTAN 2002, SGI IRIX 64 (mips4); Irvine, CA, 2002.
35. Frisch, M. J., et al. Gaussian 03, B.04; Gaussian Inc.: Pittsburgh, PA, 2003.
36. Fraley, P. E.; Rao, K. N., J. Mol. Spectrosc. 1969, 29, (1-3), 348.
37. Poully, J. C.; Grégoire, G.; Schermann, J. P., J. Phys. Chem. A 2009, 113, (28), 8020.
38. Mahjoub, A.; Chakraborty, A.; Lepere, V.; Le Barbu-Debus, K.; Guchhait, N.; Zehnacker, A., Phys. Chem. Chem. Phys. 2009, 11, (25), 5160.
39. Bouteiller, Y.; Gillet, J.-C.; Grégoire, G.; Schermann, J. P., J. Phys. Chem. A 2008, 112, (46), 11656.
40. Gorelsky, S. I. SWizard program, 4.1; 2005.
41. Irikura, K. K. THERMO.PL, National Institute of Standards and Technology: 2002.

Chapter 2: Hydrated Rubidium Cluster Ions*

Introduction

In recent years, there have been many experimental and theoretical studies of metal ion solvation.[1-5] Gas-phase infrared spectroscopy experiments combined with mass spectrometric techniques make it possible to study the competition between various noncovalent interactions (ion-water and water-water) present in size-selected systems. When ion-water interactions are strong, structures are favored that have fewer hydrogen bonds than the corresponding structures in systems with relatively weak ion-water interactions.

Previous studies from this laboratory have reported the infrared photodissociation (IRPD) spectra of $M^+(H_2O)_{n=2-5}$ and $M^+(H_2O)_{n=1-5}Ar$ with M = Li, Na, K and Cs.[6-11] While the smaller alkali metal ions (M = Li, Na and K) shared many similar spectral features, cesium often exhibited distinct and notable differences. Because cesium has the largest ionic radius (and corresponding lowest charge density), it has the weakest ion-water interaction of the ions studied, and water-water interactions quickly dominate over the Cs^+-water interaction. The rubidium ion, with an ionic radius (and therefore charge density) intermediate between that of K^+ and Cs^+, makes for an inviting target of solvation studies.

Temperature can add complexity to the competition between the various noncovalent interactions. At low temperatures, enthalpic considerations have the greatest effect on the preferred structures for the cluster ions, which tend to maximize the number of hydrogen bonds, and the structures observed in the experiment are generally in good agreement with the lowest-

---

* Reproduced with permission from Amy L. Nicely, Dorothy J. Miller and James M. Lisy, *J. Mol. Spectrosc.* **2009,** 257, (2), 157. Copyright 2009 Elsevier.

energy isomer(s) predicted by theory. When the temperatures increase, entropic contributions to the free energy become significant and isomers with fewer hydrogen bonds are favored. In our experiments, cluster ions can be stabilized through evaporation of water molecules or argon atoms. The internal energy (or temperature) of the cluster ions is directly related to the binding energy of the evaporating species. In other words, evaporation of a ligand with a higher binding energy will result in cluster ions with a higher temperature.[8, 12] The use of a "messenger" atom (in this case Ar) was first suggested by Lee and coworkers[13, 14] and is now widely used to reduce the internal energy content of cluster ions. Evaporation of water (binding energies of ~30–50 kJ/mol) produces $Rb^+(H_2O)_n$ cluster ions with temperatures in the range of ~250–500 K, while $Rb^+(H_2O)_nAr$ ions formed by evaporation of argon (binding energies of ~5 kJ/mol) have temperatures of ~40–120 K, depending on the size of the cluster ion. By changing the cluster ion composition, we can alter the temperature of the clusters, facilitating comparison of the spectra produced by warm and cold cluster ions.

Assignment of the IRPD spectra would not be possible without the parallel use of *ab initio* calculations. Calculated minimum-energy structures of hydrated rubidium cluster ions are shown in Figure 2.1. In addition, thermodynamic analysis in these cluster ion systems has aided our understanding of entropic effects by suggesting which isomers are preferred as a function of temperature. The balance between competing noncovalent interactions, as reflected by the cluster ion structures, is heavily dependent on the internal energy (temperature) of the cluster ions.

Results and Discussion

$Rb^+(H_2O)Ar$, $Rb^+(H_2O)_2Ar$ and $Rb^+(H_2O)_2$

The experimental and theoretical spectra of $Rb^+(H_2O)Ar$ are shown in Figure 2.2 along with the experimental spectra for $Rb^+(H_2O)_2Ar$ and $Rb^+(H_2O)_2$. In the gas phase, the symmetric (ν_{sym}) and asymmetric (ν_{asym}) OH stretching modes of H_2O are located at 3657 and 3756 cm^{-1}, respectively.[15] When the water molecule interacts with a rubidium cation, the frequencies are expected to shift to lower frequency as the water-ion interaction slightly weakens the OH bonds. Previous studies in our lab[9] have shown that the presence of an argon atom, while decreasing the average temperature of the cluster ions, does not significantly affect the vibrational frequencies of the stretching modes, so the calculated spectra shown here are used interchangeably for the argonated and non-argonated species. The experimental and theoretical spectra of $Rb^+(H_2O)Ar$ have a feature near 3637 cm^{-1} which is assigned to the symmetric stretching mode. The $Rb^+(H_2O)Ar$ experimental spectrum also has a series of bands ranging from 3650 to 3850 cm^{-1}. This has been previously observed in our lab for other $M^+(H_2O)Ar$ cluster ions, and arises from $\Delta K = \pm 1$ rotational subbands of the asymmetric OH stretching mode.[8] Since harmonic frequency calculations do not predict these rotational subbands, the simulated spectrum of $Rb^+(H_2O)Ar$ was generated manually. The symmetric stretching mode was modeled using a Gaussian curve, while the asymmetric stretching mode was modeled with a series of weighted Lorentzian curves. Analysis of the intensities of the rotational subbands yields a rotation temperature of 100 K. The RRKM-EE analysis yields a temperature of 60 K, somewhat lower than the experimental temperature. The $Rb^+(H_2O)_2Ar$ and $Rb^+(H_2O)_2$ spectra share similar features with the $Rb^+(H_2O)Ar$ spectrum and have corresponding assignments: a relatively sharp peak near 3640 cm^{-1} from ν_{sym} and a broad band (3600–3800 cm^{-1}) with rotational substructure from ν_{asym}.

$Rb^+(H_2O)_3Ar$ and $Rb^+(H_2O)_3$

Figure 2.3 shows the IPRD spectra for $Rb^+(H_2O)_3Ar$ and $Rb^+(H_2O)_3$, which are strikingly different. Most notable is the region below 3600 cm^{-1}, typically associated with water-water hydrogen bonding. The $Rb^+(H_2O)_3Ar$ spectrum has a strong, sharp feature near 3550 cm^{-1}, while the $Rb^+(H_2O)_3$ spectrum has a much weaker, broader band centered near 3450 cm^{-1}. As the shift in the OH stretching frequency is indicative of the strength of the hydrogen bond interaction, these two spectra indicate that different isomers are present. The relative intensity of the hydrogen bond features also provides additional information about the abundances of hydrogen-bonded isomers in the experiments. In this case, the argonated species appears to be more extensively hydrogen-bonded.

Four stable structural isomers of $Rb^+(H_2O)_3Ar$ are shown in Figure 2.1. The isomers identified for $Rb^+(H_2O)_3$ are identical (after removing the argon atom) but with slightly different relative zero-point energies, so values are given in Figure 2.1 for both the argonated and non-argonated relative energies. The calculated IR spectra for these isomers are shown in Figure 2.4. There are a total of six unique features in these spectra, two of which (ν_{sym} and ν_{asym}) have already been identified in the smaller cluster ions. In the three hydrogen-bonded isomers, a new feature near 3720 cm^{-1} is assigned to the ν_{free} OH stretching mode. This occurs when one OH oscillator in a water molecule can freely vibrate while the other OH oscillator is involved in a hydrogen bond as a proton donor. In our experimental spectra, the ν_{free} and ν_{asym} OH stretching modes tend to overlap and are often difficult to resolve. The remaining three features in the calculated spectra come from three different types of hydrogen bonds: cyclic, bent and linear. Cyclic hydrogen bonds arise when each water acts as both a proton donor and a proton acceptor

to the other water molecules, as in isomer R3b. A bent hydrogen bond is formed when two water molecules in the first solvent shell act as proton donors to secure a water molecule in the second solvent shell, as displayed by R3a. Finally, a linear hydrogen bond involves a single water molecule in the first solvent shell that acts as a proton donor to a water in the second solvent shell, as depicted in R3d. As seen in Figure 2.4, the progression of cyclic→bent→linear leads to stronger (more red-shifted) hydrogen bonds as the O–H–O angle approaches 180° (129°→164°→170°). Previous calculations of hydrated rubidium ions[2, 16, 17] have not reported any structures containing linear hydrogen bonds, but we find these species to be among the low-energy structures for clusters containing three to five water molecules.

The hydrogen bond feature in the $Rb^+(H_2O)_3Ar$ spectrum is well matched to the calculated spectrum for the R3a isomer (with bent hydrogen bonds), which is the preferred isomer based on the zero-point energies. The experiment, however, also shows a prominent feature associated with the ν_{sym} stretch. Since this stretch would not be expected to be as intense if the experiment consisted only of molecules in the R3a configuration, it is possible that another isomer such as R3c may be present as well.

Figure 2.5 shows relative free energy values reported in kJ/mol as a function of temperature for each of the four calculated isomers of $Rb^+(H_2O)_3$. The relative stability of the isomers is highly dependent on the temperature of the clusters. At temperatures from 0–50 K, the energy ordering favors cluster ions with multiple hydrogen bonds (R3a and R3b). As the temperature increases, these isomers become entropically unfavorable, and the most stable isomers are those with fewer hydrogen bonds (R3c and R3d).

The temperature of the $Rb^+(H_2O)_3Ar$ cluster ions is estimated using RRKM theory to be between 40–100 K, somewhat cooler than for $Rb^+(H_2O)Ar$. In this temperature range, the R3a

isomer is favored, with the R3c isomer lying slightly higher in energy, as can be seen in Figure 2.5. All of the $Rb^+(H_2O)_3Ar$ spectral features can be explained by the R3a isomer contributing to the strong feature near 3550 cm^{-1} and both the R3a and R3c isomers contributing to the ν_{sym} feature at 3642 cm^{-1} and the ν_{asym}/ ν_{free} peak above 3700 cm^{-1}. These structural isomers were also observed for $K^+(H_2O)_3Ar$, however the isomer comparable to R3c was the major contributor and the isomer comparable to R3a was the minor contributor.[11] In contrast, the $Cs^+(H_2O)_3Ar$ spectrum was consistent with an isomer comparable to R3b containing a cyclic water trimer. Figure 2.6 shows a comparison of the potassium, rubidium and cesium spectra. It is particularly interesting to note the decrease in the intensity of the ν_{sym} band and corresponding increase in hydrogen-bonded features from potassium to rubidium to cesium. There is a clear shift favoring water–water interactions over ion–water interactions as the size of the ion increases.

Unlike the colder $Rb^+(H_2O)_3Ar$ spectrum, the $Rb^+(H_2O)_3$ spectrum has no feature near 3550 cm^{-1}, so the R3a isomer must not be present under these experimental conditions. The low intensity of the only hydrogen-bonded feature (near 3450 cm^{-1} in Figure 2.3) relative to the ν_{sym} and ν_{asym} bands suggests that the major contributor to this spectrum must be one in which no hydrogen bonds are present. Since R3c is the only isomer without any hydrogen bonds, it is predicted to be the major contributor under these conditions. Near 300 K, the estimated temperature of the $Rb^+(H_2O)_3$ cluster ions, this isomer has the lowest free energy (as shown in Figure 2.5), with the R3d linearly hydrogen-bonded isomer lying ~7 kJ/mol higher. The relative free energies of each non-argonated isomer at 300 K are given in Figure 2.1 below the relative zero-point energies for easy comparison. The R3d spectrum in Figure 2.4 corresponds most closely to the frequency of the feature near 3450 cm^{-1} in the experiment, so this isomer is likely the minor contributor. The relatively large separation in free energy supports the assignments of

R3c and R3d as major and minor contributors, respectively. In similar $M^+(H_2O)_3$ (M = Li, Na, K) experiments, an isomer comparable to R3c has been assigned as the only contributor.[10] For the case of M = Cs, small contributions from the isomers analogous to R3a, R3b and R3d were also observed.

$Rb^+(H_2O)_4Ar$ and $Rb^+(H_2O)_4$

Figure 2.7 shows the experimental spectra of $Rb^+(H_2O)_4Ar$ and $Rb^+(H_2O)_4$. The features in the $Rb^+(H_2O)_4Ar$ spectrum are located near the same frequencies as those in the $Rb^+(H_2O)_3Ar$ spectrum (Figure 2.3), although the relative intensities of the peaks have changed. The similarity in the feature located between 3530–3570 cm^{-1} indicates that hydrogen bonding is again favored for $Rb^+(H_2O)_4Ar$. On the other hand, the significant decrease in intensity of the ν_{sym} feature near 3640 cm^{-1} and increase in the ν_{free} feature near 3710 cm^{-1} suggests that the degree of hydrogen bonding is more extensive than was observed for $Rb^+(H_2O)_3Ar$.

From a geometry search, five low-lying structural isomers of $Rb^+(H_2O)_4Ar$ were found (Figure 2.1), and their calculated spectra are shown in Figure 2.8. Again, similar structures were found for $Rb^+(H_2O)_4$, with the exception of the R4d tetrahedral, non-hydrogen-bonded isomer, which is only stable if the argon atom is present. There are two isomers with spectral features that nearly match the $Rb^+(H_2O)_4Ar$ experimental spectrum—one containing a bent hydrogen bond (R4b) and one which has a cyclic water trimer subunit (R4c). Interestingly, the R4a isomer, with a cyclic water tetramer, is the global minimum on the potential energy surface. This particular configuration was identified as the major contributor to the $Cs^+(H_2O)_4Ar$ spectrum,[11] but the low-frequency, hydrogen-bonded OH stretch calculated for the R4a structure is not consistent with these experimental results. The results of a thermodynamics evaluation indicate

that the R4a isomer actually has the lowest relative free energy from 0–100 K, with R4b and R4c lying between 0.25–4.1 kJ/mol higher in energy, so it is a bit surprising that it is not observed in the experimental spectrum. The $M^+(H_2O)_4Ar$ comparison spectrum in Figure 2.9 emphasizes the difference between the rubidium and cesium spectra and suggests that the assignments for the rubidium spectrum may more closely resemble those of potassium.

In similar experiments, features in the spectra of $M^+(H_2O)_4Ar$ (M = Li, Na, K) were all assigned to a bent hydrogen-bonded isomer comparable to R4b.[11] This makes it likely that the features near 3540 and 3558 cm^{-1} come from R4b, but additional contributions from the R4c isomer cannot be ruled out. Indeed, the relative intensity of the 3540 and 3558 cm^{-1} bands strongly suggests the presence of the second, R4c, conformer. The higher-frequency feature near 3710 cm^{-1} is assigned to the dominant ν_{free} stretch, with some overlap from the ν_{asym} stretch of these same two isomers.

As seen already for the cluster ions with three water molecules, the features observed in the $Rb^+(H_2O)_4$ spectrum are clearly different from those of the $Rb^+(H_2O)_4Ar$ spectrum (Figure 2.7), so we expect to find different isomers contributing to this spectrum. The experimental spectrum of $Rb^+(H_2O)_4$ has three features in common with the $Rb^+(H_2O)_3$ spectrum—ν_{sym} near 3640 cm^{-1}, overlapping ν_{asym} and ν_{free} peaks from 3690–3740 cm^{-1} and a broad hydrogen bond feature near 3450 cm^{-1}. This last feature was assigned to the R3d isomer with a linear hydrogen bond. Isomer R4e has a structure and calculated spectrum similar to that of R3d and is also the thermodynamically favored isomer near 300 K. This isomer is likely the major contributor to the ν_{sym} (3640 cm^{-1}), ν_{asym}/ν_{free} (3690–3740 cm^{-1}) modes and the low-frequency (~3450 cm^{-1}) hydrogen-bonded peak. The isomer with a cyclic tetramer (R4a) is also calculated to have a

feature near 3450 cm^{-1}, but this isomer has a free energy 24.2 kJ/mol higher than the R4e conformer near 300 K and is unlikely to contribute to the experiment.

The remaining feature in the $Rb^+(H_2O)_4$ spectrum, a hydrogen bond peak near 3550 cm^{-1}, is located near the frequency of the doublet feature in the $Rb^+(H_2O)_4Ar$ spectrum, which was attributed to a combination of isomers R4b and R4c. The relative free energies of these isomers at 300 K are similar (9.7 kJ/mol and 8.6 kJ/mol, respectively), so both are likely to give intensity to the hydrogen bond feature centered near 3550 cm^{-1} and also contribute to the ν_{asym}/ν_{free} feature. The $Rb^+(H_2O)_4$ spectrum looks very similar to the $Cs^+(H_2O)_4$ spectrum, and assignments of isomers analogous to R4e, R4b and R4c were also made for that spectrum.[10] In contrast, the $K^+(H_2O)_4$ spectrum contained relatively little evidence of hydrogen bonding, and the major contributor to that experiment was assigned as a non-hydrogen-bonded isomer. Under these elevated temperature conditions and at a larger cluster size, we again see how the increase in ion size tends to favor structures with water-water interactions.

$Rb^+(H_2O)_5Ar$ and $Rb^+(H_2O)_5$

The $Rb^+(H_2O)_5Ar$ and $Rb^+(H_2O)_5$ experimental spectra are shown in Figure 2.10. It was not computationally feasible to calculate structures or spectra for the $Rb^+(H_2O)_5Ar$ cluster ions, so the analysis of this experimental spectrum relies on vibrational assignments of the smaller hydrated/argonated species and on *ab initio* calculations for $Rb^+(H_2O)_5$. The low intensity at 3640 cm^{-1} for the ν_{sym} peak in the $Rb^+(H_2O)_5Ar$ spectrum indicates that almost all of the water molecules under these conditions must be involved in some form of hydrogen bonding. With at least five separate peaks in the hydrogen-bonded region, there must be more than just one or two isomers present. By comparison with the smaller clusters, the feature at 3553 cm^{-1} likely comes

from some type of bent or cyclic trimer isomer. This feature also corresponds well with the prominent hydrogen-bonded feature near 3546 cm^{-1} in the $K^+(H_2O)_5Ar$ spectrum (shown in Figure 2.11) which was assigned to a conformer with a bent hydrogen bond.[11] Cyclic tetramers or pentamers and linear hydrogen-bonded isomers are likely responsible for the remaining $Rb^+(H_2O)_5Ar$ features at 3512, 3494, 3473 and 3429 cm^{-1}. The $Cs^+(H_2O)_5Ar$ spectrum (Figure 2.11) contained bands arising from cyclic water pentamer, tetramer and trimer subunits as well as an isomer containing a bent hydrogen bond.[11]

Seven stable isomers were identified for $Rb^+(H_2O)_5$ (shown in Figure 2.1 with their simulated spectra in Figure 2.12). Thermodynamic analysis revealed that the five lowest-energy isomers have relative free energies within a 10 kJ/mol range at 300 K. This again suggests that the experimental spectrum is a result of multiple isomers. As hydrogen-bonded OH bands broaden at higher temperatures, it becomes more difficult to assign the spectral features to particular isomers since many isomers have peaks near the same frequencies. As noted earlier, the cyclic trimer and bent hydrogen-bonded peaks overlap, as do cyclic pentamer, cyclic tetramer and linear hydrogen-bonded bands. To further complicate the assignment, several of the possible isomers of $Rb^+(H_2O)_5$ (such as R5e and R5f) have more than one type of hydrogen bond. Thermodynamically, the three isomers with the lowest relative free energies at 300 K are the R5g, R5e and R5d isomers. These isomers are entropically favored as they contain fewer hydrogen bonds compared to the other isomers. While additional isomers cannot be unambiguously excluded, these three isomers can account for all of the features present in the $Rb^+(H_2O)_5$ spectrum. It is suggestive (although not definitive) that the linear hydrogen bonds in R5e could contribute to the band at ~3400cm^{-1}, linear hydrogen bonds in R5g at 3470 cm^{-1}, and a low-frequency symmetric stretch from R5e and bent hydrogen bonds from R5d at 3560 cm^{-1}.

Although definite assignments cannot be made, it is clear from the experimental spectrum that at least three different types of hydrogen bonding are present, with some water molecules not involved in hydrogen bonding as noted by the presence of the ν_{sym} peak at 3643 cm^{-1}. This is in direct contrast to the colder $Rb^+(H_2O)_5Ar$ spectrum with little intensity for the ν_{sym} mode. The analyses of the $K^+(H_2O)_5$ and $Cs^+(H_2O)_5$ spectra were also complicated by the number of spectral features present and many stable structures within several kJ/mol of relative free energy. Because of this, it's easier to compare the M = K, Rb and Cs spectra (Figure 2.13) rather than their assignments, and in doing so it becomes clear that the rubidium spectrum acts as a bridge between the other two. The spectrum of $Rb^+(H_2O)_5$ appears to be a convolution of the spectra of $K^+(H_2O)_5$ and $Cs^+(H_2O)_5$. The band at 3400 cm^{-1} indicates that a stronger hydrogen bond is present for Rb^+ and Cs^+ that is not present in $K^+(H_2O)_5$. The weaker ion-water interaction enables this bond to occur (likely a linear hydrogen bond from a structure with reduced first hydration shell occupation). K^+, which has a stronger ion-water interaction, tends to keep at least four waters in the first hydration shell.

Conclusions

The formation and relative abundance of $Rb^+(H_2O)_n$ and $Rb^+(H_2O)_nAr$ isomers are heavily dependent on the temperature of the cluster ions. Clusters formed through the evaporative loss of argon are much cooler (~40–120 K) than those formed by evaporation of water (~300 K), and the IPRD spectra—particularly for the clusters with $n \geq 3$—reflect this difference. For n=3, the dominant isomer of $Rb^+(H_2O)_3Ar$ has a water molecule in the second solvent shell secured by two bent hydrogen bonds from the remaining waters in the first shell, while the warmer $Rb^+(H_2O)_3$ favored a structure with no hydrogen bonds that maximized water-

ion interactions. For n=4, the dominant configurations for both the warm and cold cluster ions exhibit hydrogen bonding. The cold cluster ions had multiple hydrogen bonds, with bent and cyclic structures, while the warm cluster ions are dominated by a single linear hydrogen bond. Thermodynamically, the isomers with more hydrogen bonds tend to be structurally preferred at low temperatures, but at higher temperatures, breaking some of these bonds results in free rotation of the water molecules, leading to structures that are entropically favored.

This work complements previous studies from our lab, particularly those of hydrated potassium and cesium cluster ions.[10, 11] In general, the smaller potassium cation tends to form clusters that favor the ion-water interactions while the larger cesium cation tends to form clusters that favor the water-water interactions through the formation of hydrogen bonds. Rubidium tends to bridge the difference in behavior between these two ions as seen in Figures 2.6, 2.9 and 2.13. For the argonated cluster ions, the rubidium spectra resemble the potassium spectra for the n=3 and n=4 cases but resembles cesium for n=5. In the warmer experiments, the rubidium spectra reflect a combination of both the potassium and cesium spectra at each cluster size.

Figures

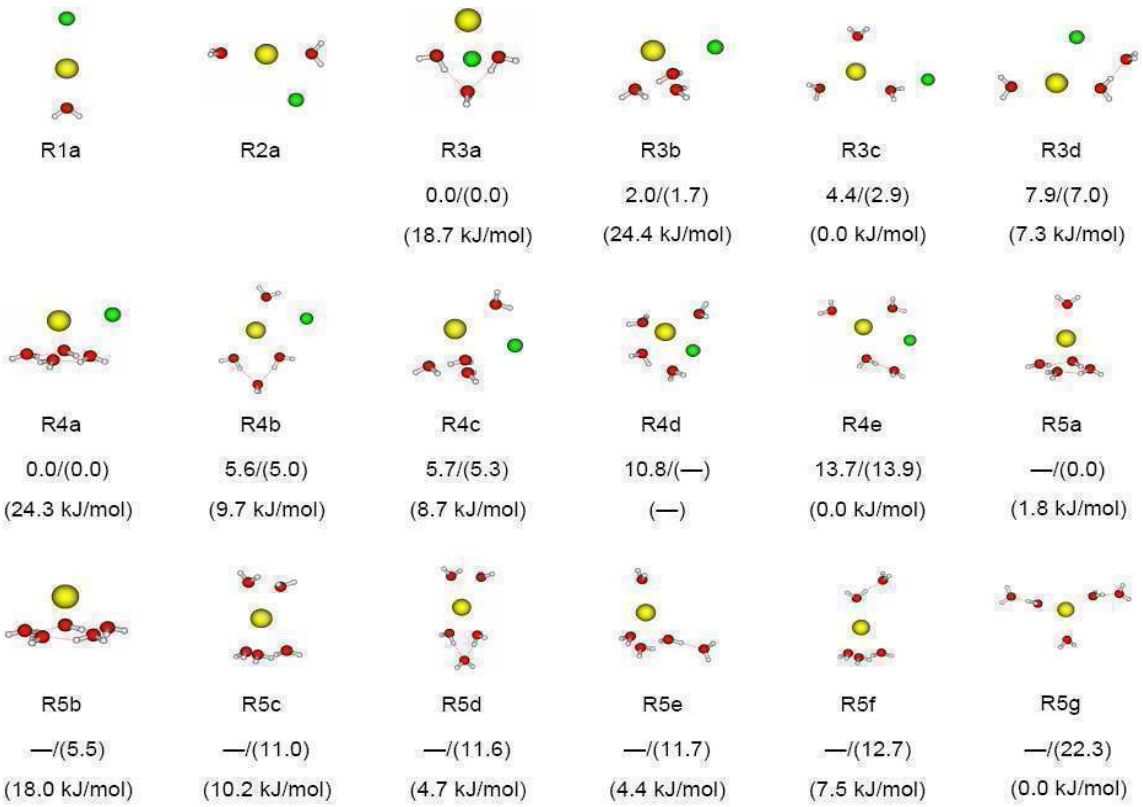

Figure 2.1: Calculated structures for $Rb^+(H_2O)_{n=1-4}Ar$ and $Rb^+(H_2O)_5$ cluster ions. Relative zero-point energies (in kJ/mol) are given in the first row below each image for both the argonated and non-argonated (in parentheses) structures. Relative free energies of the non-argonated structures at 300 K are given in the second row below each image.

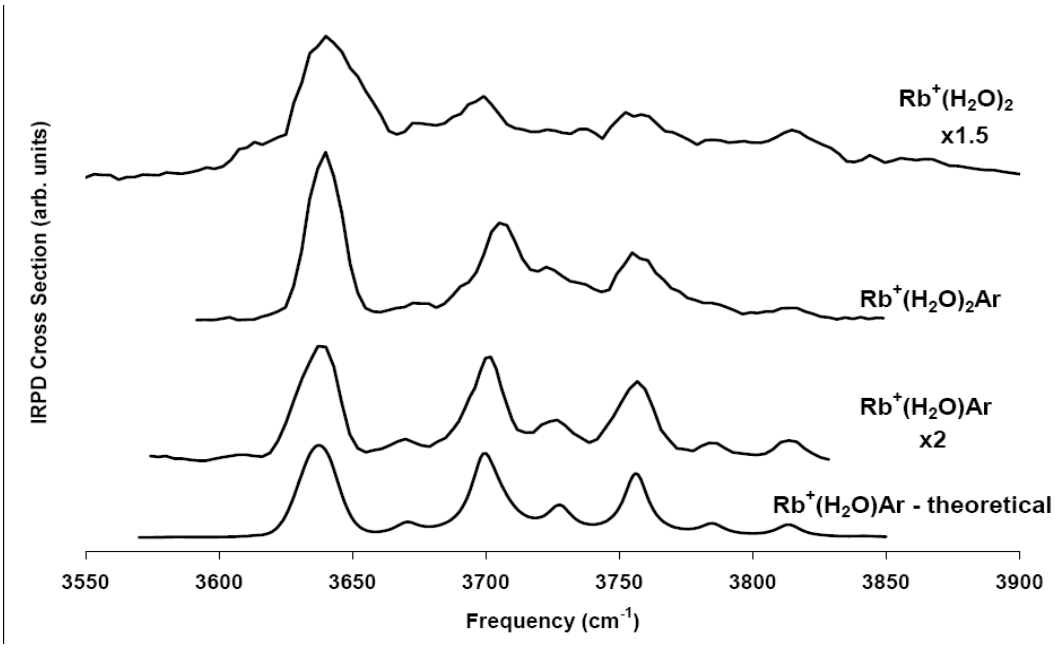

Figure 2.2: Calculated spectrum of $Rb^+(H_2O)Ar$ and IRPD spectra of $Rb^+(H_2O)Ar$, $Rb^+(H_2O)_2Ar$ and $Rb^+(H_2O)_2$. The $Rb^+(H_2O)Ar$ and $Rb^+(H_2O)_2$ spectra were scaled to have the same intensity as the $Rb^+(H_2O)_2Ar$ spectrum near 3640 cm^{-1}.

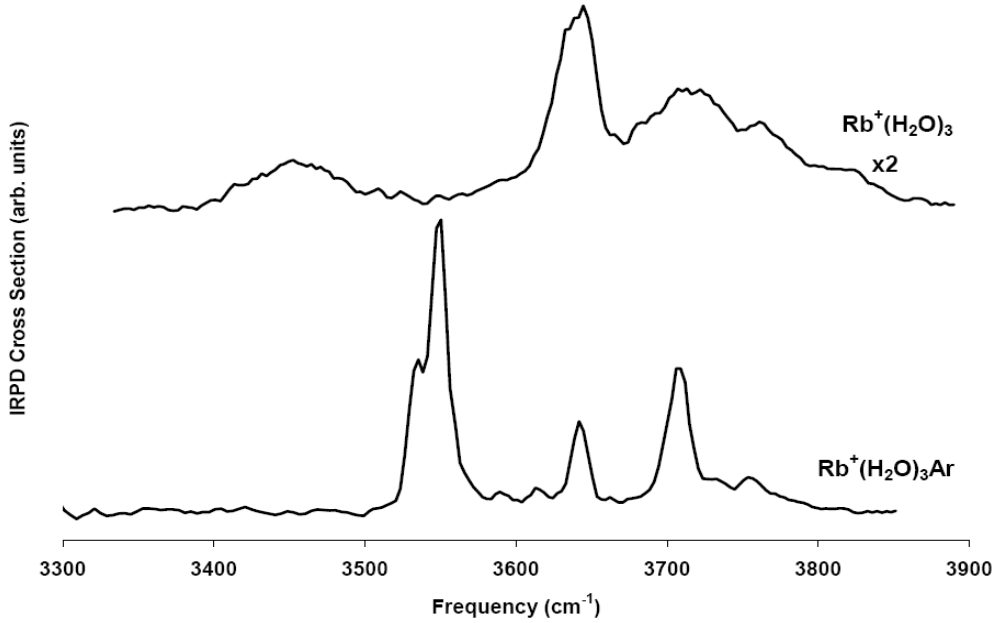

Figure 2.3: IRPD spectra of $Rb^+(H_2O)_3$ and $Rb^+(H_2O)_3Ar$.

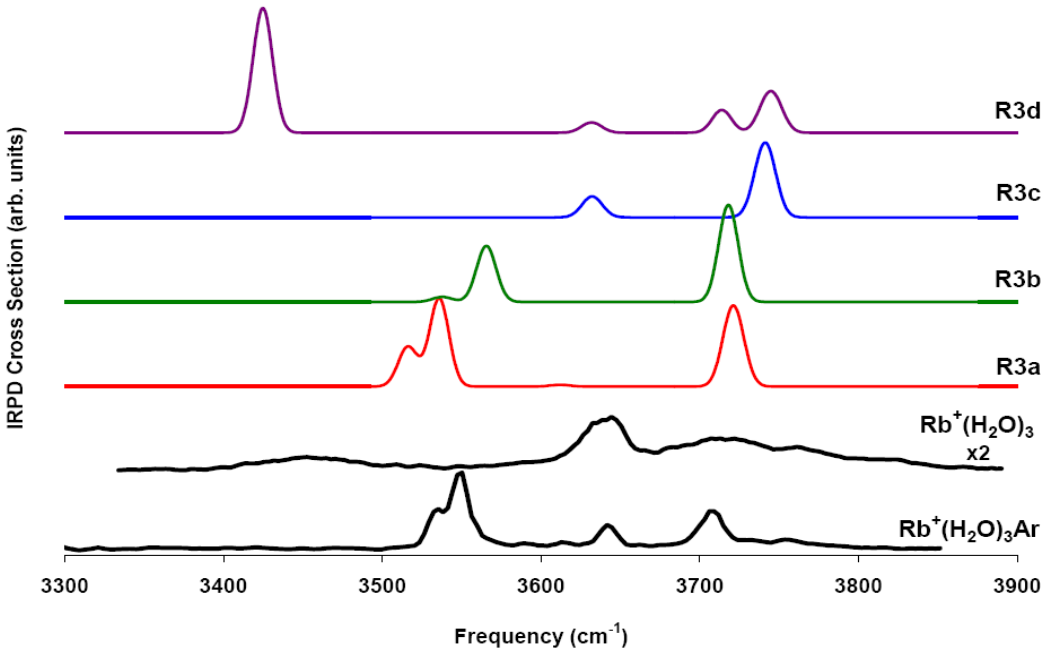

Figure 2.4: IRPD spectra of $Rb^+(H_2O)_3$ and $Rb^+(H_2O)_3Ar$ along with calculated spectra for the four structural isomers identified in Figure 2.1.

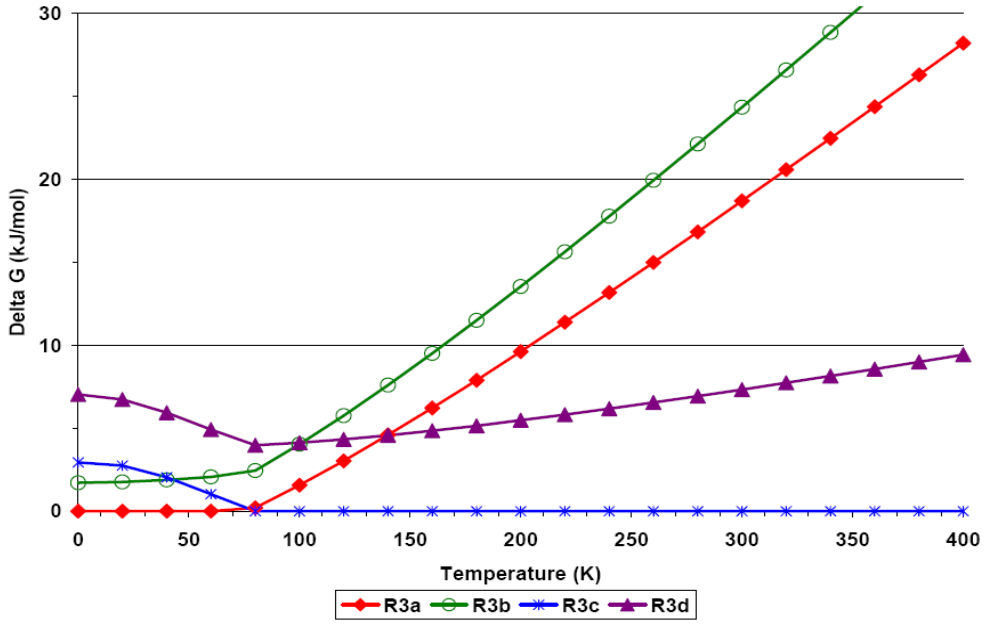

Figure 2.5: Plot of relative free energy versus temperature for the four structural isomers of $Rb^+(H_2O)_3$.

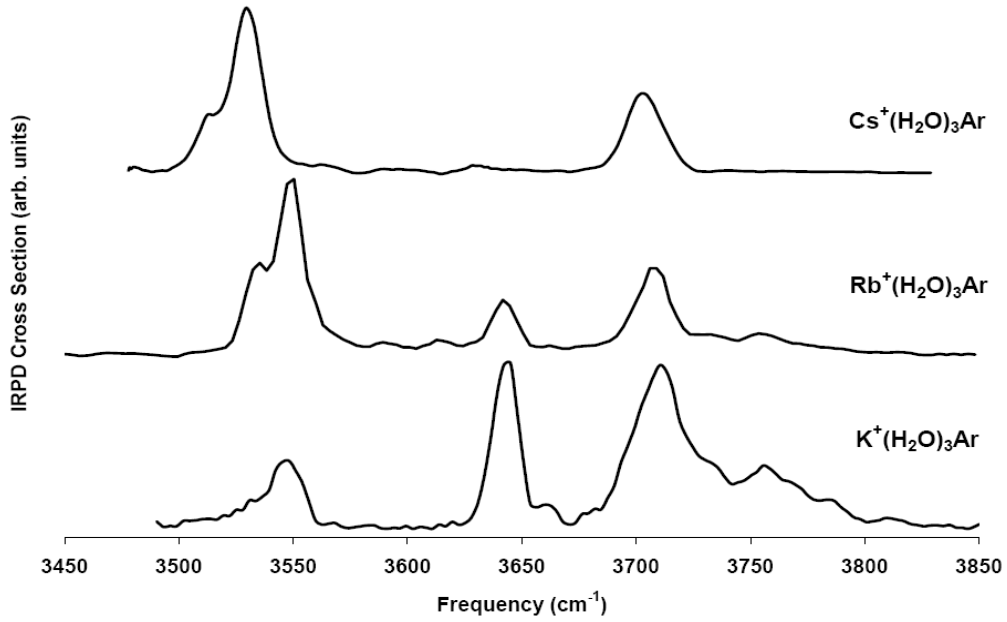

Figure 2.6: IRPD spectra of $K^+(H_2O)_3Ar$, $Rb^+(H_2O)_3Ar$ and $Cs^+(H_2O)_3Ar$. Potassium and cesium spectra were adapted from Ref. [11].

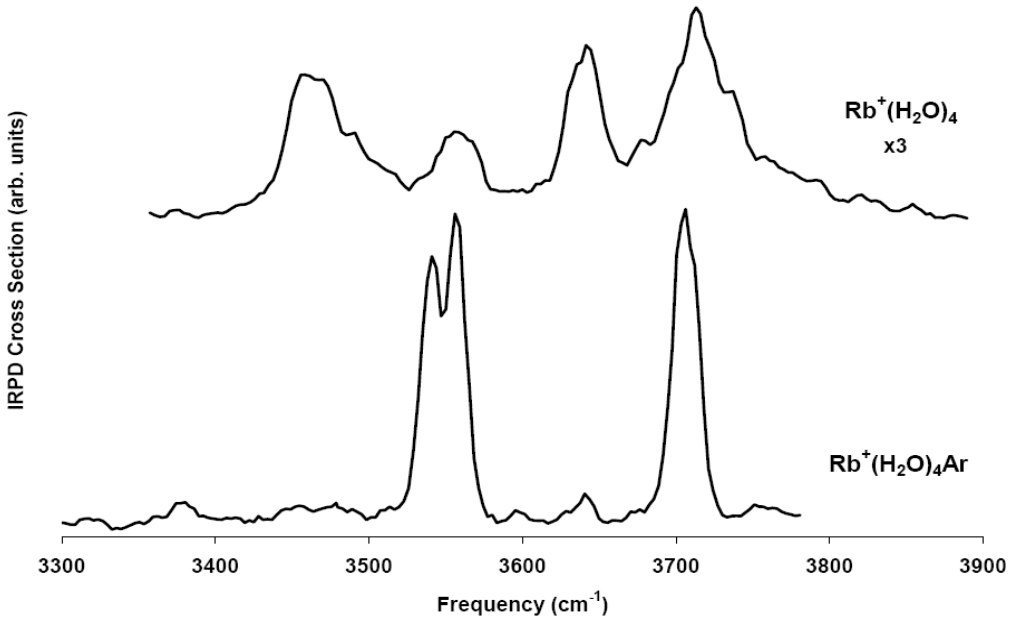

Figure 2.7: IRPD spectra of $Rb^+(H_2O)_4$ and $Rb^+(H_2O)_4Ar$.

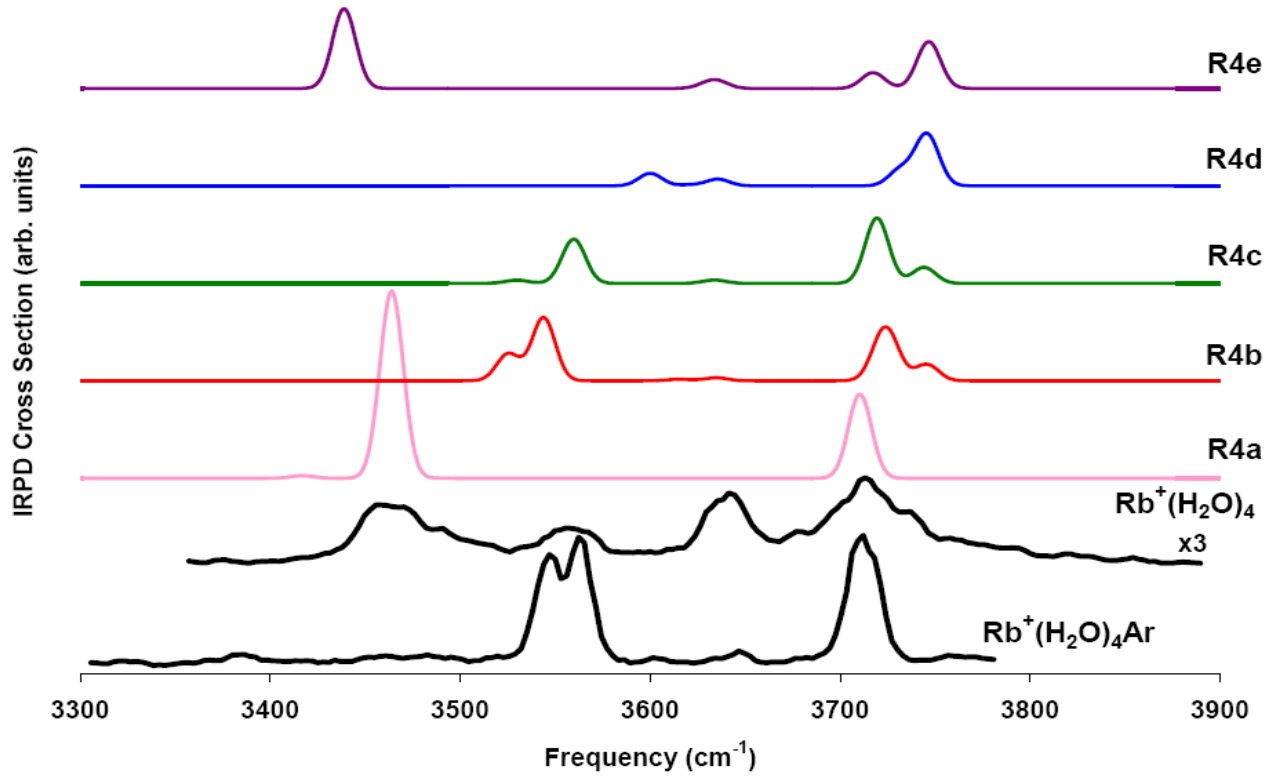

Figure 2.8: IRPD spectra of $Rb^+(H_2O)_4$ and $Rb^+(H_2O)_4Ar$ along with calculated spectra for the five structural isomers identified in Figure 2.1.

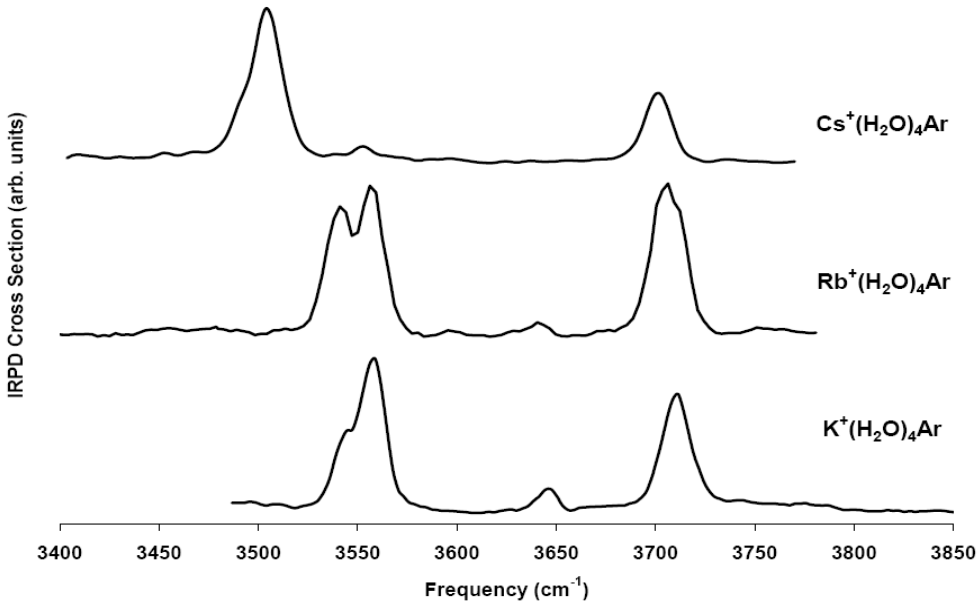

Figure 2.9: IRPD spectra of $K^+(H_2O)_4Ar$, $Rb^+(H_2O)_4Ar$ and $Cs^+(H_2O)_4Ar$. Potassium and cesium spectra were adapted from Ref. [11].

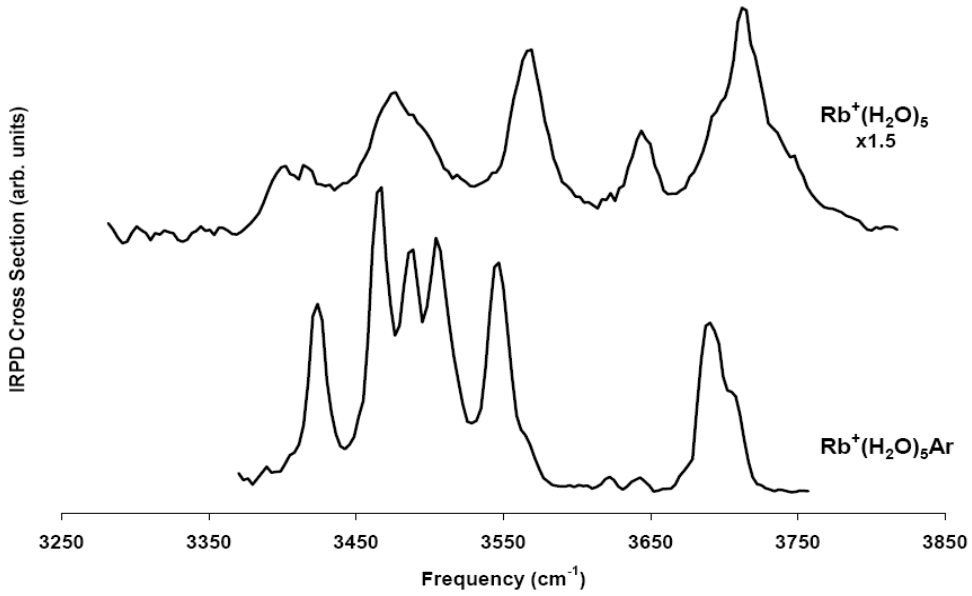

Figure 2.10: IRPD spectra of $Rb^+(H_2O)_5$ and $Rb^+(H_2O)_5Ar$.

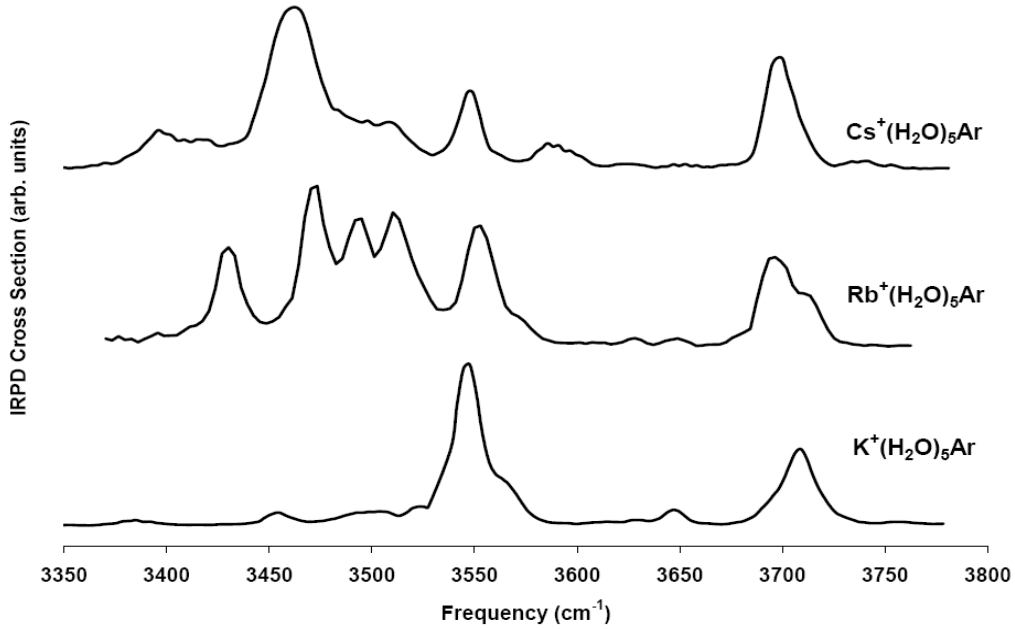

Figure 2.11: IRPD spectra of $K^+(H_2O)_5Ar$, $Rb^+(H_2O)_5Ar$ and $Cs^+(H_2O)_5Ar$. Potassium and cesium spectra were adapted from Ref. [11].

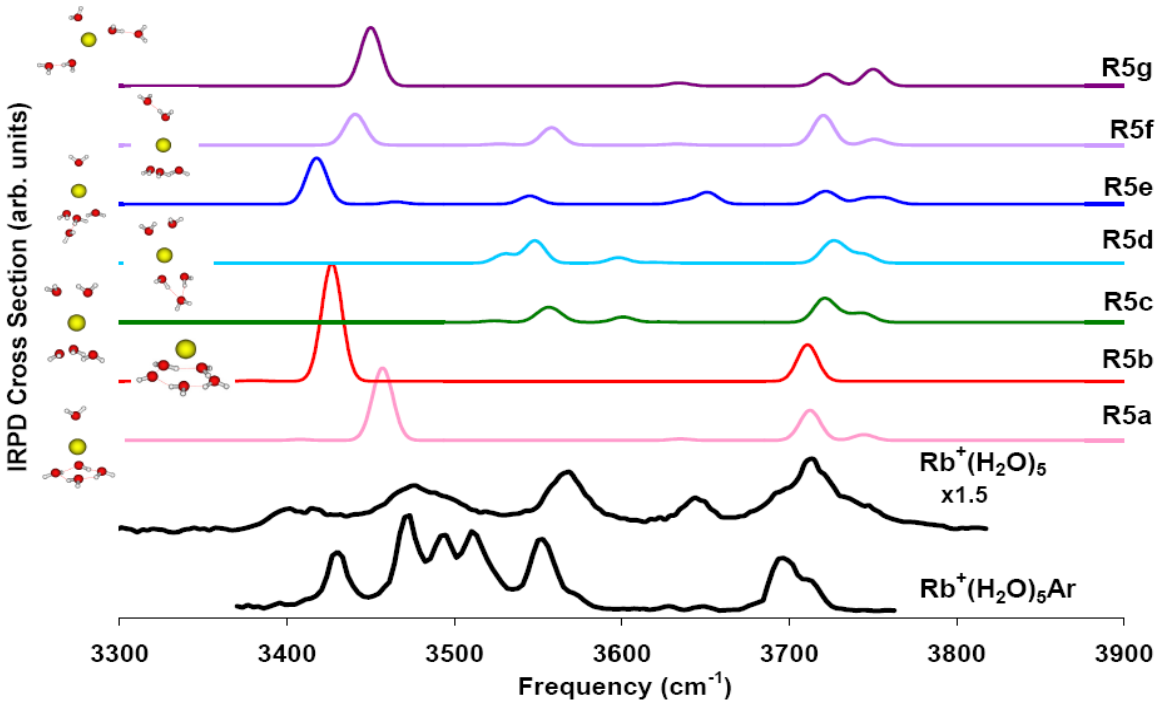

Figure 2.12: IRPD spectra of $Rb^+(H_2O)_5$ and $Rb^+(H_2O)_5Ar$ along with calculated spectra for the seven structural isomers identified in Figure 2.1.

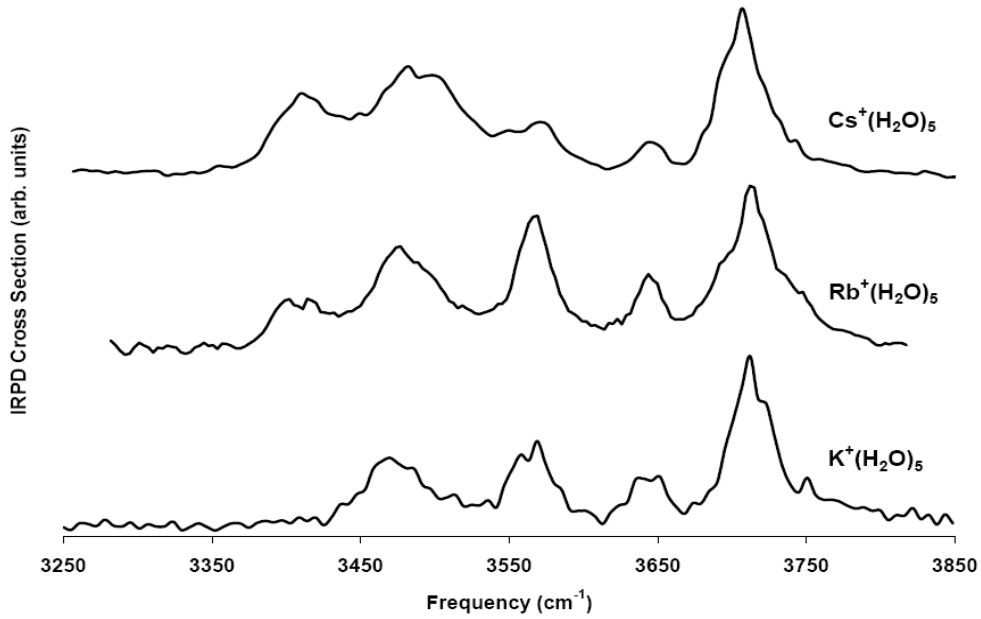

Figure 2.13: IRPD spectra of $K^+(H_2O)_5$, $Rb^+(H_2O)_5$ and $Cs^+(H_2O)_5$. Potassium and cesium spectra were adapted from Ref. [10].

References

1. Duncan, M. A., *Int. Rev. Phys. Chem.* **2003,** 22, (2), 407.
2. Lee, H. M.; Tarakeshwar, P.; Park, J.; Kolaski, M. R.; Yoon, Y. J.; Yi, H. B.; Kim, W. Y.; Kim, K. S., *J. Phys. Chem. A* **2004,** 108, (15), 2949-2958.
3. Walker, N. R.; Walters, R. S.; Duncan, M. A., *New J. Chem.* **2005,** 29, (12), 1495-1503.
4. Lisy, J. M., *J. Chem. Phys.* **2006,** 125, (13), 132302.
5. Beyer, M. K., *Mass Spectrom. Rev.* **2007,** 26, (4), 517-541.
6. Kolaski, M.; Lee, H. M.; Choi, Y. C.; Kim, K. S.; Tarakeshwar, P.; Miller, D. J.; Lisy, J. M., *J. Chem. Phys.* **2007,** 126, (7), 074302.
7. Miller, D. J.; Lisy, J. M., *J. Chem. Phys.* **2006,** 124, (2), 024319.
8. Vaden, T. D.; Weinheimer, C. J.; Lisy, J. M., *J. Chem. Phys.* **2004,** 121, (7), 3102.
9. Vaden, T. D.; Forinash, B.; Lisy, J. M., *J. Chem. Phys.* **2002,** 117, (10), 4628.
10. Miller, D. J.; Lisy, J. M., *J. Am. Chem. Soc.* **2008,** 130, (46), 15393-15404.
11. Miller, D. J.; Lisy, J. M., *J. Am. Chem. Soc.* **2008,** 130, (46), 15381-15392.
12. Cabarcos, O. M.; Weinheimer, C. J.; Lisy, J. M., *J. Phys. Chem. A* **1999,** 103, (44), 8777-8791.
13. Boo, D. W.; Lee, Y. T., *Int. J. Mass Spectrom. Ion Processes* **1996,** 159, (1-3), 209.
14. Okumura, M.; Yeh, L. I.; Myers, J. D.; Lee, Y. T., *J. Chem. Phys.* **1986,** 85, (4), 2328-2329.
15. Fraley, P. E.; Rao, K. N., *J. Mol. Spectrosc.* **1969,** 29, (1-3), 348.
16. Park, J.; Kolaski, M.; Lee, H. M.; Kim, K. S., *J. Chem. Phys.* **2004,** 121, (7), 3108.
17. Glendening, E. D.; Feller, D., *J. Phys. Chem.* **1995,** 99, (10), 3060-3067.

Chapter 3: Hydrated M^+(Tryptamine) Cluster Ions*

Introduction

Infrared spectroscopy is an effective tool for elucidating structures of gas-phase clusters and cluster ions. This technique has often been used to study the structures of bare and hydrated neutral amino acids and other similar biological species.[1-4] The environment of these species also includes a significant concentration of monovalent ions, so an accurate assessment of biomolecule conformations should necessarily include the potential effect of these ions. Accordingly, many recent studies have probed the role of protons and metal ions in directing amino acid structure.[5-10] The M^+(amino acid) systems often have different structures than the bare amino acids,[5, 6, 10] and the structures can be metal-ion dependent.[5-8]

Tryptamine (Tryp) is built around the indole ring structure and is a derivative of the amino acid tryptophan. Along with several well-known substituted tryptamines, such as serotonin and melatonin, tryptamine is classified as a neurotransmitter and believed to play a role in neuropsychiatric disorders.[11] A number of experiments have examined the electronic spectrum of tryptamine, the first of which was obtained by Park and coworkers.[12] Further studies at higher resolution examined the transition moments, rotational constants and structures of six tryptamine conformers in the electronic spectrum.[13-15] More recent experiments included conformer-specific infrared spectra, confirming the presence of seven tryptamine conformers in the molecular beam expansion,[16, 17] while advanced multi-laser techniques have probed the energy barriers between the conformers.[18] The seven observed tryptamine conformers are a

* Reproduced with permission from Amy L. Nicely, Dorothy J. Miller and James M. Lisy, *J. Am. Chem. Soc.* **2009,** 131, (18), 6314. Copyright 2009 American Chemical Society. Portions of this chapter are also reproduced with permission from Amy L. Nicely and James M. Lisy, *J. Phys. Chem. A* **2010**, *in preparation*. Copyright 2010 American Chemical Society.

subset of the nine possible conformers which differ in the position and orientation of the amino group in the ethylamine side chain. The nomenclature used here is adopted from Zwier and coworkers.[16] The position of the amino group is described as gauche to the phenyl ring, Gph; gauche to the pyrrole ring, Gpy; or pointing away from both rings, anti. The description in parentheses gives the orientation of the amino lone pair relative to the indole rings (up, out, in, py, ph). Of the nine possible tryptamine conformers, Gpy(out) has been identified as the most prominent, while Gpy(in) and Gph(in) are the two high-energy conformers not observed in any of the previous studies. The unfavorable interaction between the amino lone pair and the pi cloud above the indole rings inhibits population of these monomer conformers.

Although seven conformers of bare tryptamine are observed experimentally, the addition of a single water molecule results in only one Tryp(H_2O) conformer.[17, 19-22] This structure locks in the Gpy(out) conformer from the bare molecule, with the amino group acting as a hydrogen bond donor to the water molecule. A similar phenomenon was observed with the addition of a methanol molecule – only one band was present in the electronic spectrum of Tryp(MeOH), suggesting that one conformer was preferred over the others.[12]

Interestingly, the subsequent addition of water molecules produces a major change in the structure of the cluster: with two or three water molecules, the tryptamine converts to a Gpy(in) configuration in order to accommodate a water bridge between the amino and indole NH positions.[17, 23] Although this configuration brings strain to the ethylamine side chain, it is stabilized by the formation of hydrogen bonds. This demonstrates that while the Gpy(out) conformer is favored for the bare and singly hydrated tryptamine molecule, the other conformers cannot be excluded *a priori* as possibilities for other tryptamine-containing clusters. The

tryptamine conformation will instead be determined by a balance of competing noncovalent interactions which are sensitive to cluster composition.

We report here the infrared spectra of $M^+(Tryp)(H_2O)_{0-3}Ar_{0,1}$, with M=K and Na, the two most prevalent monovalent ions in biological systems. Unlike the neutral $Tryp(H_2O)_n$ structures which appear to adopt different tryptamine conformations depending on the number of water molecules present,[17] the sodiated and potassiated cluster ions consistently adopt the Gpy(in) and Gph(in) tryptamine conformers.

Results and Discussion

$K^+(Tryp)(H_2O)_{0,1}Ar_{0,1}$

Vibrational spectra of $K^+(Tryp)Ar$, $K^+(Tryp)(H_2O)$ and $K^+(Tryp)(H_2O)Ar$ are shown in Figure 3.1. Zwier and coworkers showed that analysis of the alkyl CH stretching modes is essential to characterizing tryptamine configurations.[16] In Figure 3.1, the alkyl CH modes in the 2850–2980 cm^{-1} region are consistent, suggesting a common tryptamine conformer in all three species. This is particularly interesting for $K^+(Tryp)Ar$ and $K^+(Tryp)(H_2O)$, which differ in both composition and effective temperature. The broad underlying feature observed in the CH stretching region of the $K^+(Tryp)(H_2O)Ar$ spectrum is indicative of strong OH hydrogen bonding (vide infra).

Notably, the CH signatures observed in these spectra are different than those observed in the neutral tryptamine study.[16] A computational study of the $K^+(Tryp)$ conformational landscape identifies AGpy(in) and AGph(in) (shown in Figure 3.2 with their calculated spectra) as the two lowest-energy isomers, with all other calculated structures 40–50 kJ/mol higher in energy. In contrast, the neutral Gpy(in) and Gph(in) conformers were the highest-energy conformers

theoretically located and were not experimentally observed in the neutral tryptamine study.[16] The potassium cation significantly impacts the tryptamine conformation, favoring structures previously unobserved. For these optimized structures, the "A" indicates that the ion sits above the indole rings of the various tryptamine conformers. The AGpy(in) and AGph(in) isomers are in good agreement with the K^+(Tryp)Ar experimental spectrum, while the AGpy(out) isomer is predicted to have a low-frequency CH feature, resulting from a direct interaction between a CH_2 group and K^+. Figure 3.2 also includes a calculated spectrum for the AGpy(out) conformer of K^+(Tryp) to emphasize the differences in the CH stretching region that result from different conformers.

Gas-phase tryptamine monomer exhibits the indole NH stretch as a strong feature near 3525 cm^{-1}, while the significantly weaker symmetric/asymmetric amino NH_2 stretches appear between 3300–3400 cm^{-1}.[17] The indole NH stretch in K^+(Tryp)Ar is observed near 3490/3503 cm^{-1} (the doublet arises from the two low-lying AGpy(in) and AGph(in) conformers), while the NH_2 asymmetric stretch is near 3364 cm^{-1}. The symmetric NH_2 stretch is too weak to be observed.

The K^+(Tryp)(H_2O) spectrum preserves these NH stretching features near 3500 and 3360 cm^{-1}. While a single water molecule should give rise to only two OH stretching features, this spectrum has three distinct OH features between 3550–3750 cm^{-1}, indicating more than one structural isomer in the molecular beam. The OH asymmetric/symmetric stretches of water monomer at 3756 and 3657 cm^{-1} [24] shift to slightly lower frequencies when bound to a cation, as observed in K^+(H_2O)Ar with corresponding frequencies at 3710 and 3636 cm^{-1}, respectively.[25] The features centered at 3711 and 3640 cm^{-1} in the K^+(Tryp)(H_2O) spectrum indicate an ion-water interaction consistent with structure K1d, as depicted in Figure 3.3. Hydrogen bonding

generally shifts OH stretches below 3600 cm^{-1}, as observed for the feature centered at 3582 cm^{-1}. This shift is attributed to a π-hydrogen bond between one OH group and the indole ring, based on the assignment of a similar band observed near 3560 cm^{-1} in $K^+(Indole)(H_2O)_2$.[26] In this hydrogen-bonded configuration (K1c in Figure 3.3), the other OH oscillator remains free with a vibrational frequency near 3710 cm^{-1}.[26] The OH free and asymmetric features are not always fully resolved in our experiments, and the observed band near 3711 cm^{-1} is likely a convolution of these vibrations, arising from a combination of isomers K1c and K1d.

In total, five low-energy $K^+(Tryp)(H_2O)$ isomers, found in computations, are shown in Figure 3.3. Each of these low-energy isomers contains either a Gpy(in) or Gph(in) tryptamine conformer. Other conformers were 30–40 kJ/mol higher in energy and thus unlikely to be present in this study. A free energy analysis (Figure 3.4) indicates that while structure K1a is preferred at 0 K, it becomes entropically unfavorable as the cluster temperature increases. Structure K1d has the lowest free energy at all temperatures above 170 K and is likely the major contributor under the warmer (~300 K) experimental conditions. Structures K1a, K1b and K1c are almost isoenergetic near 300 K (and about 8 kJ/mol higher in free energy than K1d), but only K1c is in agreement with the remaining spectral features and is assigned as a second, minor contributor to the $K^+(Tryp)(H_2O)$ spectrum; K1a and K1b are, at best, very minor contributors.

The spectrum of $K^+(Tryp)(H_2O)Ar$ shows several new features compared to the warmer $K^+(Tryp)(H_2O)$ spectrum. While the intensity of the indole NH feature around 3500 cm^{-1} decreased, a new strong feature at 3330 cm^{-1} is observed. Also, a broad feature convoluted with the CH stretching modes in the 2850–2950 cm^{-1} region is now present. The intensity and breadth of these new features are hallmarks of hydrogen-bonded XH stretching modes. The reduction in temperature has allowed new hydrogen-bonded isomers to form.

Under the conditions for the $K^+(Tryp)(H_2O)Ar$ experiment (~50–150 K), conformers with more hydrogen bonds are enthalpically favored.[27, 28] The broad band underlying the CH stretching region is presumably due to a hydrogen-bonded OH mode that is strongly red-shifted. Isomers K1a and K1b—which have the lowest free energies in this temperature range—contain a hydrogen bond between the water molecule and the amino nitrogen, calculated to have an OH stretch centered around 2950 cm^{-1}. The new feature present at 3330 cm^{-1} is consistent with isomer K1e, with the indole NH group acting as a proton donor to the water molecule. Isomer K1e is about 20 kJ/mol higher in free energy than K1a and not expected to contribute to the observed spectrum, yet the presence of this feature indicates otherwise. As the ion approaches the neutral complex embedded in argon, the rapid evaporation process must allow this higher-energy conformer to form. This was noted previously for $Li^+(H_2O)_4Ar$, where a significant barrier to isomerization prevented rearrangement to a lower-energy conformer.[27] A second example of trapping a high energy conformer by rapid argon evaporation has been recently observed in K^+(18-crown-6)$H_2O{\cdot}Ar$.[29] For the other $K^+(Tryp)(H_2O)Ar$ features, the band near 3570 cm^{-1} is again assigned to the conformer with the π-hydrogen bond (isomer K1c), and the OH modes at higher frequency arise from a combination of isomers K1a, K1b, K1c and K1e.

The role of both charge and temperature has a dramatic impact on the favored conformers of tryptamine and the nature of tryptamine-water hydrogen bonding. Two previously unobserved, high-energy conformers of neutral tryptamine become the lowest–energy and *only* conformers observed in the K^+-bearing cluster ions reported here. In addition, the presence of a high-energy conformer trapped by the argon evaporative cooling process was identified. Exploration of the conformational landscape of hydrated cluster ions bearing flexible biomolecules is now possible.

Na^+(Tryp)Ar

We have previously reported the infrared spectra of K^+(Tryp)Ar, K^+(Tryp)(H_2O) and K^+(Tryp)(H_2O)Ar, [30] shown here in Figure 3.1. The corresponding sodium-containing spectra are given in Figure 3.5. The Na^+(Tryp)Ar spectrum is clearly very similar to its potassium counterpart, making spectral assignments straightforward. The prominent feature near 3500 cm^{-1} is assigned in both spectra to the free NH stretch of the indole group. The weaker amino symmetric and asymmetric stretches appear near 3300 and 3350 cm^{-1}, respectively, as shown in the inset of Figure 3.5a for Na^+(Tryp)Ar. Only the amino asymmetric stretch was observed in the K^+(Tryp)Ar spectrum. The remaining features in the spectra (from 2850-3100 cm^{-1}) are assigned to CH stretches. A comparison of the CH stretching region of the spectra in Figures 3.1 and 3.5 suggests the same tryptamine conformers contribute to all of these spectra.

The K^+(Tryp)Ar spectrum reported was assigned with contributions from both the AGpy(in) and AGph(in) cluster ions.[30] For both K^+ and Na^+, the zero-point energies of these two isomers are very close (0.3 kJ/mol for K^+; 1.9 kJ/mol for Na^+) and both isomers are expected to be present in the experiments. One difference between the Na^+(Tryp)Ar and K^+(Tryp)Ar spectra occurs, however, at the NH stretching feature near 3500 cm^{-1}. The K^+(Tryp)Ar spectrum has a doublet feature here because the NH stretching vibration of AGpy(in) occurs slightly lower (~9 cm^{-1}) compared to that of AGph(in). In the case of sodium, the NH stretching vibrations of the two isomers are predicted to be within 1 cm^{-1} of each other, which is beyond the resolution of the current apparatus.

$Na^+(Tryp)(H_2O)$

The addition of a single water molecule does little to perturb the underlying structure of the sodium-containing cluster ions. This is demonstrated by the similarity of the Na^+(Tryp)Ar and Na^+(Tryp)(H_2O) spectra (Figure 3.5). The only significant new features in the Na^+(Tryp)(H_2O) spectrum are in the range of 3550-3750 cm^{-1} and are assigned to OH stretching vibrations. Since there are no changes in the CH stretching region (2800-3100 cm^{-1}), it is concluded that the hydrated cluster ions are composed from the same tryptamine conformers as the non-hydrated cluster ions – in other words, the Gph(in) and Gpy(in) conformers. A slight increase in intensity near 3310 cm^{-1} is observed in the Na^+(Tryp)(H_2O) spectrum, but this is a minor component of a feature that will be discussed shortly for the Na^+(Tryp)(H_2O)Ar spectra.

We have previously given a full analysis of the K^+(Tryp)(H_2O) spectrum in which isomers K1d and K1c from Figure 3.3 were able to account for all of the observed features,[30] and that same analysis can be applied to the Na^+(Tryp)(H_2O) spectrum. The prominent feature near 3500 cm^{-1} is assigned to the indole NH stretch from both isomers. The weaker features between 3550-3750 cm^{-1} can be assigned to a π-hydrogen bond from Na1c (~3585 cm^{-1}), a symmetric OH stretch from Na1d (~3655 cm^{-1}) and a combination of free OH and asymmetric OH stretches from Na1c and Na1d (~3710 cm^{-1}). Unfortunately, we have not been able to identify the Na1d isomer as a stable minimum on the Na^+(Tryp)(H_2O) potential energy surface. All attempts at optimizing this structure ultimately resulted in a rearrangement to structure Na1c, but this result is not entirely surprising. Geometry calculations take place at a temperature of 0 K, while the actual cluster temperature is estimated to be around 300 K. At higher temperatures, clusters with hydrogen bonds tend to be less favored because they have large entropic energy contributions. This has been demonstrated recently for both K^+(Tryp)(H_2O) and $Rb^+(H_2O)_n$ cluster ions.[30, 31]

As shown in Figure 3.4, the K1d isomer is predicted to be several (~2) kJ/mol higher in energy than the K1c isomer at 0 K, but becomes the favored isomer as the temperature increases. Similar behavior is expected for the Na1d and Na1c structures, which would allow both isomers to be present in this experiment.

$Na^+(Tryp)(H_2O)Ar$

The colder $Na^+(Tryp)(H_2O)Ar$ spectrum (Figure 3.5) contains many of the same features as the $Na^+(Tryp)(H_2O)$ spectrum, with several exceptions: a new, prominent feature has appeared near 3315 cm^{-1} as well as a large, broad band centered at ~2780 cm^{-1}. In the OH stretching region, a new feature near 3735 cm^{-1} also appeared, which is higher in frequency than any of the features observed in the $Na^+(Tryp)(H_2O)$ spectrum.

Before concentrating on the new features, it is helpful to first examine the features which have already been assigned in the warmer $Na^+(Tryp)(H_2O)$ spectrum. The indole NH stretch and the characteristic CH stretches from the $Na^+(Tryp)(H_2O)$ and $Na^+(Tryp)Ar$ spectra remain unchanged, indicating that the Gph(in) and Gpy(in) tryptamine conformers are still present in the $Na^+(Tryp)(H_2O)Ar$ cluster ions. All of the Na1x (x=a,b,c…) calculated isomers shown in Figure 3.3 contain the tryptamine molecule in one of these two configurations. The features near 3570 and 3710 cm^{-1} are much sharper and better resolved compared to the $Na^+(Tryp)(H_2O)$ spectrum, and thus easily assigned to the OH stretches in π-hydrogen bond and free vibrations. Isomer Na1c can account for all of the CH, NH and OH features listed here except for the two OH stretches near 3645 and 3735 cm^{-1}, which are addressed below.

The prominent new features in the $Na^+(Tryp)(H_2O)Ar$ spectrum are similar to the features near 3330 cm^{-1} and in the CH stretching region of the $K^+(Tryp)(H_2O)Ar$ spectrum. The feature

near 3330 cm^{-1} was assigned to isomer K1e which contains a hydrogen bond between the indole NH group and the water molecule.[30] With sodium as the cation, calculations for Na1e predict the NH-OH_2 hydrogen bonded NH stretch to appear at 3313 cm^{-1}, in good agreement with the experimental value of 3317 cm^{-1}. The symmetric and asymmetric water OH stretches calculated at 3647 and 3753 cm^{-1} are also quite close to the observed frequencies of 3646 and 3734 cm^{-1}. It should also be noted that the NH_2 symmetric and asymmetric stretches should still be present near 3300 and 3350 cm^{-1}, respectively, but they're obscured by the intense hydrogen-bonded NH feature from isomer Na1e. Isomer Na1e is calculated to be more than 30 kJ/mol higher in energy than the minimum-energy isomer (Na1c), so it can only be populated by a "trapping" mechanism during the cluster ion formation. A similar phenomenon was observed for K^+(Tryp)(H_2O)Ar: the isomer K1e was clearly present in the experimental spectrum even though it was predicted to be ~20 kJ/mol above the minimum-energy isomer.[30] In order for these high-energy isomers to be populated in the experiment, a rapid argon evaporation process must trap them following the impact of the cation into the neutral tryptamine/water/argon cluster.

The broad and intense feature overlapping with the CH stretches in the K^+(Tryp)(H_2O)Ar spectrum was assigned as a hydrogen-bonded OH stretch, resulting from the structures depicted as isomers K1a and K1b.[30] Both isomers contain a hydrogen bond between the water and the tryptamine amino group where the water acts as a proton donor while still interacting with the potassium cation. In the Na^+(Tryp)(H_2O)Ar spectrum, the stronger electrostatic interaction between the sodium cation and the water molecule further enhances this hydrogen bond and shifts the OH stretch to lower frequency, so the peak absorption is below the CH stretching region. In comparison to K^+, calculations with Na^+ predict a shift of about -120 cm^{-1}, placing the feature near 2830 cm^{-1} for isomer Na1a or 2860 cm^{-1} for isomer Na1b. The experimental feature

is centered near 2780 cm^{-1}, which is lower than calculations predict, but still within reasonable agreement. It has been suggested that a different, smaller local scaling factor may be appropriate for strongly hydrogen-bonded interactions,[32] which would further red-shift the calculated frequencies and lead to better agreement with the experiments, but a reliable value for this additional scaling factor is not yet available. In addition to the low-frequency feature, the Na1a and Na1b isomers would also contribute to the CH stretches between 2900-3100 cm^{-1}, the indole NH stretch near 3500 cm^{-1} and the free OH stretch near 3710 cm^{-1}.

The $Na^+(Tryp)(H_2O)Ar$ spectrum is assigned then to a combination of isomers Na1a, Na1b, Na1c and Na1e which are the same four isomers previously assigned to the $K^+(Tryp)(H_2O)Ar$ spectrum.[30] From Figure 3.4, the low-temperature energy ordering of the $K^+(Tryp)(H_2O)$ isomers is K1a<K1b<K1c. A similar analysis for $Na^+(Tryp)(H_2O)$ gives Na1c<Na1a<Na1b. While the energy ordering suggests a preference for isomers K1a and Na1c at low temperatures, there appears to be sufficient internal energy to produce all three of the lowest-energy isomers. Isomers K1e and Na1e are present too, but due to the trapping mechanism discussed earlier.

$M^+(Tryp)(H_2O)_2$

The spectrum of $Na^+(Tryp)(H_2O)_2$ (Figure 3.6) is virtually identical to that of $Na^+(Tryp)(H_2O)$ (Figure 3.5). Because of the similarities, it is straightforward to assign the experimental features. The CH stretching signature indicates that the tryptamine is still in a Gpy(in) or Gph(in) conformation. The remaining features can easily be assigned to the indole NH stretch near 3500 cm^{-1} and OH π-hydrogen bonding, symmetric and free/asymmetric stretches near 3580, 3640 and 3710 cm^{-1}, respectively. It is reasonable to assume that isomers

similar to Na1d and Na1c (the two isomers assigned to $Na^+(Tryp)(H_2O)$) are also present in this case since the spectral features are so similar. Among the seven isomers of $Na^+(Tryp)(H_2O)_2$ presented in Figure 3.3, isomer Na2c is most noteworthy, as a "combination" of both Na1c and Na1d. It contains a water molecule involved in a π-type hydrogen bond (as in isomer Na1c) and a water molecule interacting only with the sodium cation (as in isomer Na1d). The calculated spectrum of isomer Na2c, shown at the top of Figure 3.6, is almost an exact match to the experimental spectrum. Isomer Na2c is also calculated to be the lowest-energy isomer at all temperatures in the range from 0-400K, making this assignment clear-cut.

The $K^+(Tryp)(H_2O)_2$ spectrum (Figure 3.7, bottom) has the same four features in the NH and OH stretching regions as well as the same CH signature as the $Na^+(Tryp)(H_2O)_2$ spectrum. From 2800-3300 cm^{-1}, however, the spectrum contains an additional, very broad feature, similar to that observed in the CH stretching region of the $K^+(Tryp)(H_2O)Ar$ spectrum, due to a strongly-shifted, hydrogen-bonded OH stretch. Two of the major isomers assigned in that case (K1a and K1b) contained a water molecule "sandwiched" between the potassium cation and the amino group of the ethylamine side chain. Analogous structures in the two-water cluster are depicted in the two lowest-energy conformers: K2a and K2b. The hydrogen bond formed between the water and the amino group was predicted to result in a very strong red-shift of the OH group and a corresponding increase in intensity. In addition, they each contain a second water molecule which is allowed to interact freely with the potassium cation (similar to isomer K1d). This interaction is in good agreement with the symmetric and asymmetric spectral features in the OH stretching region near 3640 and 3710 cm^{-1}. While higher-energy conformers (K2e and K2f) could contribute, trapping such species requires the presence of argon, at least in our laboratory experience, and as seen below, such high-energy conformers are not needed in the spectral

assignment. Based on the $K^+(Tryp)(H_2O)$ and $Na^+(Tryp)(H_2O)_2$ spectra, the remaining feature near 3580 cm^{-1} can be assigned to an OH π-hydrogen bond, as in isomer K2c. To account for all of the features in the $K^+(Tryp)(H_2O)_2$ spectrum, a minimum of three isomers (K2a, K2b and K2c) must be used, and as shown in Figure 3.7, these three do an excellent job of reproducing the observed experimental spectrum. While twelve minima were detected in a geometry search, only the seven shown in Figure 3.3 have energies within 25 kJ/mol of the minimum-energy isomer, K2a. However, isomers K2d-K2g display hydrogen-bonding configurations which would exhibit bands near 3320 cm^{-1} (hydrogen-bonded indole NH) or 3425 cm^{-1} (water-water hydrogen bond). These are inconsistent with the observed spectral features, so they can be excluded from consideration for this experiment.

Both $M^+(Tryp)(H_2O)_2$ spectra have apparent contributions from an isomer containing one free water molecule and one π-hydrogen-bonded water molecule. For M=Na this was the energetically-preferred isomer and the only one assigned to the spectrum. For M=K, the energetics shifted, and this isomer is expected to be ~5 kJ/mol higher in energy than the K2a and K2b isomers near 300 K.

$M^+(Tryp)(H_2O)_2Ar$

The spectrum of $K^+(Tryp)(H_2O)_2Ar$ (Figure 3.8, bottom) is similar to that of $K^+(Tryp)(H_2O)_2$ with a few exceptions: the spectral features are generally narrower, reflecting a lower internal energy for the argonated species; a new doublet feature is present near 3325 and 3345 cm^{-1}; and the features in the CH and OH stretching regions are better resolved. All of the features identified for $K^+(Tryp)(H_2O)_2$ are still present in the $K^+(Tryp)(H_2O)_2Ar$ spectrum, which suggests that the same three isomers (K2a, K2b and K2c) are contributing along with additional

isomers to account for the new spectral features. The intense doublet near 3330 cm^{-1} in the $K^+(Tryp)(H_2O)_2Ar$ spectrum is similar to the feature in the $K^+(Tryp)(H_2O)Ar$ spectrum assigned to two conformers containing a hydrogen-bonded indole NH which acted as a proton donor to the water molecule. As shown in Figure 3.3, isomers K2e, K2f and K2g all contain this type of interaction. At low temperatures, these isomers are predicted to be ~15-18 kJ/mol higher in energy than the minimum-energy K2a isomer. With energy differences this large, these isomers would not generally be expected to contribute to the observed spectrum, but the observed doublet suggests that at least two of these isomers must be present.

Upon further inspection, isomers K2e and K2f are quite similar to the reported structure for $Tryp(H_2O)_2$.[17] This cluster contained a water bridge stretching from the indole NH group to the side-chain amino group. Although this bridge involved significant strain of the ethylamine side chain, it was proposed that the added stabilization of the water bridge was sufficient to populate that configuration. If one were to then imagine a potassium cation approaching the water bridge, it is easy to see how isomers K2e and K2f could form with K^+ inserting between the waters, preserving the indole NH hydrogen bond with one water and the OH hydrogen bond with the amine group. Isomer K2g would be a little more difficult to form because it would involve breaking two hydrogen bonds, but it can't be excluded spectroscopically. The low internal energy of the cluster ions (a result of the argon binding) would preclude rearrangement from the K2e and K2f isomers to the more energetically-favorable K2a and K2b isomers.

In order to account for the features in the $K^+(Tryp)(H_2O)_2Ar$ spectrum, a minimum of isomers K2a, K2b, K2c, K2e and K2f must be present in the molecular beam, with isomer K2g remaining a possibility as well. Of the seven isomers in Figure 3.3, only K2d can be excluded

definitively because it contains a water-water hydrogen bond that is calculated to appear spectroscopically as a strong feature near 3425 cm^{-1}.

The $Na^+(Tryp)(H_2O)_2Ar$ (Figure 3.9, bottom) features are based on those of $K^+(Tryp)(H_2O)_2Ar$. Above 3000 cm^{-1}, these two spectra are quite similar. The feature near 3330 cm^{-1}, now a singlet, comes from an indole NH which acts as a hydrogen bond donor to a water molecule, while the feature near 3510 cm^{-1} comes from a free indole NH stretching vibration. The higher-frequency features near 3560, 3650, 3715 and 3730 cm^{-1} come from OH π-hydrogen bonded, symmetric, free and asymmetric stretches, respectively. The CH stretching region contains the Gpy(in)/Gph(in) tryptamine signatures as well as a low-frequency OH hydrogen-bonded feature near 2860 cm^{-1} which is assigned to a water molecule "sandwiched" between the sodium ion and the side-chain amino group. This low-frequency feature has shifted ~80 cm^{-1} higher in frequency compared to the $Na^+(Tryp)(H_2O)_1Ar$ spectrum, which indicates a weaker water-ion interaction upon addition of the second water molecule.

Isomer Na2c, the isomer assigned to the $Na^+(Tryp)(H_2O)_2$ spectrum, can account for many of the features in the $Na^+(Tryp)(H_2O)_2Ar$ spectrum, with the exception of the peaks near 2860 and 3330 cm^{-1}. These remaining features could be attributed to the Na2e isomer, which contains both a "sandwiched" water molecule and one bound to the indole NH group. At low temperatures, this isomer is calculated to be almost 30 kJ/mol higher in energy than isomer Na2c, but is merely another example of the high-energy isomer trapping in argonated clusters that was noted earlier. Assigning the $Na^+(Tryp)(H_2O)_2Ar$ spectral features exclusively to isomers Na2c and Na2e is certainly the simplest approach, but it would be naïve to exclude other possible isomers from consideration. For example, isomer Na2a is virtually isoenergetic with Na2c, and with one free water molecule and one "sandwiched" water molecule, there are no

distinguishing features that would separate this isomer from the two already assigned to the $Na^+(Tryp)(H_2O)_2Ar$ spectrum. In truth, it is almost impossible to rule out any of the isomers shown in Figure 3.3, with the exception of isomer Na2d, which is expected to have a water-water hydrogen-bonded feature near 3390 cm^{-1}, a feature that is not present in the experimental spectrum. Although assignment of this spectrum to specific isomers may not be feasible, the dominant features and underlying intermolecular interactions, as noted in Na2c and Na2e, are quite clear.

The $M^+(Tryp)(H_2O)_2Ar$ assignments are an interesting mix of thermodynamically-preferred and trapped isomers. The sodium spectrum comes from at least one of each, while the additional splitting of features in the potassium spectrum suggests that several of each contribute to that experiment.

$M^+(Tryp)(H_2O)_3$

The $Na^+(Tryp)(H_2O)_3$ spectrum (Figure 3.10, bottom) contains many of the same features which have been assigned repeatedly for the smaller spectra. From high to low frequency, these include the OH free/asymmetric, symmetric and π-hydrogen-bonded stretches, the free indole NH stretch and the aliphatic CH stretches characteristic of the Gpy(in) and/or Gph(in) tryptamine conformers. The only new feature, near 3470 cm^{-1}, is a low-frequency shoulder to the free indole NH stretch. This feature is likely due to a hydrogen-bonded OH stretch, which in this spectral region has been associated with water-water hydrogen bonding in a number of $M^+(H_2O)_n$ systems.[27, 28, 31] Seven isomers of $Na^+(Tryp)(H_2O)_3$ are shown in Figure 3.3. Thermodynamically, isomers Na3a, Na3e and Na3f are expected to be the preferred isomers near 300K and have relative free energies within 3 kJ/mol of each other. Isomer Na3e contains one

water molecule involved in a π-hydrogen bond while a second water molecule and the tryptamine amino group act as proton donors to the third water molecule, which is in the second solvent shell. The calculated spectrum for this isomer (shown in Figure 3.10) has very good agreement with the experimental spectrum. Isomer Na3f has two water molecules acting as proton donors to secure the third water molecule in the second solvent shell. One of the first-shell water molecules is also involved in a π-hydrogen bond and has a vibrational feature calculated to be ~100 cm^{-1} higher in frequency and significantly more intense than the usual π-hydrogen bond. However, this feature is not observed in the experimental spectrum, making it unlikely for this isomer to be present. Isomer Na3a, with a predicted low-frequency, intense hydrogen-bonded OH stretch from a water "sandwiched" between the ion and the NH_2 group, can also be ruled out. The remaining $Na^+(Tryp)(H_2O)_3$ isomers shown in Figure 3.3 include either a "sandwiched" water molecule or a water molecule bound to the indole NH group, but the infrared features associated with these configurations are not present in the experimental spectrum. Thus, they can all be eliminated from consideration. That leaves isomer Na3e as the sole isomer that accurately reproduces the salient features in the $Na^+(Tryp)(H_2O)_3$ spectrum.

In the $K^+(Tryp)(H_2O)_3$ spectrum (Figure 3.11, bottom), however, there is a broad and intense band in the vicinity of the CH stretching region, which strongly suggests that an isomer containing a "sandwiched" water molecule contributes to this spectrum. The remaining features are similar to the $Na^+(Tryp)(H_2O)_3$ spectrum, although the low-frequency shoulder to the NH stretching feature is not as prominent.

Eight $K^+(Tryp)(H_2O)_3$ isomers are shown in Figure 3.3, and their calculated spectra are given in Figure 3.11. Immediately, isomers K3d and K3h can be eliminated from consideration because they each contain a hydrogen bond between the indole NH and a water molecule, but no

feature appears spectroscopically near 3330 cm^{-1} to correspond with this type of interaction. Isomer K3g is also not very likely because it contains an enhanced hydrogen bond that is predicted to be lower in frequency than any of the experimental features.

Of the isomers remaining, the "sandwiched" water molecule could come from K3a, K3b or K3c. Isomers K3a, K3b, K3e and K3f all contain some type of water-water hydrogen bond, predicted to appear somewhere between 3435-3480 cm^{-1} which would give rise to the low-frequency shoulder on the indole NH feature. This gives a total of five K3x isomers which could contribute to the $K^+(Tryp)(H_2O)_3$ spectrum. Thermodynamically, they are all calculated to be within 8 kJ/mol of the minimum-energy conformer (K3a) near 300 K, so it is possible for any (or all) of these conformers to contribute to the experimental spectrum. This is in sharp contrast to the $Na^+(Tryp)(H_2O)_3$ spectrum which could be assigned to a single isomer.

$M^+(Tryp)(H_2O)_3Ar$

The $Na^+(Tryp)(H_2O)_3Ar$ spectrum (Figure 3.12, top) is a bit more complicated than the $Na^+(Tryp)(H_2O)_3$ spectrum, but the features are still very similar to those already assigned for the smaller cluster ions, with two exceptions. First, there is now a high-frequency shoulder to the indole NH stretching vibration centered near 3530 cm^{-1}, most likely caused by some type of water-water hydrogen bonding. Second, there is a noticeable shift to higher frequency as well as a significant decrease in intensity of the hydrogen-bonded NH stretch compared to the other $Na^+(Tryp)(H_2O)_nAr$ spectra. This feature has progressed from ~3320 cm^{-1} to ~3330 cm^{-1} and now to ~3350 cm^{-1} as the argonated sodium cluster ions have grown in size from one to two to three water molecules. Since both the free NH and the hydrogen-bonded NH stretching features

are present in the spectrum, isomers with each of these configurations must be contributing to this experiment.

The $K^+(Tryp)(H_2O)_3Ar$ spectrum (Figure 3.12, bottom) has a number of notable changes compared to the other spectra. The symmetric OH stretching feature has disappeared, and a number of new features attributed to hydrogen bonds are present throughout the entire spectral range, but particularly between 3200-3600 cm^{-1}. There is also a very broad feature below the CH stretching region, with a maximum near 2800 cm^{-1}. This suggests that essentially all of the water molecules are involved as proton donors in various types of hydrogen bonds, either with themselves or with the tryptamine. Unfortunately, the sheer number of features in the spectrum makes assignments to particular isomers virtually impossible, and in this case, the computational studies were not particularly helpful. The ability to obtain conformer-specific spectra would be required to make definitive assignments for the isomers contributing to the $M^+(Tryp)(H_2O)_3Ar$ experiments.

K^+(Serotonin)Ar

One of the goals of the tryptamine project was to start with a relatively simple, biologically-relevant molecule and subsequently add functional groups. The IRPD spectra of tryptamine would be used as a guide in interpreting the spectra of more complicated molecules.

The structure of serotonin (5-hydroxytryptamine) differs from tryptamine only by the addition of a hydroxy group on the indole ring. The possible conformations are close analogues to those of tryptamine, but the hydroxy group has the possibility of orienting either *syn* or *anti* in relation to the indole NH, giving a total of 18 possible conformers. The structure of neutral serotonin has been studied experimentally and theoretically.[33-36] The observations from these

previous studies coupled with the analysis of the M^+(Tryptamine)$(H_2O)_n$ spectra would provide an excellent starting point for the examination of M^+(Serotonin) complexes.

The IRPD spectrum of K^+(Serotonin)Ar is shown in Figure 3.13. This spectrum can be compared to the K^+(Tryptamine)Ar spectrum shown in Figure 3.1. In addition to the CH and NH stretching features identified in the tryptamine spectrum, the K^+(Serotonin)Ar spectrum has a new feature centered near 3650 cm^{-1} which can be attributed to the OH stretching vibration of the hydroxy group. Additional spectra and supporting calculations are needed to provide a full analysis of the conformational behavior of serotonin in the presence of a potassium cation.

Conclusions

We have presented IRPD spectra of M^+(Tryp)$(H_2O)_{0-3}Ar_{0-1}$ (M=Na, K) and have examined the possible isomers for the cluster ions involved in each experiment. All of the spectra contained the CH "signature" of tryptamine in the Gph(in) or Gpy(in) configuration. This is in contrast to neutral Tryp$(H_2O)_n$ experiments which reported the Gpy(out) configuration for n=0 and n=1.[17, 21]

The M^+(Tryp)Ar, M^+(Tryp)(H_2O) and M^+(Tryp)(H_2O)Ar spectra were not particularly ion-dependent. The isomers assigned to the sodium spectra were all identical to those previously assigned to the potassium spectra.[30] Except for K^+(Tryp)Ar and K^+(Tryp)(H_2O), the potassiated cluster ions displayed evidence of "sandwiched" water molecules. In contrast, these water sandwiches were only observed for the sodiated cluster ions containing argon. The warmer Na^+(Tryp)$(H_2O)_{1-3}$ spectra were assigned to isomers containing mostly free or π-hydrogen-bonded water molecules.

For $K^+(Tryp)(H_2O)_{2,3,}$ the spectra were assigned to contributions from a greater number of isomers compared to the corresponding sodium-containing cluster ions. It appears that the stronger electrostatic interactions between sodium and water leads to a preference for one or two structural isomers in any given cluster ion. In contrast, the potassium-water electrostatic interactions are weaker and must compete with water-Tryp and water-water interactions of comparable strength, which leads to population of multiple low-energy isomers. These differences were reflected in the n=3 spectra, where extensive hydrogen bonding in the spectrum of $K^+(Tryp)(H_2O)_3Ar$ was more pervasive than for any other size and/or composition studied.

The argonated spectra reflected contributions from a combination of isomers, both thermodynamically favored and trapped during cluster ion formation. The low internal energy and low argon binding energy in these cluster ions prevented rearrangement to the thermodynamically-favored structures.

The results presented here can act as a baseline for the vibrational spectra of similar biomolecules. Molecules such as serotonin, which differs from tryptamine only in the addition of a single functional group, are inviting targets for future study.

Figures

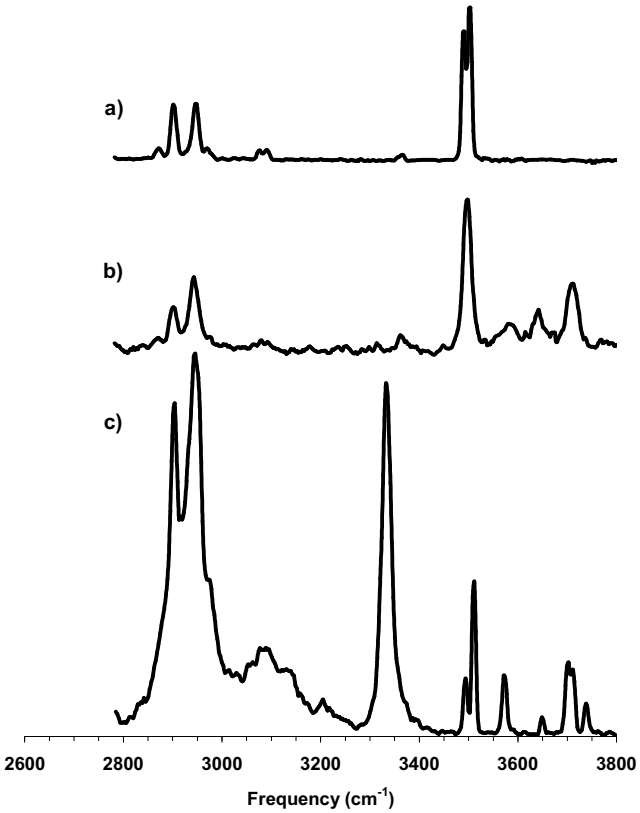

Figure 3.1: From top to bottom, IRPD spectra of a) K^+(Tryp)Ar, b) K^+(Tryp)(H_2O) and c) K^+(Tryp)(H_2O)Ar.

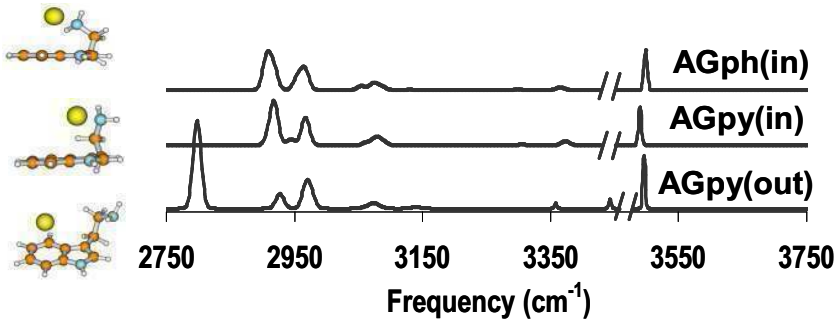

Figure 3.2: From top to bottom, calculated spectra and structures for the AGph(in), AGpy(in) and AGpy(out) isomers of K^+(Tryp).

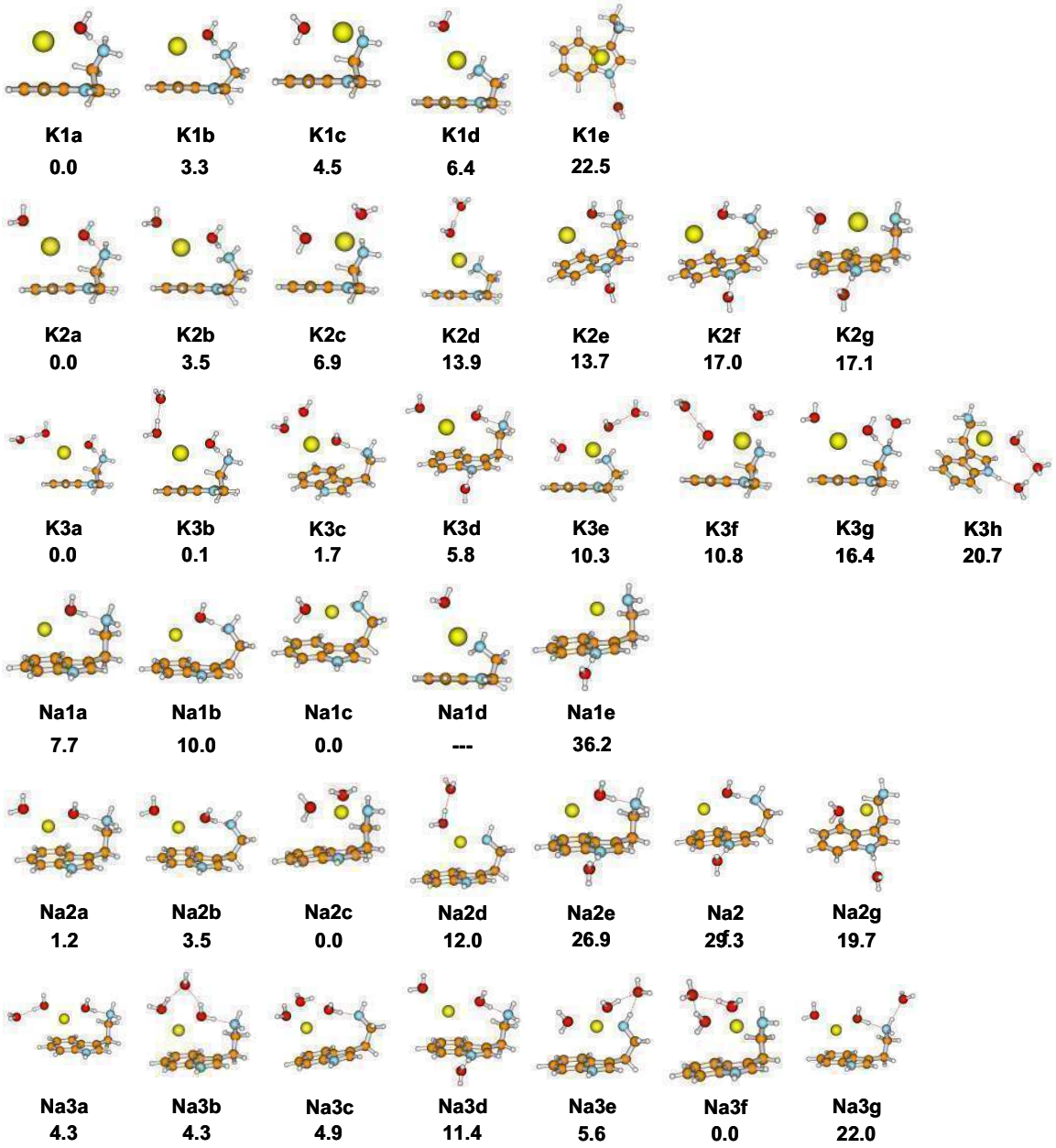

Figure 3.3: Calculated structures for $M^+(Tryp)(H_2O)_{1-3}$ (M=K, Na) cluster ions. Relative energies (kJ/mol), to the global minimum for each cluster size (corrected for zero-point energy), are given below each structure.

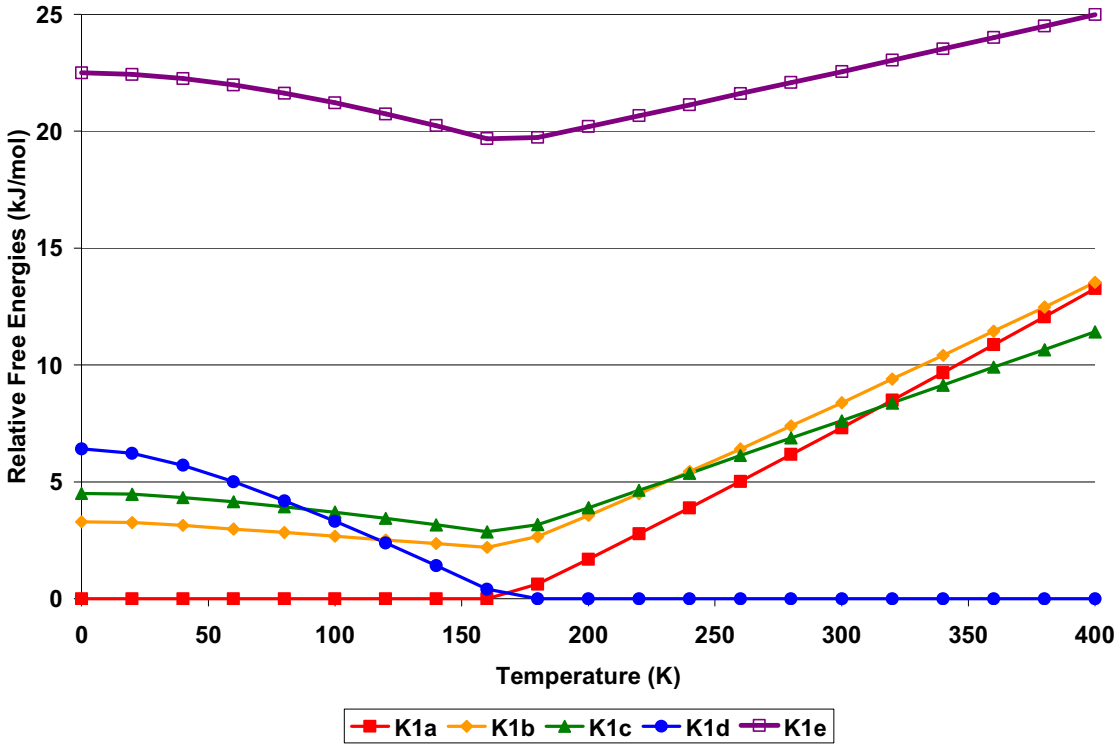

Figure 3.4: Plot of relative free energy as a function of temperature for the five structural isomers of $K^+(Tryp)(H_2O)$.

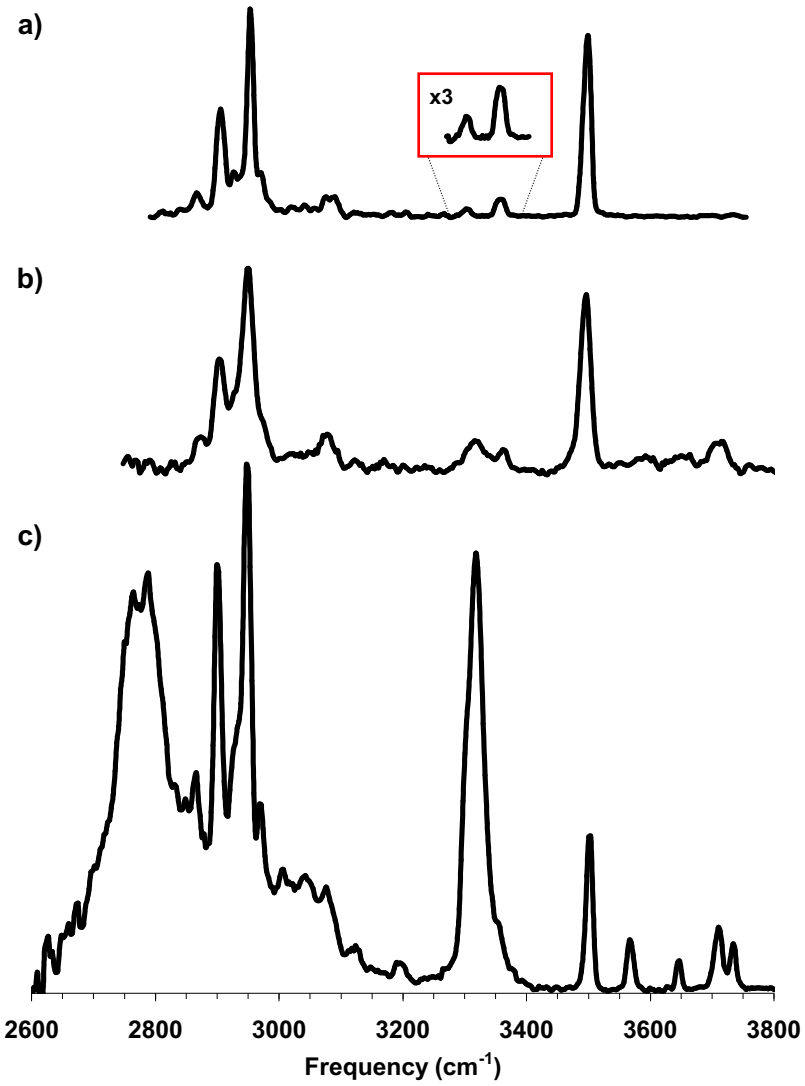

Figure 3.5: From top to bottom, IRPD spectra of a) Na^+(Tryp)Ar, b) Na^+(Tryp)(H_2O) and c) Na^+(Tryp)(H_2O)Ar. The amine NH stretching region is enlarged in the Na^+(Tryp)Ar spectrum for clarity.

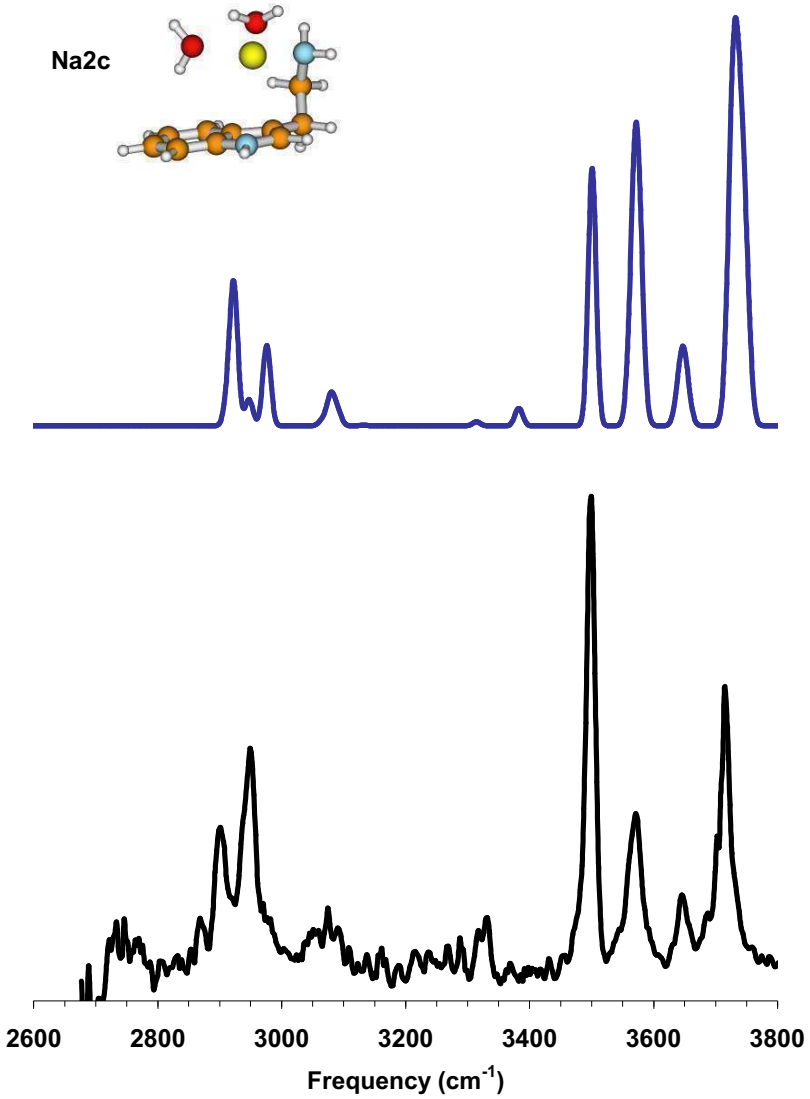

Figure 3.6: Calculated spectrum of isomer Na2c shown above the experimental $Na^+(Tryp)(H_2O)_2$ spectrum.

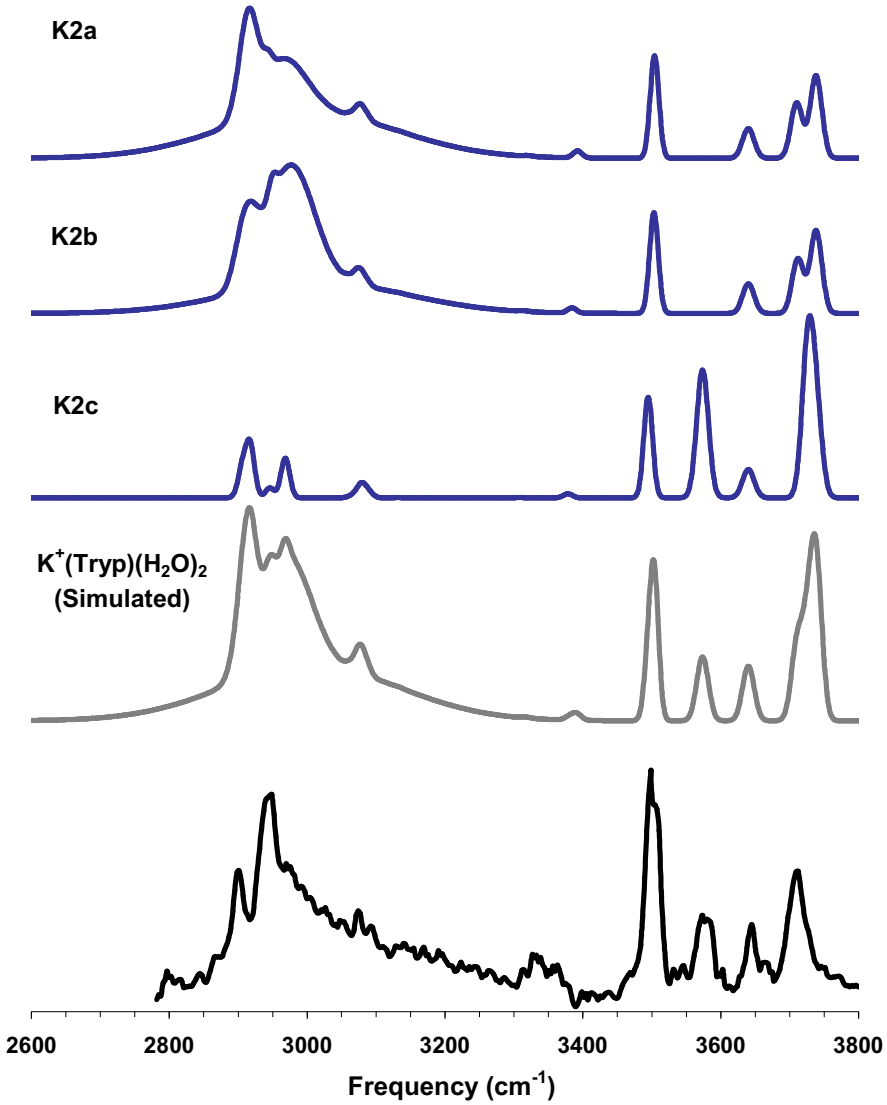

Figure 3.7: Calculated spectra of isomers K2a, K2b and K2c shown individually and then combined with a 1.6:1.1:1.0 weighting to form a simulated spectrum that corresponds with the $K^+(Tryp)(H_2O)_2$ experimental spectrum located at the bottom of the figure.

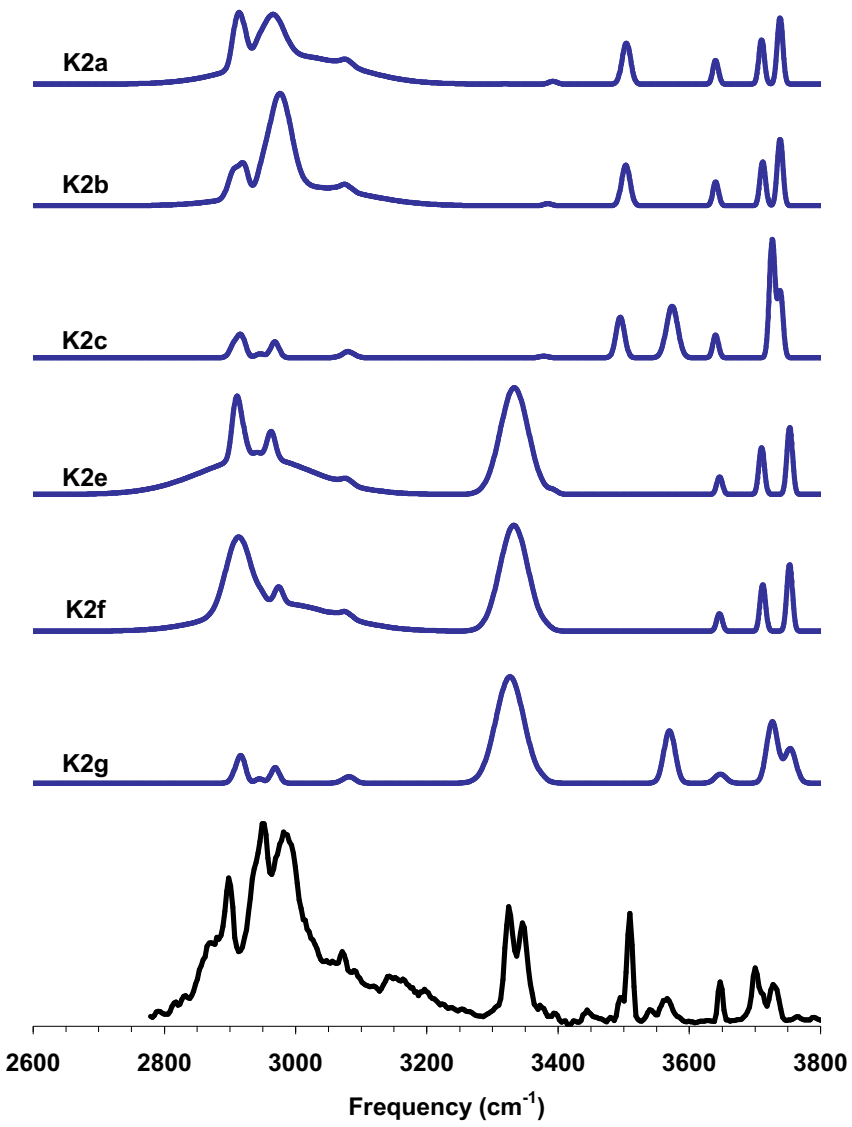

Figure 3.8: Calculated spectra of isomers K2a-K2c and K2e-K2g, with the $K^+(Tryp)(H_2O)_2Ar$ experimental spectrum located at the bottom of the figure.

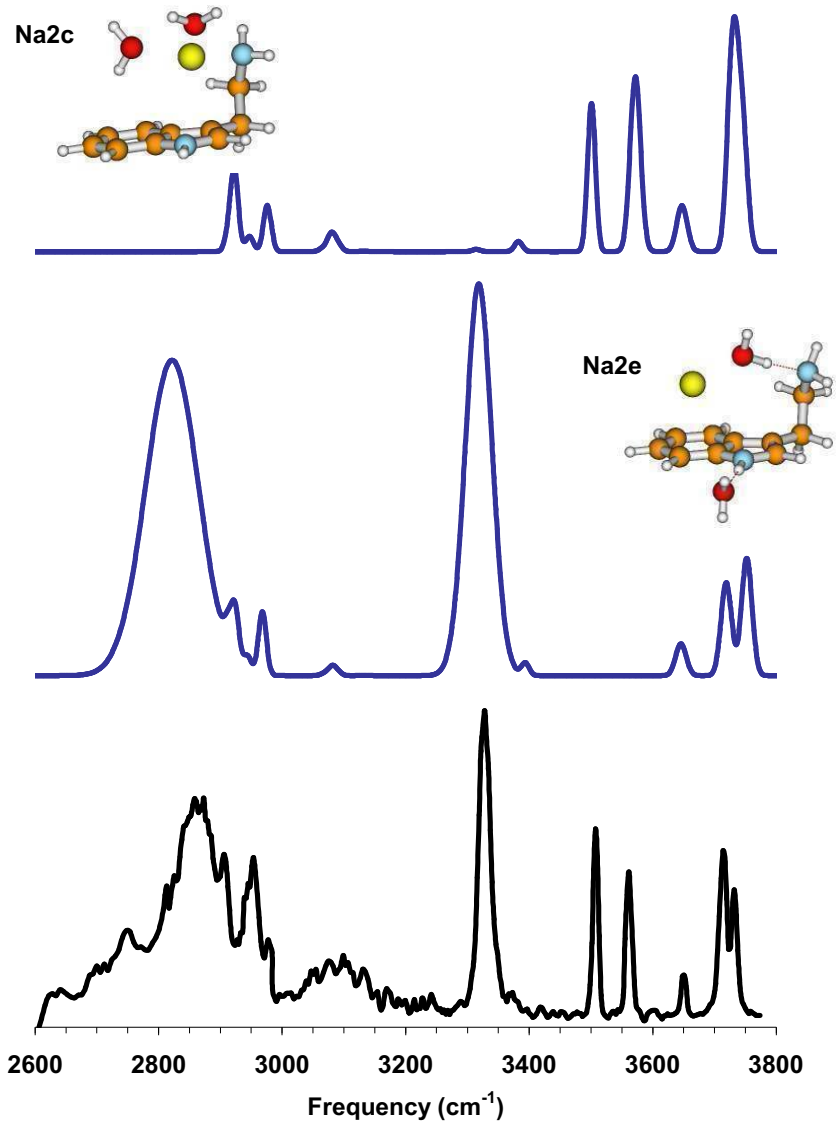

Figure 3.9: Calculated spectra of isomers Na2c and Na2e shown above the experimental $Na^+(Tryp)(H_2O)_2Ar$ spectrum.

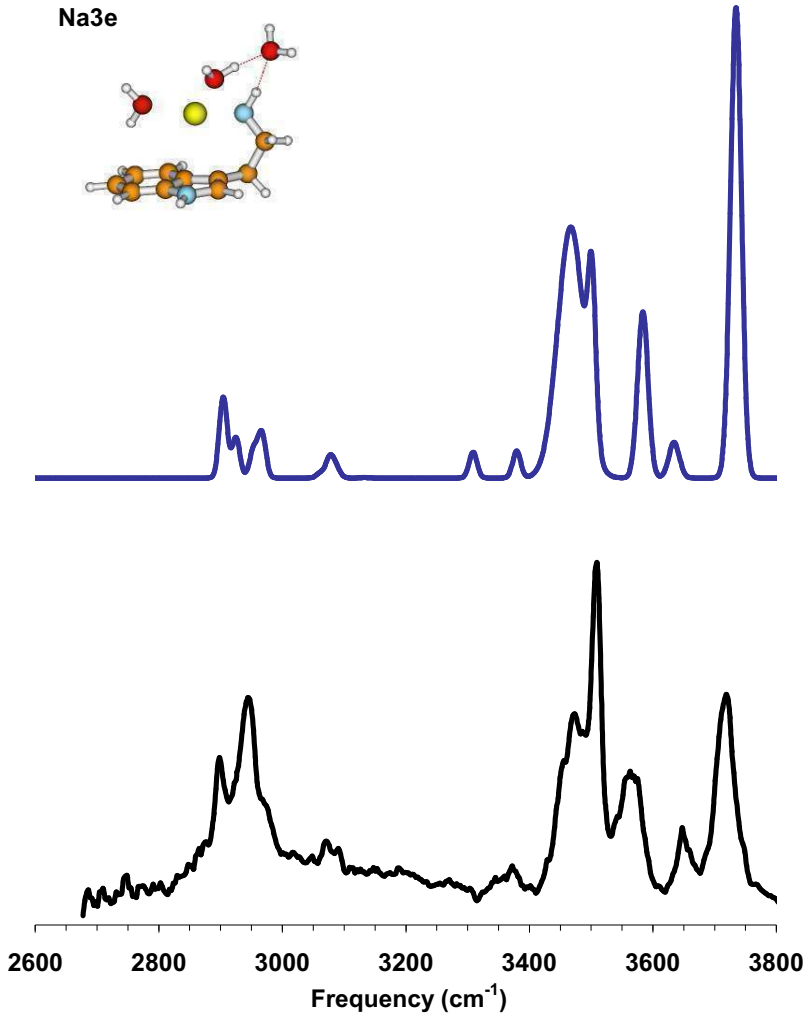

Figure 3.10: Calculated spectrum of isomer Na3e shown above the experimental $Na^+(Tryp)(H_2O)_3$ spectrum

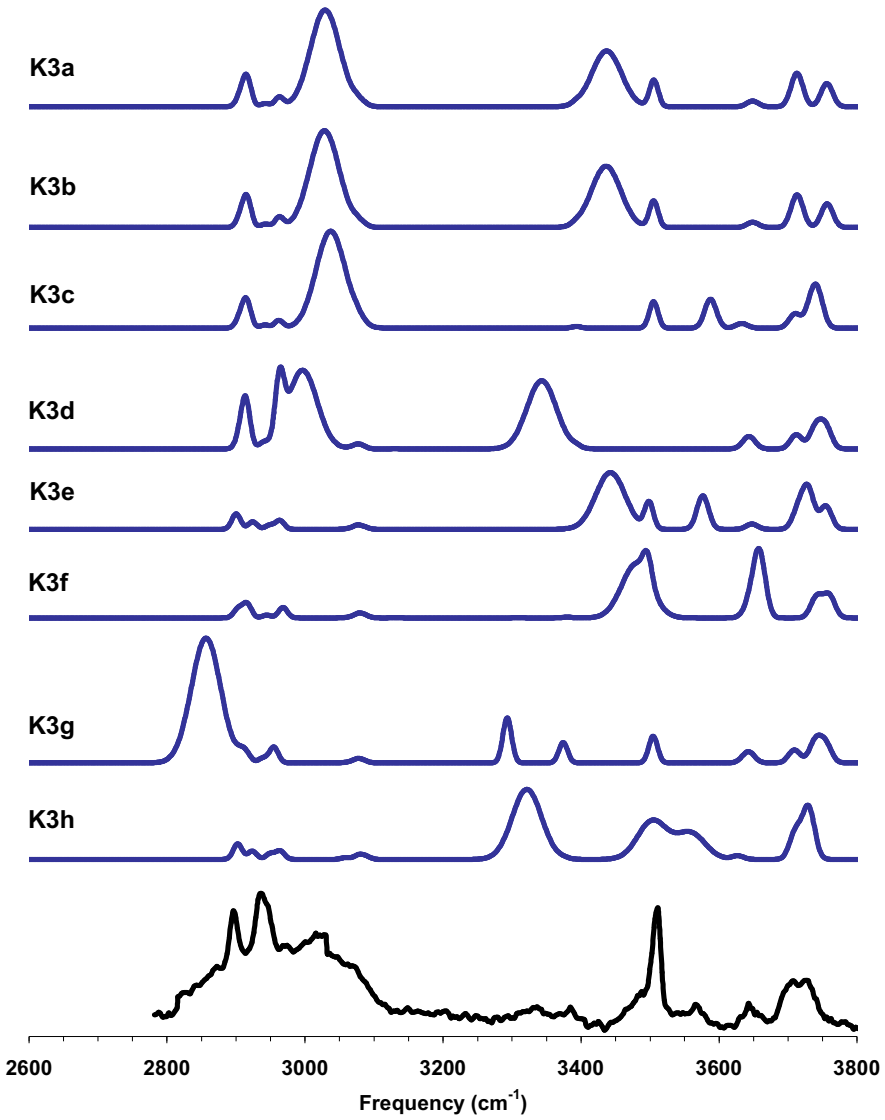

Figure 3.11: Calculated spectra of the eight $K^+(Tryp)(H_2O)_3$ isomers shown in Figure 1, with the $K^+(Tryp)(H_2O)_3$ experimental spectrum shown at the bottom of the figure.

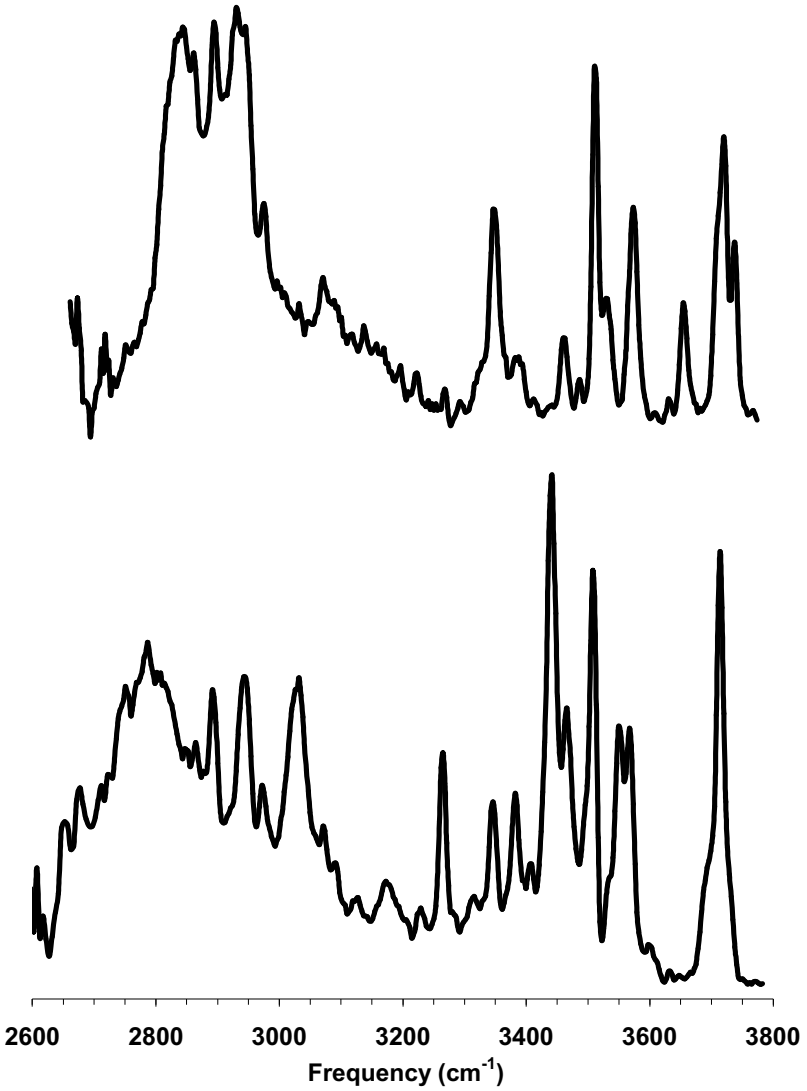

Figure 3.12: IRPD spectra of $Na^+(Tryp)(H_2O)_3Ar$ (top) and $K^+(Tryp)(H_2O)_3Ar$ (bottom).

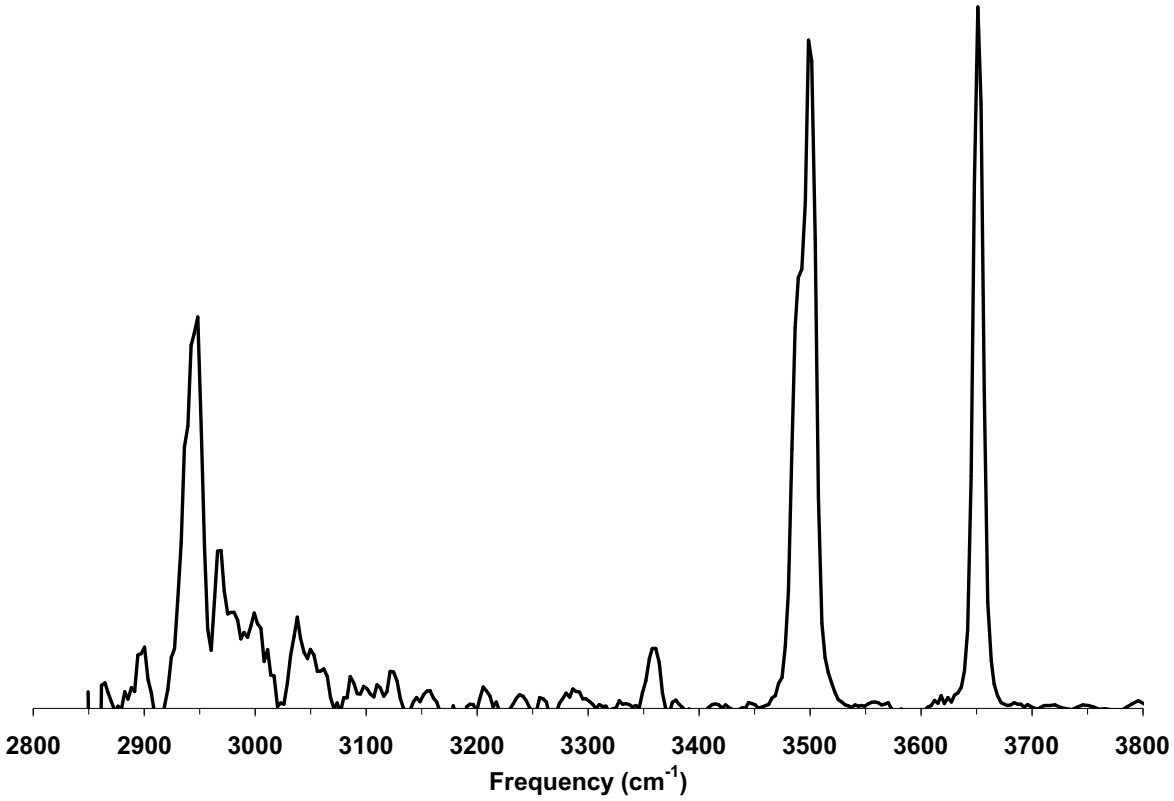

Figure 3.13: IRPD spectrum of K+(Serotonin)Ar

References

1. Von Helden, G.; Compagnon, I.; Blom, M. N.; Frankowski, M.; Erlekam, U.; Oomens, J.; Brauer, B.; Gerber, R. B.; Meijer, G., Phys. Chem. Chem. Phys. 2008, 10, (9), 1248.
2. Yongjun, H.; Da, X., Progress in Chemistry 2009, 21, (7-8), 1592.
3. Ebata, T.; Hashimoto, T.; Ito, T.; Inokuchi, Y.; Altunsu, F.; Brutschy, B.; Tarakeshwar, P., Phys. Chem. Chem. Phys. 2006, 8, (41), 4783.
4. Ebata, T., Bull. Chem. Soc. Jpn. 2009, 82, (2), 127.
5. Armentrout, P. B.; Rodgers, M. T.; Oomens, J.; Steill, J. D., J. Phys. Chem. A 2008, 112, (11), 2248.
6. Rodgers, M. T.; Armentrout, P. B.; Oomens, J.; Steill, J. D., J. Phys. Chem. A 2008, 112, (11), 2258.
7. Bush, M. F.; Oomens, J.; Saykally, R. J.; Williams, E. R., J. Phys. Chem. A 2008, 112, (37), 8578-8584.
8. Bush, M. F.; Forbes, M. W.; Jockusch, R. A.; Oomens, J.; Polfer, N. C.; Saykally, R. J.; Williams, E. R., J. Phys. Chem. A 2007, 111, (32), 7753-7760.
9. Remko, M.; Fitz, D.; Rode, B. M., J. Phys. Chem. A 2008, 112, (33), 7652.
10. Kamariotis, A.; Boyarkin, O. V.; Mercier, S. R.; Beck, R. D.; Bush, M. F.; Williams, E. R.; Rizzo, T. R., J. Am. Chem. Soc. 2006, 128, (3), 905-916.
11. Mousseau, D. D.; Butterworth, R. F., J. Neurochem. 1994, 63, (3), 1052-1059.
12. Park, Y. D.; Rizzo, T. R.; Peteanu, L. A.; Levy, D. H., J. Chem. Phys. 1986, 84, (12), 6539.
13. Philips, L. A.; Levy, D. H., J. Phys. Chem. 1986, 90, (21), 4921.
14. Philips, L. A.; Levy, D. H., J. Chem. Phys. 1988, 89, (1), 85-90.
15. Nguyen, T. V.; Korter, T. M.; Pratt, D. W., Mol. Phys. 2005, 103, (11), 1603 - 1613.
16. Carney, J. R.; Zwier, T. S., J. Phys. Chem. A 2000, 104, (38), 8677-8688.
17. Zwier, T. S., J. Phys. Chem. A 2001, 105, (39), 8827-8839.
18. Dian, B. C.; Clarkson, J. R.; Zwier, T. S., Science 2004, 303, (5661), 1169-1173.
19. Clarkson, J. R.; Herbert, J. M.; Zwier, T. S., J. Chem. Phys. 2007, 126, (13), 134306.
20. Peteanu, L. A.; Levy, D. H., J. Phys. Chem. 1988, 92, (23), 6554-6561.
21. Schmitt, M.; Bohm, M.; Ratzer, C.; Vu, C.; Kalkman, I.; Meerts, W. L., J. Am. Chem. Soc. 2005, 127, (29), 10356-10364.
22. Sipior, J.; Sulkes, M., J. Chem. Phys. 1988, 88, (10), 6146.
23. Carney, J. R.; Dian, B. C.; Florio, G. M.; Zwier, T. S., J. Am. Chem. Soc. 2001, 123, (23), 5596.
24. Fraley, P. E.; Narahari Rao, K., J. Mol. Spectrosc. 1969, 29, (1-3), 348.
25. Vaden, T. D.; Weinheimer, C. J.; Lisy, J. M., J. Chem. Phys. 2004, 121, (7), 3102.
26. Miller, D. J.; Lisy, J. M., J. Chem. Phys. 2006, 124, (18), 184301.
27. Miller, D. J.; Lisy, J. M., J. Am. Chem. Soc. 2008, 130, (46), 15381-15392.
28. Miller, D. J.; Lisy, J. M., J. Am. Chem. Soc. 2008, 130, (46), 15393-15404.
29. Rodriguez, J. D.; Lisy, J. M., Int. J. Mass Spectrom. 2009, 283, (1-3), 135-139.
30. Nicely, A. L.; Miller, D. J.; Lisy, J. M., J. Am. Chem. Soc. 2009, 131, (18), 6314.
31. Nicely, A. L.; Miller, D. J.; Lisy, J. M., J. Mol. Spectrosc. 2009, 257, (2), 157.
32. Bouteiller, Y.; Gillet, J.-C.; Grégoire, G.; Schermann, J. P., J. Phys. Chem. A 2008, 112, (46), 11656.
33. LeGreve, T. A.; James, W. H.; Zwier, T. S., J. Phys. Chem. A 2009, 113, (2), 399.

34. LeGreve, T. A.; Clarkson, J. R.; Zwier, T. S., J. Phys. Chem. A 2008, 112, (17), 3911.
35. LeGreve, T. A.; Baquero, E. E.; Zwier, T. S., J. Am. Chem. Soc. 2007, 129, (13), 4028.
36. Bayari, S.; Saglam, S.; Ustundag, H. F., J. Mol. Struct. THEOCHEM 2005, 726, (1-3), 225.

Chapter 4: Hydrated M^+(2-amino-1-phenyl ethanol) Cluster Ions

Introduction

The molecule 2-amino-1-phenyl ethanol (APE) serves as a building block for neurotransmitters such as ephedrine and adrenaline. Spectroscopic and theoretical studies of APE, protonated APE and hydrated APE have been reported in the literature,[1-6] but no group has studied the effects of a cation such as sodium or potassium, two monovalent ions abundant in biological systems. Electrostatic interactions compete with other noncovalent interactions (water-water and APE-water) to direct the structures of hydrated APE cluster ions. It is understood that the structure and function of biomolecules are linked, so an accurate understanding of the structure of APE in different environments is a crucial first step in understanding the function of APE and other related neurotransmitters.

The first spectroscopic study of bare and singly-hydrated APE was performed by Simons and coworkers using UV-UV holeburning and IR-UV ion dip spectroscopy.[2] Two stable isomers of APE were identified, with each containing an intramolecular hydrogen bond in which the OH group acts as a proton donor to the nitrogen. The two structures, shown in Figure 4.1, differed in the orientation (either anti or gauche) of the C-C-C-N chain, and the anti configuration (named AG_1) was assigned as the experimentally-preferred conformer by a ratio of almost 3:1.[2] Torsional path integral Monte Carlo (TPIMC) simulations support the preference for the AG_1 structure.[5]

$APE(H_2O)_n$ structures can be classified as "addition" or "insertion" depending on whether the water molecule acts as a proton donor to the alcohol group (leaving the intramolecular hydrogen bond intact) or inserts into the intramolecular hydrogen bond. The

preferred APE(H_2O) configuration is the latter, which creates an OH···OH···NH chain.[2, 3] Addition of a second and third water molecule result in similar structures in which a chain of water molecules is inserted into the APE intramolecular hydrogen bond.[3] This creates a 4- or 5-member chain in which each oxygen and nitrogen acts as both a single donor and single acceptor.

When a cation is present, the possible configurations are expanded beyond the simple "addition" or "insertion" classification. The cation can interrupt the intramolecular hydrogen bond or be positioned over the phenyl ring, leaving the hydrogen bond intact. The water molecules then have the opportunity to interact with the cation or the APE molecule, creating many possibilities for the $M^+(APE)(H_2O)_n$ structures. Figure 4.2 shows the structures of the low-energy $Na^+(APE)(H_2O)_n$ and $K^+(APE)(H_2O)_n$ cluster ions identified during a geometry search.

The infrared photodissociation (IRPD) spectra of $Na^+(APE)(H_2O)_{0\text{-}3}Ar_{0,1}$ and $K^+(APE)(H_2O)_{0\text{-}3}Ar_{0,1}$ are presented here along with density functional theory (DFT) calculations which were used to aid the interpretation of the spectra. The spectra generated with and without the use of argon tagging are compared to study the influence of internal energy on the observed cluster ion structures.

Results and Discussion

$M^+(APE)Ar$

The Na^+(APE)Ar spectrum (Figure 4.3, top) is fairly simple, but yet very different from the spectrum of the APE monomer.[2, 3] In the previously-reported APE spectra, the strongest feature (attributed to the APE intramolecular hydrogen bond) appeared near 3530 cm^{-1}, while the most prominent feature in the Na^+(APE)Ar spectrum appears near 3225 cm^{-1}. The features

below 3150 cm^{-1} are typically assigned to CH stretching vibrations. Specifically, the region from 3000-3150 cm^{-1} is attributed to aromatic CH stretches, and the region from 2850-3000 cm^{-1} is attributed to aliphatic CH stretches from the APE molecule. It is difficult to compare the features in this spectral region based on DFT-predicted frequencies, so the focus will be instead on the higher-frequency portion of the spectrum. In addition to the CH stretches, the Na^+(APE)Ar cluster ion should have one OH stretching vibration and two NH stretching vibrations. Depending on the orientation of the APE molecule, the OH group could either be free or involved in an intramolecular hydrogen bond with the amino group. A free OH group would produce a feature between 3650-3680 cm^{-1}, which is clearly inconsistent with the observed spectrum. Instead, the strong feature near 3225 cm^{-1} must come from a hydrogen-bonded OH stretch in which the OH group acts as a proton donor to the amino group (as observed for the APE monomer). The remaining features near 3365 and 3435 cm^{-1} are assigned to the symmetric and asymmetric stretches of the terminal amino group, respectively. Several calculated Na^+(APE) spectra are shown in Figure 4.4, and the one associated with isomer Na0c clearly has the best agreement with the experimental spectrum. This isomer is essentially the same as the AG_1 isomer previously assigned to the bare APE molecule (with the Na^+ interacting with the phenyl ring and the oxygen lone pairs),[2, 3] but the hydrogen-bonded feature in this case appears almost 300 cm^{-1} lower in frequency because the sodium cation enhances the intramolecular hydrogen bond.

Isomer Na0c has the best agreement with the experimental spectrum, but it was not predicted to be the preferred isomer for Na^+(APE). Based on our calculations, isomer Na0a (which has the sodium ion positioned between the OH and NH_2 groups) is almost 20 kJ/mol lower in energy. The higher-energy isomer must be trapped during cluster ion formation. When

the cations impact the neutral APE$(Ar)_n$ clusters, the argon atoms evaporate quickly, removing internal energy from the cluster ions. In this case, the cluster ions do not have sufficient energy to overcome the barrier to reach the energetically-favorable conformation. We have recently reported similar trapping mechanisms for a variety of systems.[7-9]

The K^+(APE)Ar spectrum (Figure 4.3, bottom) is virtually identical to the Na^+(APE)Ar spectrum, which makes the assignment very straightforward. Again, the isomer with the cation interrupting the intramolecular hydrogen bond (K0a) is the energetically-preferred isomer, but the isomer which leaves the hydrogen bond intact (K0b) has the best agreement with the experimental spectrum. Interestingly, there is not a strong energetic preference (Figure 4.2) for isomer K0a compared to K0b as there was for Na0a compared to Na0c.

Since the potassium ion has a weaker electrostatic interaction with the APE molecule than the sodium cation, the spectral feature assigned to the intramolecular hydrogen bond is closer to that of the bare molecule. Calculations predict this feature to appear near 3325 cm^{-1} for K^+(APE), compared to ~3290 cm^{-1} for Na^+(APE). The actual features are centered near 3290 (K^+) and 3225 cm^{-1} (Na^+), so the calculations are not quite able to reproduce the magnitude of the frequency shifts associated with the enhanced intramolecular hydrogen bonds.

The CH stretching regions of both M^+(APE)Ar spectra are very consistent. This supports the conclusion that the same APE conformation is present in both spectra.

$M^+(APE)(H_2O)Ar$

When a single water molecule is added to the M^+(APE)Ar cluster ions, the only new features in the spectra (Figure 4.5) appear near 3585 and 3710 cm^{-1} for both Na^+(APE)(H_2O)Ar and K^+(APE)(H_2O)Ar (with the new features in the sodium spectrum appearing ~5 cm^{-1} higher in

frequency compared to the potassium spectrum). This simplicity in the OH stretching region suggests that only one isomer is present in each of these experiments. A gas-phase water molecule exhibits symmetric and asymmetric vibrational stretches at 3657 and 3756 cm^{-1}, respectively.[10] In the presence of a cation such as sodium or potassium, these stretches are expected to be red-shifted slightly.[9, 11-13] For the $M^+(APE)(H_2O)Ar$ cluster ions, calculations predict the symmetric and asymmetric stretches to be located near 3640 and 3730 cm^{-1}, respectively, for a "free" water molecule. In this case, a free water molecule is one which interacts with the cation but not the APE molecule, such as in isomers Na1a, Na1b, Na1d, K1a and K1b. These would not be good assignments, however, for the $M^+(APE)(H_2O)Ar$ spectra since the lower-frequency OH stretch appears significantly below 3640 cm^{-1}. Instead, isomers Na1c and K1c are in much better agreement. These isomers contain a π-hydrogen bond between the water molecule and the APE phenyl ring, with a predicted vibrational frequency close to 3600 cm^{-1}.

Thermodynamically, the energies of isomers K1a, K1b and K1c are within 2 kJ/mol, so any of the three isomers could potentially contribute to the experimental spectrum; however, there is clearly a preference for isomer K1c to be populated. Isomer Na1c is almost 20 kJ/mol higher in energy than the minimum-energy sodium structure (Na1a), so once again, this isomer must be trapped during the cluster ion formation process.

$M^+(APE)(H_2O)$

When the cluster ions are stabilized via evaporation of water rather than evaporation of argon, the resulting cluster ions contain a greater amount of internal energy, which can be used to overcome barriers to isomerization. As a result, the infrared spectra of the "warmer" species can

be significantly different than those of the "colder" species. The spectra of $Na^+(APE)(H_2O)$ and $K^+(APE)(H_2O)$ are no exception. As shown in Figure 4.6, these spectra are lacking the intense features attributed to the APE intramolecular hydrogen bond and have much different features in the OH stretching region compared to the $M^+(APE)(H_2O)Ar$ spectra.

The $Na^+(APE)(H_2O)$ spectrum has one intense feature near 3640 cm^{-1} and a progression of weaker features that span from 3600-3850 cm^{-1}. These weaker features are a signature of a water molecule which is allowed to freely rotate within a cluster ion.[14] This can only occur for water molecules that are not acting as hydrogen bond donors. In other words, the water molecule for this cluster ion cannot be participating in a π-hydrogen bond, which was the configuration assigned to the $Na^+(APE)(H_2O)Ar$ cluster ions. Instead, a configuration like Na1a or Na1b should be considered since both of these involve a free water molecule. The feature attributed to the APE intramolecular hydrogen bond is not present in this spectrum, so isomer Na1b can be eliminated from consideration, leaving only isomer Na1a. The free OH vibrational stretch from the APE molecule is predicted to occur near 3650 cm^{-1} in isomer Na1a, which overlaps spectroscopically with the symmetric stretch of the free water molecule.

The $K^+(APE)(H_2O)$ spectrum resembles the $Na^+(APE)(H_2O)$ spectrum, but with additional features in the range of 3200-3400 cm^{-1}. This is the region associated with features from the APE intramolecular hydrogen bond, but the features in this spectrum are not nearly as intense as those in the $K^+(APE)Ar$ or $K^+(APE)(H_2O)Ar$ spectra. Most likely, an isomer with the intramolecular hydrogen bond is present in this experiment, but as a minor contributor. Four isomers of $K^+(APE)(H_2O)$ are shown in Figure 4.2. Isomers K1a and K1b each contain a free water molecule which would contribute to the spectral features located above 3600 cm^{-1}. Isomer K1a has the ion positioned between the lone pairs of the APE oxygen and nitrogen (which breaks

the intramolecular hydrogen bond), while isomer K1b preserves the intramolecular hydrogen bond and has the ion positioned above the APE phenyl ring. Near 300 K, these isomers are predicted to be within ~2 kJ/mol of energy, so it is probable for both of them to be present in the molecular beam. There is one small feature near 3590 cm^{-1}, however, that cannot be attributed to either of these isomers. This feature appears in the region associated with π-hydrogen-bonding, as seen in the $K^+(APE)(H_2O)Ar$ spectrum. Isomer K1c has this type of interaction but is calculated to be almost 12 kJ/mol higher in energy than isomer K1a near 300K. Overall, this suggests that isomer K1a is likely the major contributor to the experimental spectrum, isomer K1b is a minor contributor, and isomer K1c is a very minor contributor.

$M^+(APE)(H_2O)_2Ar$

There are three major differences in the $Na^+(APE)(H_2O)_2Ar$ spectrum (Figure 4.7) compared to that of $Na^+(APE)(H_2O)Ar$. First, the feature attributed to the APE intramolecular hydrogen bond has moved up in frequency from ~3225 to ~3260 cm^{-1}. Second, a new feature has appeared near 3650 cm^{-1}, which is the region associated with either the APE free OH stretch or a water symmetric stretch. Finally, a high-frequency shoulder has appeared near 3730 cm^{-1} on the water free OH stretching feature. It is important to recognize, however, that no features from the $Na^+(APE)(H_2O)Ar$ spectrum have disappeared, and that the CH stretching region appears virtually unchanged. This suggests that the second water molecule fits into the cluster in such a way so that it does not disturb the $Na^+(APE)(H_2O)Ar$ configuration. Isomer Na1c was characterized by a π-hydrogen bond and an APE intramolecular hydrogen bond. Of the seven isomers shown in Figure 4.2, only Na2c has both of these characteristics. The second water molecule in this isomer is a free water and interacts only with the sodium ion, causing no

disturbance to the APE configuration. The predicted frequencies for the symmetric and asymmetric OH stretching features of the free water molecule are 3646 and 3741 cm^{-1}, respectively, in good agreement with the two new features in the $Na^+(APE)(H_2O)_2Ar$ spectrum. While the assignment of isomer Na2c is sufficient to explain all of the spectral features, it is still possible for additional isomers to contribute as well. Isomer Na2a (with two free water molecules and no intramolecular hydrogen bond) is the minimum-energy structure (~10 kJ/mol below Na2c) identified in our geometry search. All of the features in the calculated spectrum of this isomer overlap with features in the Na2c calculated spectrum, so it cannot be definitively excluded from consideration.

The $K^+(APE)(H_2O)_2Ar$ spectrum (Figure 4.8) contains quite a few features which were not present in the $K^+(APE)(H_2O)Ar$ spectrum, including high- and low-frequency shoulders on the free water OH stretching feature, two new features near 3630 and 3645 cm^{-1} and a variety of features across the entire range from 3025-3550 cm^{-1}. This spectral congestion makes it difficult to assign specific isomers to the $K^+(APE)(H_2O)_2Ar$ cluster ions. It is clear, however, that multiple isomers must be contributing to this experimental spectrum, and that significant hydrogen bonding has taken place.

Near 100K, isomers K2b, K2c and K2d are calculated to be within 6 kJ/mol of the minimum-energy isomer, K2a. In contrast, no sodium-containing isomers are within 6 kJ/mol of isomer Na2a. This corresponds well with the observation that more isomers were contributing to the potassium spectrum than the sodium spectrum.

$M^+(APE)(H_2O)_2$

The $Na^+(APE)(H_2O)_2$ spectrum (Figure 4.7) has considerably fewer features compared to the $Na^+(APE)(H_2O)_2Ar$ spectrum and is in fact virtually identical to the $Na^+(APE)(H_2O)$ spectrum. The only significant difference is a more defined feature near 3720 cm^{-1} instead of the broad feature in this region of the $Na^+(APE)(H_2O)$ spectrum. The $Na^+(APE)(H_2O)$ cluster ions were assigned to structure Na1a, which contained a single free water molecule. Since the spectral features are so similar for the $Na^+(APE)(H_2O)_2$ spectrum, it is highly probable that these cluster ions contain two free water molecules, as shown in isomer Na2a. In this scenario, the feature near 3720 cm^{-1} is assigned to water asymmetric stretches, the feature near 3645 cm^{-1} to symmetric water stretches, the feature near 3375 cm^{-1} to the NH_2 asymmetric stretch, and the features in the range 2900-3150 cm^{-1} are assigned to CH stretches. All of the other $Na^+(APE)(H_2O)_2$ structures shown in Figure 4.2 contain some form of hydrogen bonding (water-water or intramolecular APE), which is inconsistent with the reported spectrum.

Although considerably simpler than the $K^+(APE)(H_2O)_2Ar$ spectrum, the $K^+(APE)(H_2O)_2$ spectrum (Figure 4.8) still has quite a few features. Unlike the $Na^+(APE)(H_2O)_2$ spectrum, it must have more than one contributing isomer. Fortunately, the spectral features are similar to those in the $K^+(APE)(H_2O)$ spectrum. The features in the OH stretching region come from a combination of free/asymmetric (~3715 cm^{-1}), symmetric (~3645 cm^{-1}) and π-hydrogen-bonded (~3590 cm^{-1}) stretches. The features in the middle of the spectrum come from the asymmetric and symmetric NH_2 stretches as well as the intramolecular APE hydrogen bond. Isomers K2b and K2a contain all of these interactions. Isomer K2b (with two free water molecules) is the minimum-energy isomer near 300K, while isomer K2a (with one free water molecule and one involved in a π-hydrogen-bond) is only about 3 kJ/mol higher in energy.

The ion dependence of the n=2 spectra is quite striking. For both the warm and cold spectra, the potassium version is significantly more complex than the sodium version. The cold potassium spectrum was so complex that it couldn't even be assigned to specific isomers. The $K^+(APE)(H_2O)_2$ spectrum appears to come from a combination of isomers with both free and π-hydrogen-bonded water molecules. In addition, contributions from isomers with (K2a) and without (K2b) the intramolecular APE hydrogen bond were detected. There does not appear to be a strong preference for the position of the K^+, while the preferred location for the Na^+ is the four-coordinated position that interrupts the APE intramolecular hydrogen bond.

$M^+(APE)(H_2O)_3Ar$

The progression from $Na^+(APE)(H_2O)Ar$ to $Na^+(APE)(H_2O)_2Ar$ involved only minor spectral changes, but the addition of a third water molecule to the cluster ion created a dramatic change in the observed features, as shown in Figure 4.9. The features associated with a free water molecule and a π-hydrogen-bonded water molecule are still present near 3730, 3720, 3650 and 3585 cm^{-1}, but new features have popped up in the OH stretching region near 3700, 3540, 3495 and 3455 cm^{-1}. There appear to be smaller features which are also present in this region that are not fully resolved, particularly near 3565 and 3510 cm^{-1}. The features between 3450-3600 cm^{-1} are indicative of water-water hydrogen bonding.[9, 12] With so many OH stretching features present, there must be several isomers contributing to this spectrum. The minimum-energy isomer, Na3a, contains a "bent" hydrogen bond in which two water molecules in the first solvent shell act as single donors to secure a water molecule in the second solvent shell. This isomer is calculated to exhibit strong features near 3549 and 3520 cm^{-1}. Of the five isomers shown in Figure 4.2, only Na3a is thermodynamically expected to contribute to this experiment.

The remaining features must come from isomers which are trapped in the molecular beam. Unfortunately, this limits the ability to assign specific isomers to a spectrum which is as cluttered as this one. Instead, we can only propose several bonding motifs which *could* contribute to the experiment. The first is a water chain, as shown in Na3e, which is predicted to exhibit hydrogen-bonded stretches near 3510 and 3455 cm^{-1}. Another good possibility is isomer Na3c. This isomer has a bent hydrogen bond, much like isomer Na3a, but in this case one of the first-shell water molecules also participates in a weak π-hydrogen bond with the APE phenyl ring. The weak hydrogen bond is calculated to appear near 3710 cm^{-1} and could be assigned to the new feature near 3700 cm^{-1} in the $Na^+(APE)(H_2O)_3Ar$ spectrum. In addition, isomer Na3c also contains the APE intramolecular hydrogen bond, which would contribute to the feature near 3300 cm^{-1} in the experiment. Although specific isomers cannot be identified, it is clear that significant water-water hydrogen bonding has occurred for these cluster ions.

The $K^+(APE)(H_2O)_3Ar$ spectrum (Figure 4.10) is, surprisingly, somewhat simpler than the $Na^+(APE)(H_2O)_3Ar$ spectrum. This is the only occurrence of this phenomenon in any of the $M^+(APE)(H_2O)_nAr_{0,1}$ spectra reported here. The energetically-preferred isomer at low temperatures is K3a, which contains the same bent hydrogen-bonded configuration as isomer Na3a. As seen in Figure 4.10, isomer K3a does a relatively decent job of replicating many of the spectral features, but two features are not replicated: one near 3595 cm^{-1} (possibly from a π-hydrogen bond) and one centered just below 3100 cm^{-1}. Isomers K3b and K3c each contain a π-hydrogen bond, but the intramolecular APE hydrogen bond in each of these isomers is not consistent with the experiment. The other feature which has not yet been assigned is in the region of the aromatic CH stretches. The intensity of this feature is enhanced relative to the

aliphatic CH stretches. Calculations have unfortunately not been able to replicate the increase in intensity in this region.

$M^+(APE)(H_2O)_3$

The $Na^+(APE)(H_2O)_3$ spectrum (Figure 4.11) preserves the features near 3720 and 3650 cm^{-1} from the $Na^+(APE)(H_2O)_2$ spectrum (attributed to free water molecules) and also has additional features near 3585, 3460 and 3295 cm^{-1}. The lowest feature is likely from an isomer containing the APE intramolecular hydrogen bond, while the other features are indicative of water-water hydrogen bonding. Features near 3550 cm^{-1} are often associated with bent hydrogen bonds, while features near 3450 cm^{-1} have been assigned to linear hydrogen bonds (one first-shell water molecule donates a hydrogen to a second-shell water).[9, 12, 14] It is likely that several isomers are contributing to this experiment. Isomers Na3a and Na3b are the energetically-preferred isomers near 300 K, but as shown in Figure 4.11, neither of the isomers stands out as an exceptional match for the experiment.

Compared to the $Na^+(APE)(H_2O)_3$ spectrum, the $K^+(APE)(H_2O)_3$ spectrum (Figure 4.12) has many of the same features. One of the new features appears near 3440 cm^{-1} and is consistent with a linear water-water hydrogen bond, as shown in isomers K3b, K3c and K3d. In fact, these three isomers can account for most of the features in the $K^+(APE)(H_2O)_3$ spectrum. The calculated spectra are shown in Figure 4.12. For each experimental feature, there is at least one calculated feature which corresponds to it. The one exception is the feature near 3230 cm^{-1} in the experimental spectrum, which does not correspond to any of the calculated features. The problem with these assignments, however, is that since many of the features overlap, it is not possible to definitively include or eliminate any of the individuals isomers from the assignment.

Rather, isomers K3b, K3c and K3d are simply good possibilities that *could* be contributing to the experimental spectrum.

Conclusions

The $M^+(APE)(H_2O)_nAr_{0,1}$ spectra reported here demonstrate a strong dependence on both the identity of M^+ and the evaporative cooling pathway. Cluster ions stabilized through the loss of argon are able to trap high-energy conformers, while cluster ions stabilized through the loss of water tend to reach thermodynamic equilibrium.

The cold n=0 and n=1 spectra were similar for both ions, although the features in the $Na^+(APE)Ar$ and $Na^+(APE)(H_2O)Ar$ spectra were shifted lower in frequency compared to the $K^+(APE)Ar$ and $K^+(APE)(H_2O)Ar$ due to the stronger electrostatic forces of the sodium ion. For all of the other spectra (with the exception of $M^+(APE)(H_2O)_3Ar$), the potassium spectra were more complex, and were assigned to contributions from multiple isomers. Also, almost every potassium spectrum contained features from isomers with an APE intramolecular hydrogen bond as well as those in which the potassium ion interrupted the internal hydrogen bond. This is consistent with the isomers identified in a search for minimum-energy structures (Figure 4.2). The low-energy structures for sodium-containing isomers consistently indicated a strong preference for the sodium ion to interrupt the APE internal hydrogen bond, while low-energy potassium-containing isomers were identified both with and without the internal hydrogen bond.

Figures

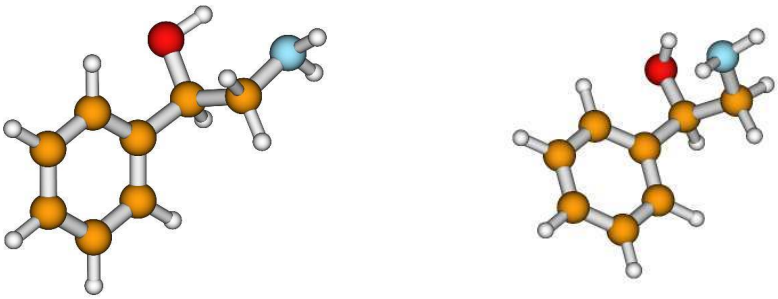

Figure 4.1: The AG_1 and GG_1 conformers of neutral APE

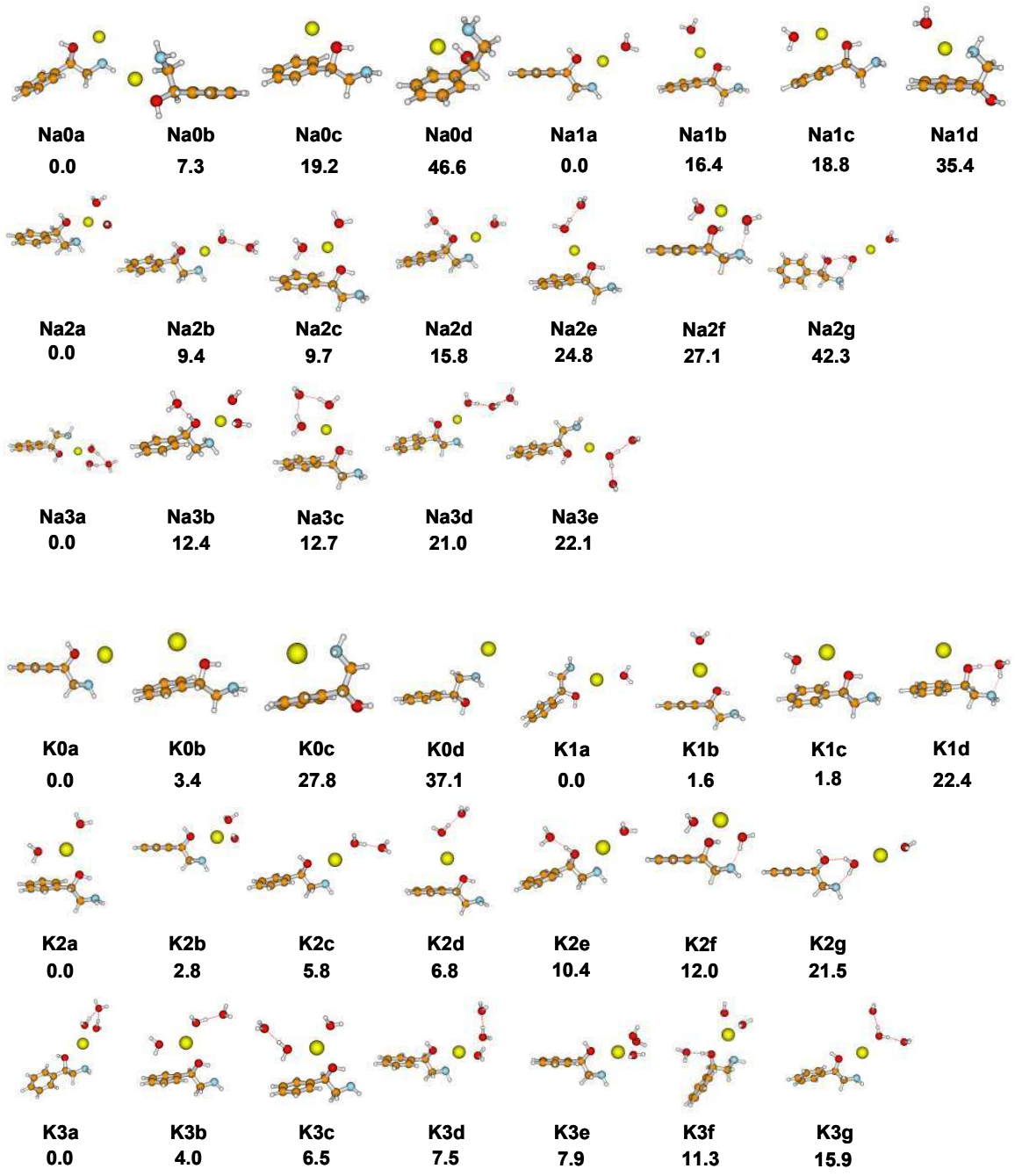

Figure 4.2: Low-energy conformers of $M^+(APE)(H_2O)_{0-3}$ for M = Na and K

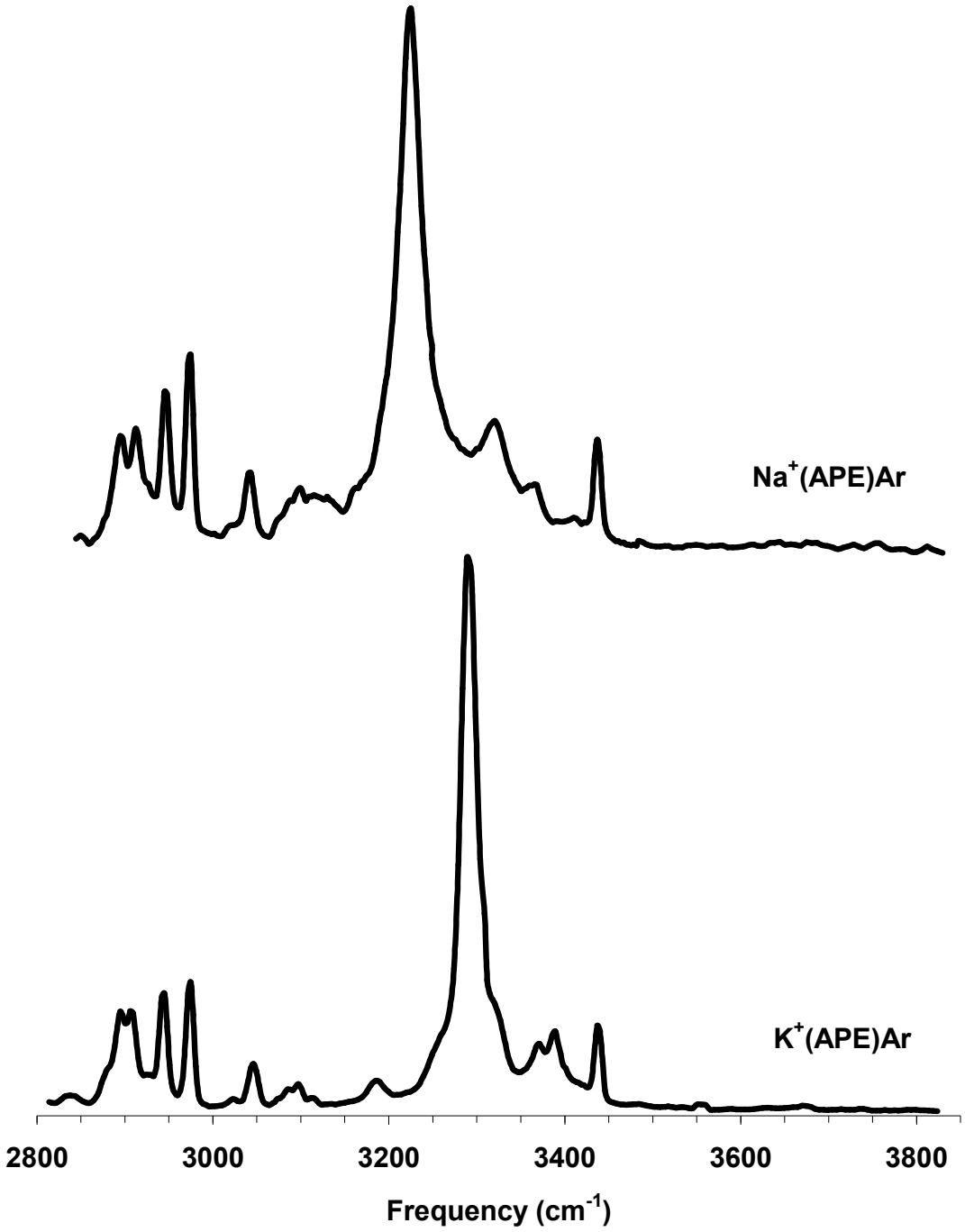

Figure 4.3: IRPD spectra of Na^+(APE)Ar (top) and K^+(APE)Ar (bottom)

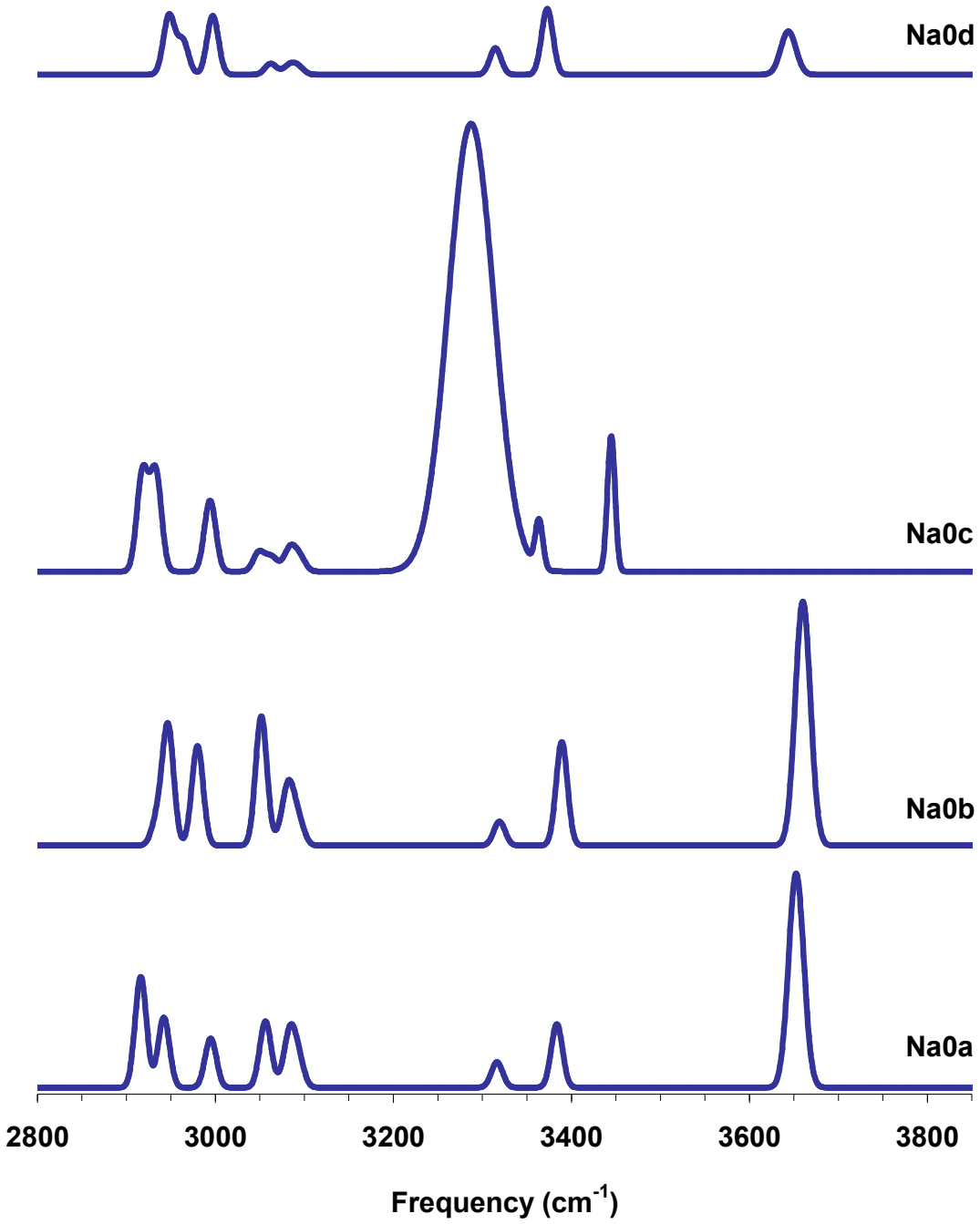

Figure 4.4: Calculated spectra corresponding to the four low-energy isomers of Na^+(APE) shown in Figure 4.2

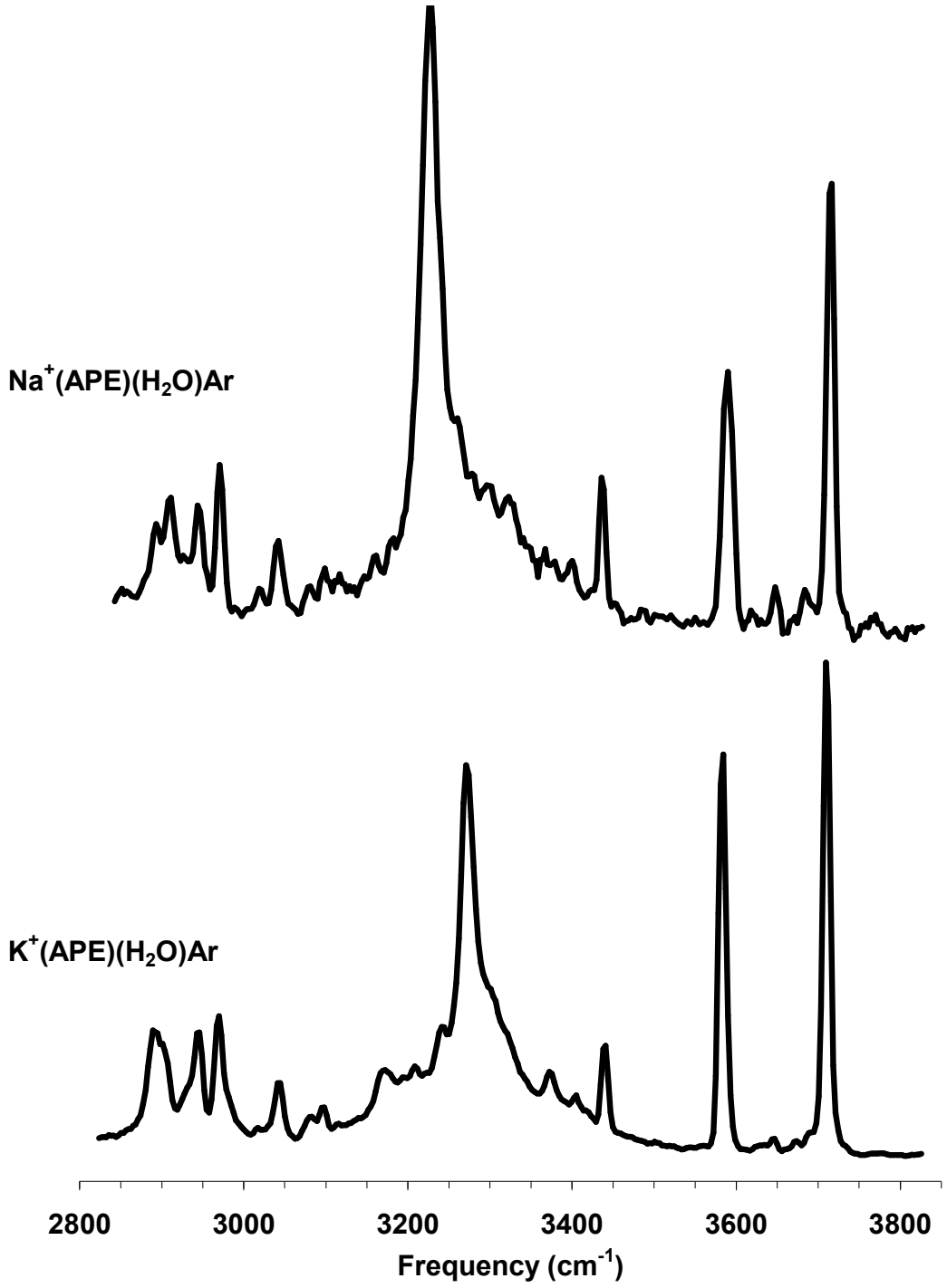

Figure 4.5: IRPD spectra of $Na^+(APE)(H_2O)Ar$ (top) and $K^+(APE)(H_2O)Ar$ (bottom)

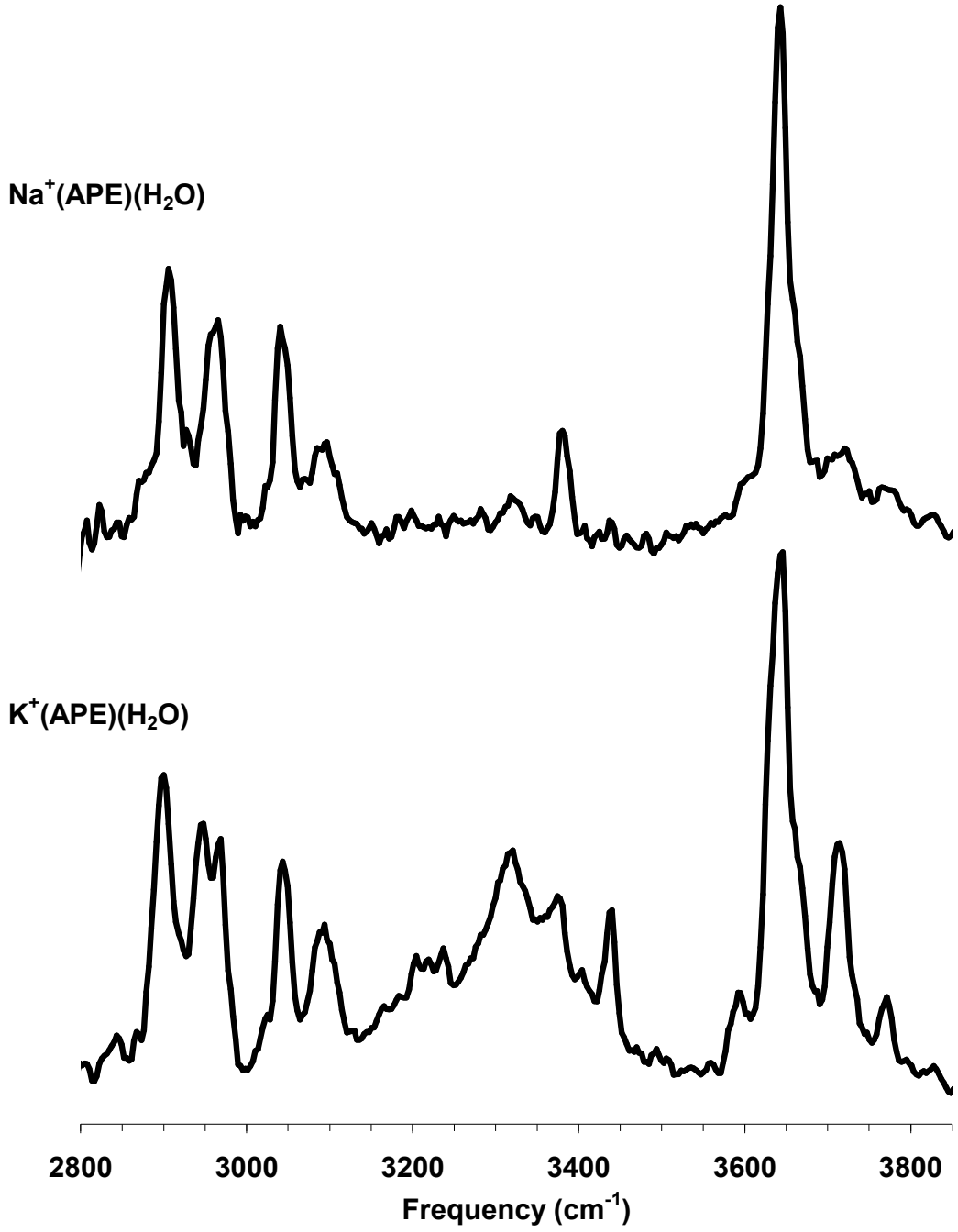

Figure 4.6: IRPD spectra of $Na^+(APE)(H_2O)$ (top) and $K^+(APE)(H_2O)$ (bottom)

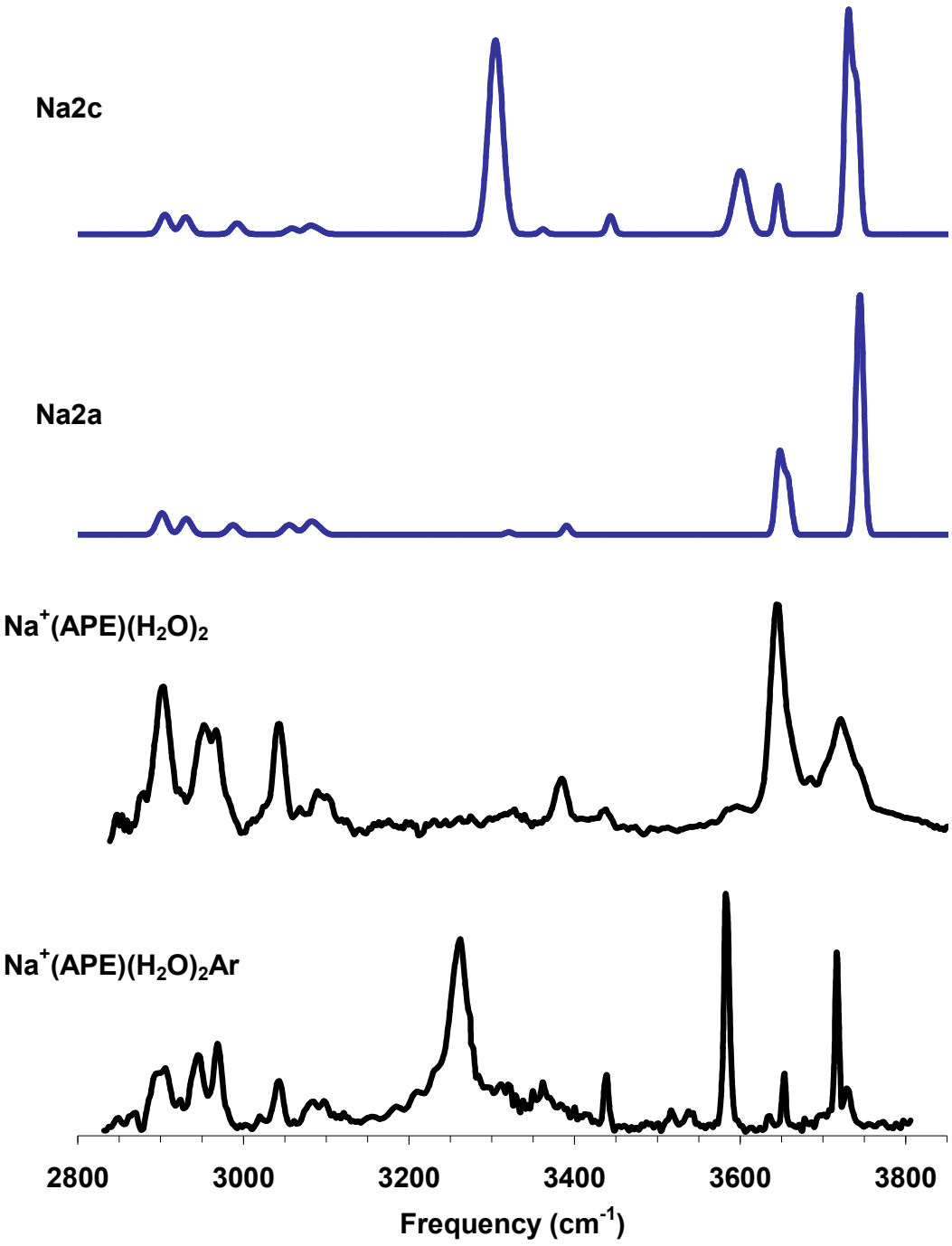

Figure 4.7: IRPD spectra of $Na^+(APE)(H_2O)_2$ and $Na^+(APE)(H_2O)_2Ar$, along with the calculated spectra corresponding to isomers Na2c and Na2a

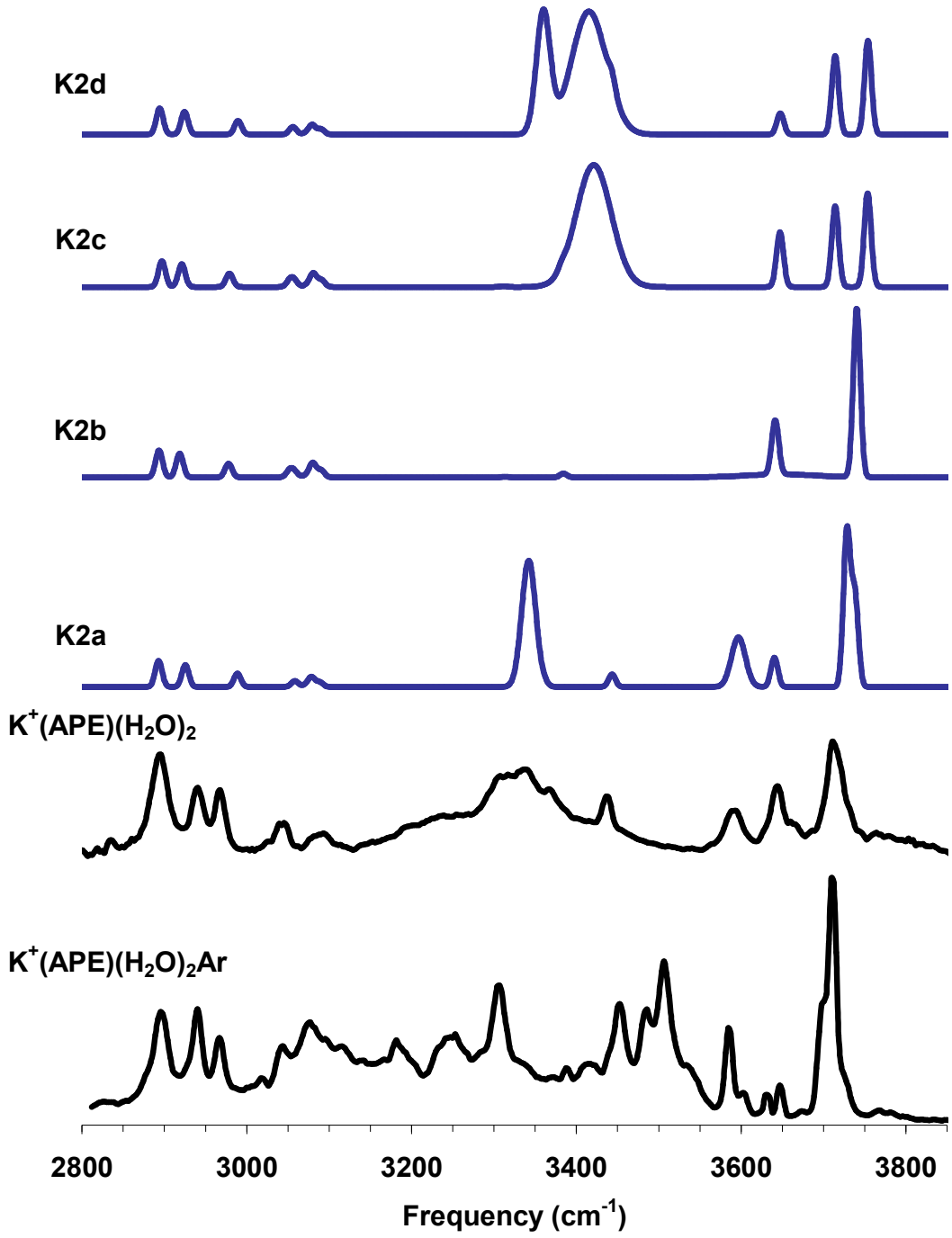

Figure 4.8: IRPD spectra of $K^+(APE)(H_2O)_2$ and $K^+(APE)(H_2O)_2Ar$, along with the calculated spectra corresponding to isomers K2a, K2b, K2c and K2d

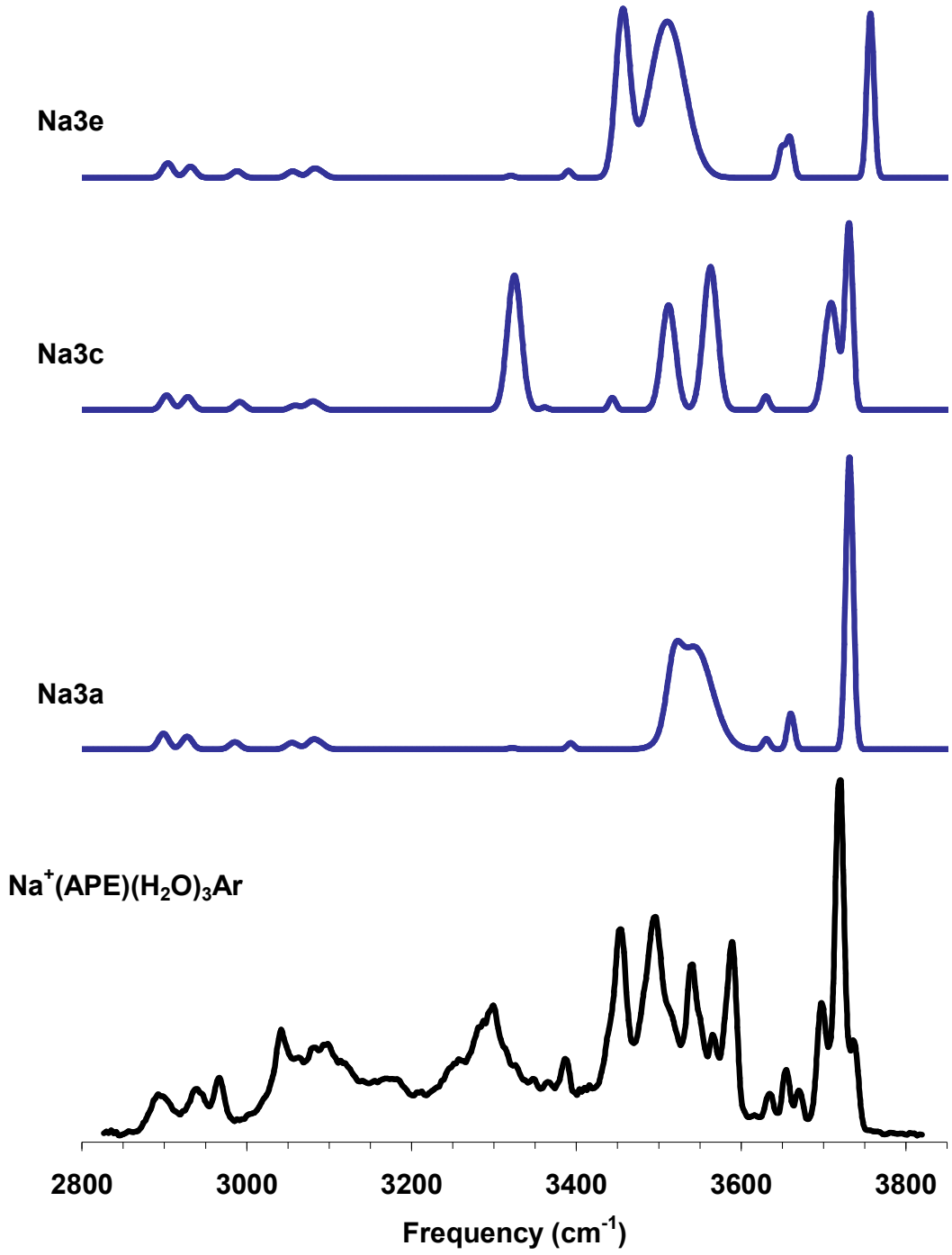

Figure 4.9: IRPD spectrum of $Na^+(APE)(H_2O)_3Ar$, along with the calculated spectra corresponding to isomers Na3a, Na3c and Na3e

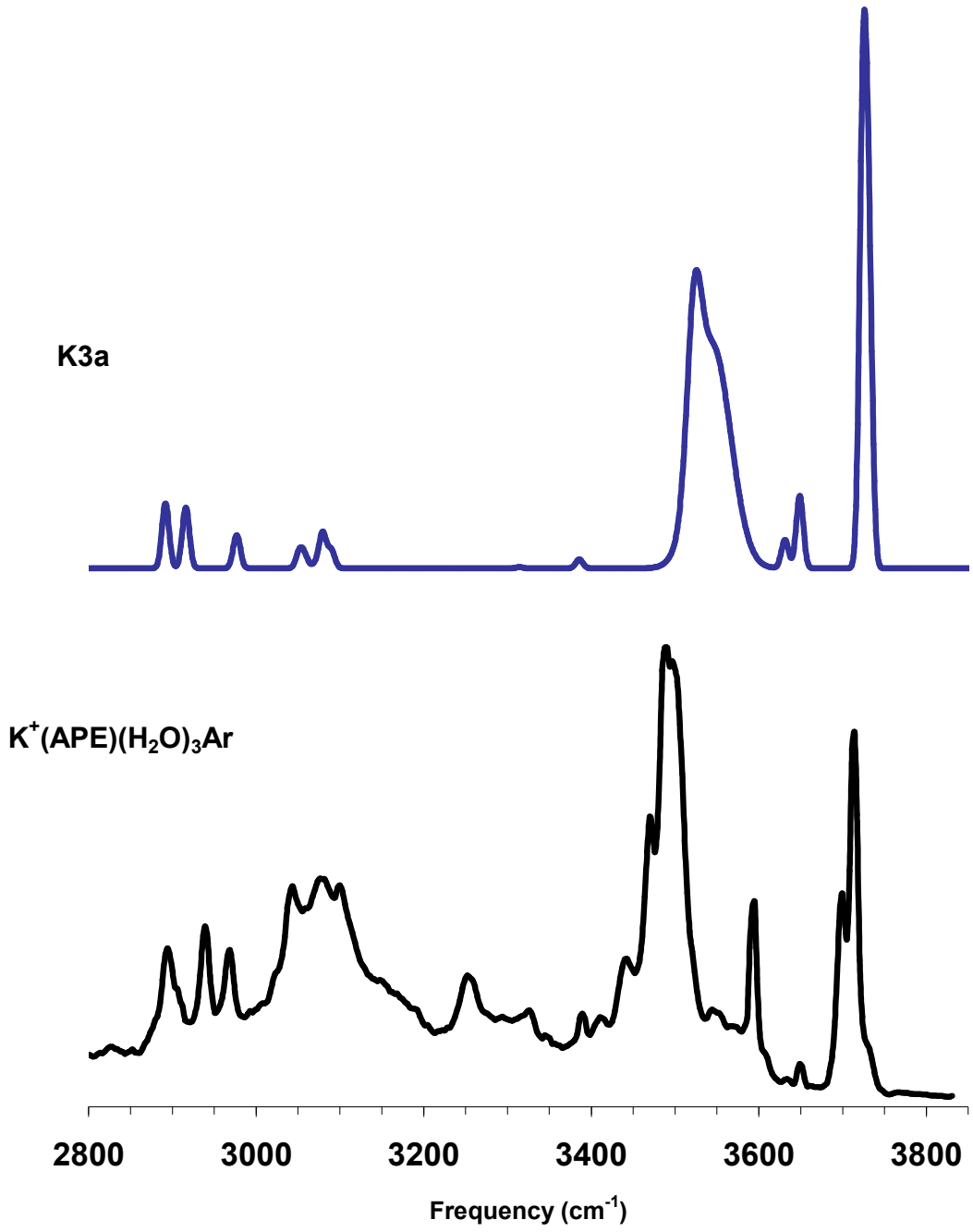

Figure 4.10: IRPD spectrum of $K^+(APE)(H_2O)_3Ar$, along with the calculated spectrum corresponding to isomer K3a

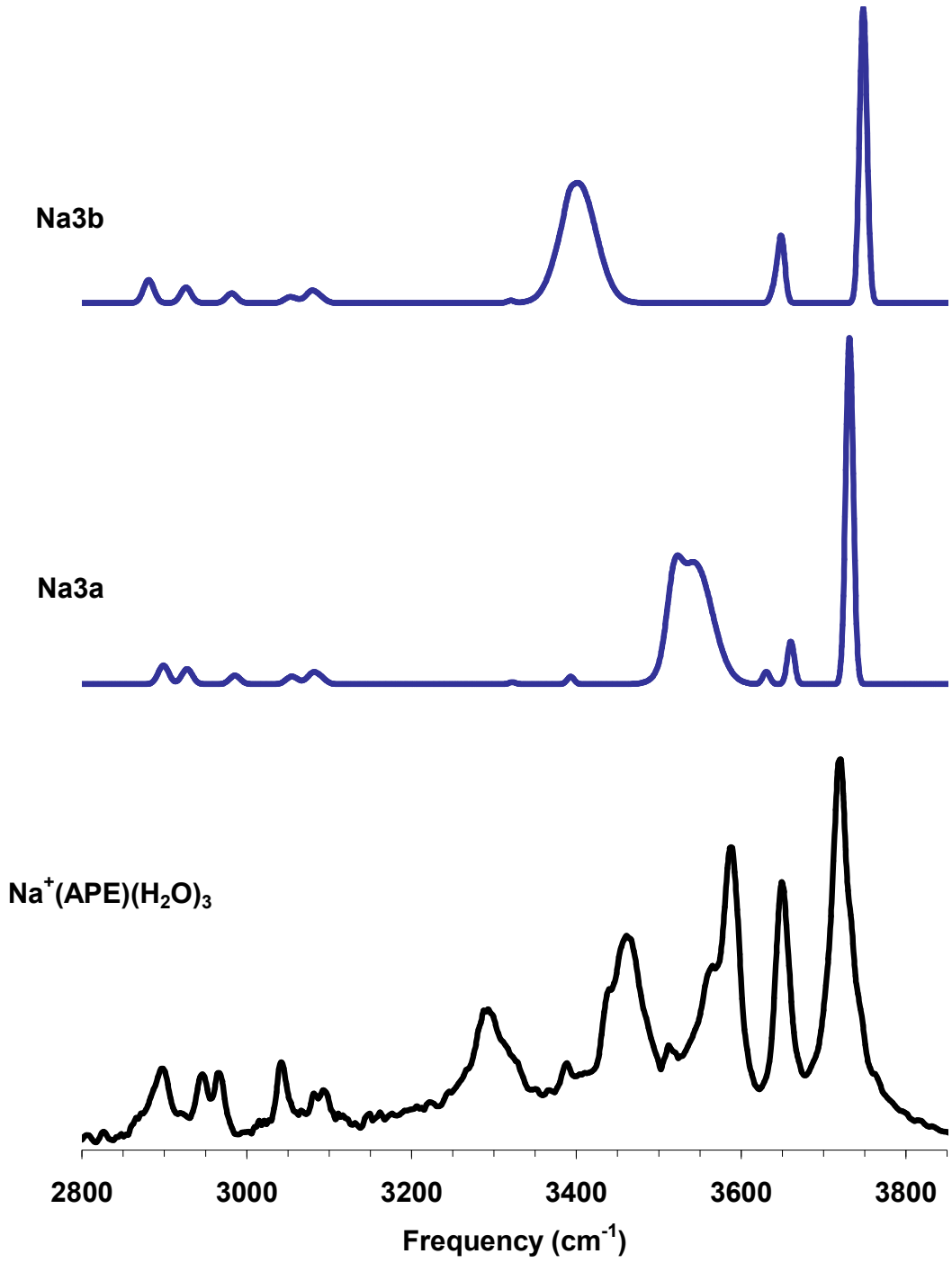

Figure 4.11: IRPD spectrum of $Na^+(APE)(H_2O)_3$, along with the calculated spectra corresponding to isomers Na3a and Na3b

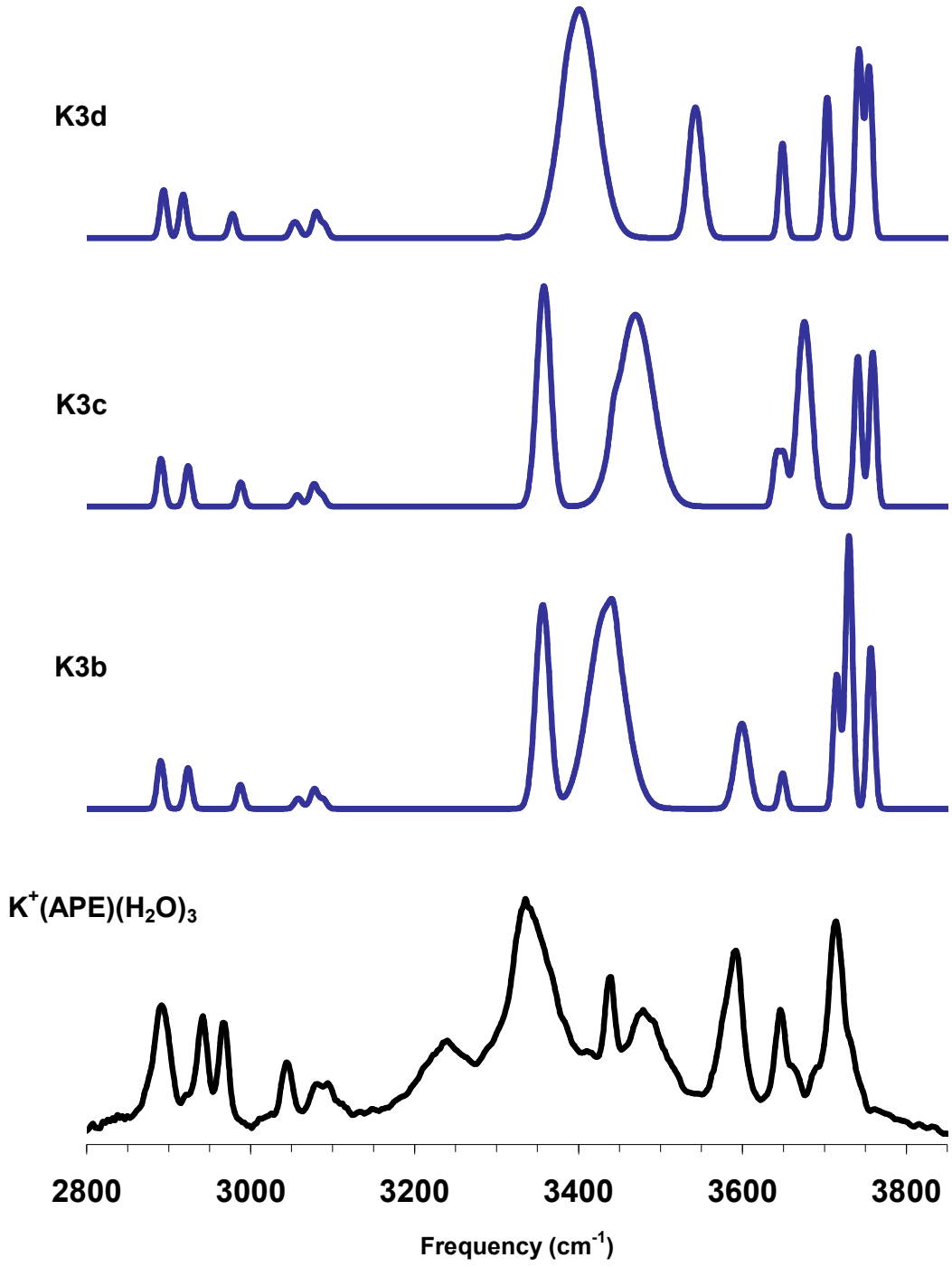

Figure 4.12: IRPD spectrum of $K^+(APE)(H_2O)_3$, along with the calculated spectra corresponding to isomers K3b, K3c and K3d

References

1. Baker, C. M.; Grant, G. H., J. Phys. Chem. B 2007, 111, (33), 9940.
2. Graham, R. J.; Kroemer, R. T.; Mons, M.; Robertson, E. G.; Snoek, L. C.; Simons, J. P., J. Phys. Chem. A 1999, 103, (48), 9706.
3. Macleod, N. A.; Robertson, E. G.; Simons, J. P., Mol. Phys. 2003, 101, (14), 2199.
4. Macleod, N. A.; Simons, J. P., Mol. Phys. 2006, 104, (20/21), 3317.
5. Miller III, T. F.; Clary, D. C., J. Phys. Chem. B 2004, 108, (7), 2484.
6. Miller III, T. F.; Clary, D. C., J. Phys. Chem. A 2006, 110, (2), 731.
7. Nicely, A. L.; Lisy, J. M., in preparation.
8. Rodriguez, J. D.; Lisy, J. M., Int. J. Mass spectrom. 2009, 283, (1-3), 135.
9. Miller, D. J.; Lisy, J. M., J. Am. Chem. Soc. 2008, 130, (46), 15381-15392.
10. Fraley, P. E.; Narahari Rao, K., J. Mol. Spectrosc. 1969, 29, (1-3), 348.
11. Miller, D. J.; Lisy, J. M., J. Chem. Phys. 2006, 124, (18), 184301.
12. Miller, D. J.; Lisy, J. M., J. Am. Chem. Soc. 2008, 130, (46), 15393-15404.
13. Nicely, A. L.; Miller, D. J.; Lisy, J. M., J. Am. Chem. Soc. 2009, 131, (18), 6314.
14. Nicely, A. L.; Miller, D. J.; Lisy, J. M., J. Mol. Spectrosc. 2009, 257, (2), 157.

Chapter 5: Hydrated M^+(Ephedrine) Cluster Ions

Introduction

In Chapter 4, the structural behavior of 2-amino-1-phenylethanol (APE) was examined in the presence of sodium and potassium cations. In this chapter, the structural preferences of a similar biomolecule, ephedrine, are studied. Ephedrine has the same phenyl ring as APE, but differs slightly in the side chain, where it has a methyl group attached to the final carbon as well as to the nitrogen. The diastereoisomer pseudoephedrine exhibits physiological effects which are quite different from those of ephedrine,[1, 2] which emphasizes the important role of chirality. The chirality of a molecule is simply one component of its overall structure, which is clearly important in determining its physiological behavior.

The conformational preferences of ephedrine (and its diastereoisomer pseudoephedrine) have been studied using a variety of techniques including UV spectroscopy, infrared ion-dip and hole-burning spectroscopy and molecular beam Fourier transform microwave spectroscopy.[3-6] It was determined that the preferred structure of ephedrine (identified as AGa) was one in which the side chain was extended away from the phenyl ring, and the side-chain oxygen formed an intramolecular hydrogen bond with the amino nitrogen. This is very similar to the neutral structure of APE,[7-10] as discussed in the previous chapter.

There are two possible structural motifs of hydrated ephedrine. The first is an "insertion" structure, in which the water molecule is positioned between the ephedrine OH and NH groups to create an OH···OH···NH chain. The second is an "addition" structure, in which the water molecule donates a proton to the alcohol group, leaving the ephedrine intramolecular hydrogen bond intact. Infrared ion-dip spectroscopy of hydrated APE indicated a strong preference for

insertion structures upon addition of one, two or three water molecules.[8, 9] Similar experiments of hydrated ephedrine, on the other hand, suggest population of both types of structures for the singly hydrated cluster, while the doubly hydrated cluster again adopts an insertion structure.[11] The ephedrine structure is determined to remain in the AGa configuration for all of the observed bare, singly hydrated and doubly hydrated ephedrine clusters.

Results and Discussion

M^+(Eph)Ar

The spectrum of K^+(Eph)Ar is shown at the bottom of Figure 5.1. The spectrum may initially seem a bit complicated, but with the help of DFT calculations it is straightforward to assign. The structures and relative zero-point energies of low-energy isomers identified in a geometry search are given in Figure 5.2. The ephedrine molecule gives rise to one OH stretching feature, one NH stretching feature and a series of CH stretching features. The CH stretching vibrations are responsible for most of the spectral features in the range of 2800-3100 cm^{-1}, with the aromatic CH stretches appearing at a higher frequency than the aliphatic CH stretches. The small experimental feature near 3380 cm^{-1} is assigned to the ephedrine NH stretching feature. DFT calculations predict this feature to occur in the range of 3320-3380 cm^{-1}, depending on the position of the potassium cation relative to the NH group. The only remaining feature in the spectrum (centered near 3130 cm^{-1}) must come from the ephedrine OH stretch. The OH group can be "free" (as in isomers K0a and K0b) or involved in an intramolecular hydrogen bond with the NH group (as in isomers K0c, K0d or K0e). A free OH stretch is calculated to appear near 3650 cm^{-1}, while the hydrogen-bonded OH stretch can appear significantly lower in frequency. Isomer K0c, for which the OH stretch is calculated to be centered just below 3200 cm^{-1}, has the

best agreement with the experiment, and the calculated spectrum is shown above the K^+(Eph)Ar experimental spectrum in Figure 5.1 for comparison.

The Na^+(Eph)Ar spectrum (Figure 5.1, top) is virtually identical to the K^+(Eph)Ar spectrum. The one notable difference is a shift of the OH stretching feature to lower frequency so that it overlaps with the CH stretching features. The sodium cation has a stronger electrostatic interaction with the ephedrine compared to the potassium cation, which results in a larger frequency shift. Isomer Na0c is in the same configuration as isomer K0c and has a similar calculated spectrum, although the hydrogen-bonded OH stretch is predicted to be centered near 3110 cm^{-1} for the sodium spectrum compared to 3200 cm^{-1} for the potassium spectrum. The actual features are even further red-shifted, suggesting that a smaller local scaling factor would be appropriate for strong hydrogen bond interactions. The similarities in the M^+(Eph)Ar spectra allow a straightforward assignment of Na0c as the sole isomer contributing to the Na^+(Eph)Ar spectrum, just as isomer K0c was assigned to the K^+(Eph)Ar spectrum.

Both K0c and Na0c preserve the intramolecular hydrogen bond that characterized the neutral ephedrine structure, and the cation is positioned near the edge of the phenyl ring, where it can interact with both the pi electrons and the oxygen lone pairs. Interestingly, this is not the minimum-energy configuration calculated for the M^+(Eph) cluster ions. Rather, K0a and Na0a – structures in which the cation interrupts the intramolecular hydrogen bond and interacts with the nitrogen and oxygen lone pairs – are energetically preferred. As noted above, this leaves a free OH group on the ephedrine which is expected to exhibit a feature near 3650 cm^{-1}, which is inconsistent with the experimental spectra in Figure 5.1. The energy difference calculated for the potassium cluster ions is only about 3 kJ/mol, but it's more than 20 kJ/mol for the sodium cluster ions (and isomer Na0b is at an intermediate energy). This is a significant energy difference and a

clear indication that the higher-energy isomers are being trapped during the evaporative cooling process. The rapid evaporation of argon removes energy from the cluster ions, preventing rearrangement to the thermodynamically-favored isomers. Similar trapping phenomena have been reported for $M^+(Tryp)(H_2O)Ar$[12, 13] and $M^+(APE)(H_2O)Ar$[14] cluster ions.

$M^+(Eph)(H_2O)Ar$

Upon addition of a water molecule, there are only a few differences in the $M^+(Eph)(H_2O)Ar$ spectra (Figure 5.3) compared to the non-hydrated spectra. First, there are two new features in the OH stretching region, centered at 3707 and 3578 cm^{-1} in the potassium spectrum and 3713 and 3589 cm^{-1} in the sodium spectrum. The feature near 3710 cm^{-1} could be assigned to either the asymmetric stretch of a free water molecule (as seen in isomers K1a, K1d, Na1a, Na1b and Na1d) or a free OH stretch of a water molecule which forms a hydrogen bond with the other OH oscillator (as seen in isomers K1b and K1c and Na1c). In the first case, the asymmetric stretch of a free water molecule would be accompanied by a symmetric stretch in the vicinity of 3650 cm^{-1}. The second option, a water free OH stretch, is accompanied in isomers K1c and Na1c by a π-hydrogen bond with a calculated frequency near 3575 cm^{-1} (K^+) or 3600 cm^{-1} (Na^+). This scenario has a much nicer agreement with the experimental $M^+(Eph)(H_2O)Ar$ spectra, and the calculated spectrum of isomer K1c is shown in the middle of Figure 5.3 for comparison.

The ephedrine intramolecular hydrogen bond is still intact, as seen by the continued presence of the broad features near the CH stretching region. An additional broad feature centered near 3200 cm^{-1} in both spectra overlaps with the intramolecular hydrogen bond features. The new feature is clearer in the $K^+(Eph)(H_2O)Ar$ spectrum, where it has a greater intensity.

This feature is likely the result of a slight rotation of the ephedrine side chain to form a second isomer with a π-hydrogen-bonded water molecule. This would also explain the presence of a second NH stretching feature near 3315 (K^+) and 3300 cm^{-1} (Na^+).

Thermodynamically, isomers K1a and K1c are virtually isoenergetic between 80-120 K. Based solely on this information, the two isomers would be expected to contribute equally to the experimental spectrum. Isomer K1a has a free water molecule, which is not a good match for the experiment, as discussed above. In addition, the ephedrine intramolecular hydrogen bond is broken in isomer K1a, resulting in an ephedrine free OH stretch with a predicted frequency of 3635 cm^{-1} – also inconsistent with the experiment. Despite the similar energies, isomer K1c is favored during cluster formation. This effect is magnified for the sodium-containing cluster ions. Isomer Na1a is more than 17 kJ/mol lower in energy than isomer Na1c at low temperatures, but isomer Na1c is clearly more consistent with the experimental features. This is yet another example of high-energy isomer trapping, as seen already for the M^+(Eph)Ar spectra.

M^+(Eph)(H_2O)

When singly hydrated ephedrine cluster ions are formed by the evaporation of water, without the use of argon tagging, significant changes in the isomer populations occur. The M^+(Eph)(H_2O) spectra are shown in Figures 5.4 and 5.5, and for the first time the spectra are ion-dependent. The K^+(Eph)(H_2O) spectrum has three resolved features in the OH stretching region near 3580, 3635 and 3710 cm^{-1}, while the Na^+(Eph)(H_2O) spectrum has one intense feature near 3640 cm^{-1} and a progression of weak, high-frequency features.

The features near 3580 and 3710 cm^{-1} in the K^+(Eph)(H_2O) spectrum are consistent with the features assigned to isomer K1c in the K^+(Eph)(H_2O)Ar spectrum. The new feature between

these two is in the region typically assigned to water symmetric stretches,[15-17] but the ephedrine free OH stretch is also calculated to appear near 3650 cm^{-1}. Isomer K1c has the lowest zero-point energy, but near 300 K, isomer K1a is the minimum-energy isomer, with isomer K1c calculated to be approximately 7 kJ/mol higher in energy. With both a free water molecule and an ephedrine free OH stretch, isomer K1a has excellent agreement with the new spectral feature. Isomer K1c corresponds with the features which were consistent with the $K^+(Eph)(H_2O)Ar$ spectrum. Both of these isomers were likely present in the experiment. Since isomer K1a is the minimum-energy isomer, it is expected to be the major contributor, with K1c as the minor contributor. A simulated spectrum containing isomers K1a and K1c in a 4:1 ratio is shown in Figure 5.4 and has excellent agreement with the $K^+(Eph)(H_2O)$ spectrum.

The $Na^+(Eph)(H_2O)$ spectrum (Figure 5.5) has one prominent feature near 3640 cm^{-1} and a broad, partially resolved progression of features at higher frequency. Also, the intensity in the CH stretching region is noticeably suppressed, and the broad feature between 3050-3200 cm^{-1} in the $Na^+(Eph)(H_2O)Ar$ spectrum is absent. This suggests that the ephedrine intramolecular hydrogen bond has been broken.

While two low-energy potassium-containing isomers were identified in a geometry search, there is a strong energetic preference for only one sodium-containing isomer, Na1a. In the entire temperature range of 0-400 K, the next isomer (Na1b) is calculated to be more than 9 kJ/mol higher in energy. Isomer Na1a, like K1a, has a free water molecule and no intramolecular hydrogen bond. The water symmetric and asymmetric stretches are calculated to appear near 3630 and 3725 cm^{-1}, respectively, but rotation of the water molecule has been shown to result in a broadened asymmetric stretching feature.[18, 19] The ephedrine free OH stretch is calculated to appear near 3650 cm^{-1}, so the experimental feature centered at 3641 cm^{-1} is likely a

combination of the free water symmetric stretch and the ephedrine free OH stretch. The calculated spectrum of isomer Na1a is shown with the experimental $Na^+(Eph)(H_2O)$ spectrum in Figure 5.5. The similarity of these two spectra support the assignment of isomer Na1a as the sole contributor to this experiment, in contrast to the $K^+(Eph)(H_2O)$ experiment which had at least two contributing isomers.

In contrast to the neutral ephedrine experiments,[11] the $M^+(Eph)(H_2O)$ and $M^+(Eph)(H_2O)Ar$ cluster ions do not adopt either insertion *or* addition structures. Rather, the water molecule demonstrates a preference for electrostatic interaction with the metal ion, either as a free water molecule or as one involved in a π-hydrogen bond. The experiments reported here show no evidence for interaction of the water molecule with the ephedrine OH or NH groups.

$M^+(Eph)(H_2O)_2$

The $Na^+(Eph)(H_2O)_2$ spectrum (Figure 5.6) is very similar to the $Na^+(Eph)(H_2O)$ spectrum: It contains one intense feature near 3640 cm^{-1} and a broader feature centered near 3724 cm^{-1}. The CH stretching region is also very consistent in both spectra, suggesting that the conformation of the ephedrine molecule has not changed with the addition of the second water molecule. The $Na^+(Eph)(H_2O)$ spectrum was assigned to an isomer with a free water molecule. If the second water molecule was interacting with the first to form a hydrogen bond, a new feature would appear in the spectrum below 3600 cm^{-1}. These hydrogen bond signatures have been well-documented for hydrated alkali metal ions.[15-17] Because there are no new features in the $Na^+(Eph)(H_2O)_2$ spectrum, the second water molecule must also be a free water. Isomer Na2a fits this description and also happens to be the minimum-energy isomer identified in the

geometry search. The calculated spectrum of Na2a is shown in Figure 5.6 and is in excellent agreement with the experimental spectrum below it. At 300 K, the next-lowest isomer, Na2b, is calculated to lie about 7 kJ/mol higher in energy. This isomer contains one free water molecule and one water molecule involved in a π-hydrogen bond (similar to that of isomer Na1c). The ephedrine molecule exhibits the intramolecular hydrogen bond in Na2b, but there is no broad feature in the CH stretching region of the $Na^+(Eph)(H_2O)_2$ spectrum to coincide with this configuration. Therefore, isomer Na1a is assigned as the sole contributor to the $Na^+(Eph)(H_2O)_2$ spectrum.

The $K^+(Eph)(H_2O)_2$ spectrum (Figure 5.7) has several features which were not present in the $Na^+(Eph)(H_2O)_2$ spectrum – one near 3585 cm^{-1} and a broad feature centered around 3230 cm^{-1} – but are very similar to features in the $K^+(Eph)(H_2O)$ spectrum. The $K^+(Eph)(H_2O)$ spectrum was assigned to a combination of isomers K1a (which contained a free water molecule and a free ephedrine OH) and K1c (which contained a π-hydrogen-bonded water molecule and an ephedrine intramolecular hydrogen bond). While it is possible to have an isomer which contains both a free water molecule and a π-hydrogen-bonded water molecule, it is not possible to have both the free ephedrine OH and the intramolecular hydrogen bond in one isomer. This would seem to suggest that a minimum of two isomers must be contributing to the experiment. There is another possibility, however, since harmonic frequency calculations predict that the symmetric water stretch overlaps with the ephedrine free OH stretch. This creates the possibility of having one isomer with a free water molecule contributing to the features near 3710 and 3640 cm^{-1}, a π-hydrogen-bonded water molecule contributing to the features near 3710 and 3585 cm^{-1} and the ephedrine intramolecular hydrogen bond contributing to the broad feature near 3230 cm^{-}

[1]. From a geometry search, there is an isomer that meets all of these criteria – isomer K2a – and is also the minimum-energy isomer across the entire temperature range of 0-400 K.

Isomer K2c, which is similar in structure to isomer Na2a with two free water molecules, should also be considered. At 300 K, this isomer is calculated to be only 3 kJ/mol higher in energy than isomer K2a. The calculated spectra of K2a and K2c are shown above the experimental spectrum in Figure 5.7. There are no features in the K2c spectrum that would separate it spectroscopically when isomer K2a is also present. Therefore, the $K^+(Eph)(H_2O)_2$ spectrum is assigned to either isomer K2a or a combination of isomers K2a and K2c.

$M^+(H_2O)_2Ar$

The spectra of $M^+(Eph)H_2O)_2Ar$ (Figures 5.8 and 5.9) exhibit many of the same features which have already been identified. Although the features are more resolved, the $Na^+(Eph)(H_2O)_2Ar$ spectrum looks quite similar to the $K^+(Eph)(H_2O)_2$ spectrum. In the OH stretching region, there are features near 3585, 3635, 3650, 3715 and 3730 cm^{-1}, which are in agreement with an isomer containing both a free water molecule (contributing to the features near 3635 and 3730 cm^{-1}) and a π-hydrogen-bonded water molecule (contributing to the features near 3585 and 3715 cm^{-1}). The remaining feature, located near 3650 cm^{-1}, likely comes from the free ephedrine OH stretch of an isomer which does not contain the intramolecular ephedrine hydrogen bond. The broad feature between 3000-3200 cm^{-1} indicates the presence of an isomer with the intramolecular hydrogen bond, so there are most likely at least two different isomers contributing to this experiment.

Comparing this information with the isomers shown in Figure 5.2 (and the assignments of the $K^+(Eph)(H_2O)_2$ spectrum) leads to the conclusion that isomers Na2a and Na2b are excellent

candidates for this experiment. The calculated spectra for both of these isomers are shown in Figure 5.8 along with the $Na^+(Eph)(H_2O)_2Ar$ for comparison. Isomer Na2b contains one free water molecule, one π-hydrogen-bonded water molecule and the ephedrine intramolecular hydrogen bond. Isomer Na2a, which contains two free water molecules and a free ephedrine OH, was assigned as the sole contributor to the $Na^+(Eph)(H_2O)_2$ spectrum. It is the lowest-energy isomer at all temperatures in the range of 0-400 K and is expected to be the major contributor to the experiment. At the same time, however, the intensity of the features near 3635, 3650 and 3730 cm^{-1} compared to those near 3585 and 3715 cm^{-1} suggest that Na2a is actually the minor contributor while isomer Na2b is the major contributor.

The $K^+(Eph)(H_2O)_2Ar$ spectrum (Figure 5.9) has the same features as the $Na^+(Eph)(H_2O)_2Ar$ and $K^+(Eph)(H_2O)_2$ spectra, plus additional features ranging from 3340-3450 cm^{-1}. At a minimum, isomer K2a (the major contributor to the $K^+(Eph)(H_2O)_2$ spectrum) is expected to contribute again to this experiment. The new features are characteristic of water-water hydrogen bonding,[15-17] but hydrogen bonding between the ephedrine OH group and water molecules should also be considered. Of the structures shown in Figure 5.2, only isomer K2d contains this type of interaction. The calculated spectra of isomers K2a and K2d are shown in Figure 5.9. Although these two spectra agree well with the experimental spectrum, there are probably more isomers which are also present in this experiment.

Thermodynamically, isomers K2a and K2b are expected to be the two main contributors at low temperatures. Isomer K2b contains a weak hydrogen bond in which one of the water molecules donates a proton to the ephedrine oxygen. This interaction is predicted to result in a feature near 3520 cm^{-1}, which is actually in the only region of the $K^+(Eph)(H_2O)_2Ar$ spectrum that remains at baseline for more than 100 cm^{-1}. This suggests that isomer K2b does not

contribute to the experiment. Isomer K2d, which has good agreement with the experimental spectrum, is about 13 kJ/mol higher in energy at low temperatures than isomer K2a. This is yet another example of high-energy isomer trapping due to the argon evaporation process. As mentioned earlier, there are probably other isomers also contributing to the $K^+(Eph)(H_2O)_2Ar$ spectrum, but without restricting the geometry search to low-energy isomers, it becomes difficult to make a definitive assignment for each of the spectral features. Instead, assignments will be limited to qualitative descriptions of the binding motifs – in this case, a free water molecule, a π-hydrogen-bonded water molecule, the ephedrine intramolecular hydrogen bond and some type of water-water or ephedrine-water hydrogen bonding.

$M^+(Eph)(H_2O)_3$

It is quite interesting that the addition of a third water molecule still does little to change the spectrum of the warm potassium-containing cluster ions. The $K^+(Eph)(H_2O)_3$ spectrum (Figure 5.10) contains all of the features seen in the $K^+(Eph)(H_2O)_2$ spectrum, plus an increase in intensity near 3350 cm^{-1} and what is perhaps a small feature near 3475 cm^{-1}. The $K^+(Eph)(H_2O)_2$ spectrum was assigned to a combination of isomers containing free and π-hydrogen-bonded water molecules, so that makes a good starting point in the geometry search for isomers contributing to this spectrum. The minimum-energy isomer identified, K3a, contains one free water molecule, one π-hydrogen-bonded water molecule and one water molecule which was originally free but shifted to donate a hydrogen bond to the ephedrine during the geometry optimization. The calculated spectrum of isomer K3a, shown in Figure 5.10, has reasonable agreement with the experimental spectrum. The one feature that is not replicated well is the one centered near 3350 cm^{-1}. This is expected to come from some type of strong hydrogen-bonding

interaction, and the geometry search continues for another low-energy isomer that is in good agreement with the experimental spectrum.

The $Na^+(Eph)(H_2O)_3$ spectrum (Figure 5.11) also has the characteristic features of a free water molecule and a π-hydrogen-bonded water molecule near 3715, 3645 and 3585 cm^{-1}. Unlike the other warm sodium-containing spectra, this spectrum also indicates the presence of at least one isomer containing the ephedrine intramolecular hydrogen bond. The one new feature that has not been seen in any of the sodium spectra thus far is one near 3455 cm^{-1}, in the region associated with water-water (or ephedrine-water) hydrogen bonding.

At warm temperatures (near 300 K), isomers Na3b and Na3c are the minimum-energy (and virtually isoenergetic) isomers of $Na^+(Eph)(H_2O)_3$. The calculated spectra of these two isomers are shown in Figure 5.11 for comparison with the experiment. Isomer Na3b contains a free water molecule, a π-hydrogen-bonded water molecule and an almost free water molecule. This final water molecule has a very weak interaction with the side chain of the ephedrine, such that the water symmetric stretch is predicted to be shifted to about 3620 cm^{-1} rather than the usual 3650 cm^{-1}. This isomer also contains the ephedrine intramolecular hydrogen bond and is expected to contribute to the broad feature between 3100-3300 cm^{-1}. Isomer Na3c contains one free water molecule and a linear hydrogen bond between the other two water molecules, which is predicted to appear near 3410 cm^{-1}. This isomer does not contain the intramolecular hydrogen bond, so the free ephedrine OH stretch would contribute to the feature near 3650 cm^{-1} in the experimental spectrum.

Isomer Na3a, which contains a bent hydrogen bond, is the minimum-energy isomer at low temperatures, but it becomes entropically unfavorable as the temperature increases. Near 300 K, this isomer is about 5 kJ/mol higher in energy than isomers Na3b and Na3c. The bent

hydrogen bond is expected to exhibit strong features near 3540 and 3480 cm^{-1}. This is not consistent with the features in the experimental spectrum, so the assignment for $Na^+(Eph)(H_2O)_3$ will be restricted to isomers Na3b and Na3c.

Conclusions

This chapter examines the role of charge and temperature on the structure of hydrated ephedrine cluster ions. While neutral ephedrine contains an intramolecular hydrogen bond, it is not expected for this conformation to be populated in the presence of a sodium or potassium cation. It was rather unexpected then, to observed a clear signature of this feature in the $M^+(Eph)Ar$ spectra.

From the spectra of the hydrated ephedrine cluster ions, it becomes clear that the warmer species are able to populate the energetically-preferred isomers, while the colder species often exhibit evidence of higher-energy, trapped configurations. This is a result of the argon evaporation process, where the removal of internal energy from the cluster prevents rearrangement to the lower-energy conformers.

The observed $M^+(Eph)(H_2O)_nAr_{0,1}$ spectra are almost all ion-dependent. While evidence of the ephedrine intramolecular hydrogen bond was present in all of the potassium-containing spectra, it was not observed in the warm sodium-containing spectra until the addition of a third water molecule. In addition, there are significant differences, mainly in the hydrogen-bonding region, between every sodium-containing spectrum and its potassium-containing counterpart except for the $M^+(Eph)Ar$ and $M^+(Eph)(H_2O)Ar$ spectra.

Figures

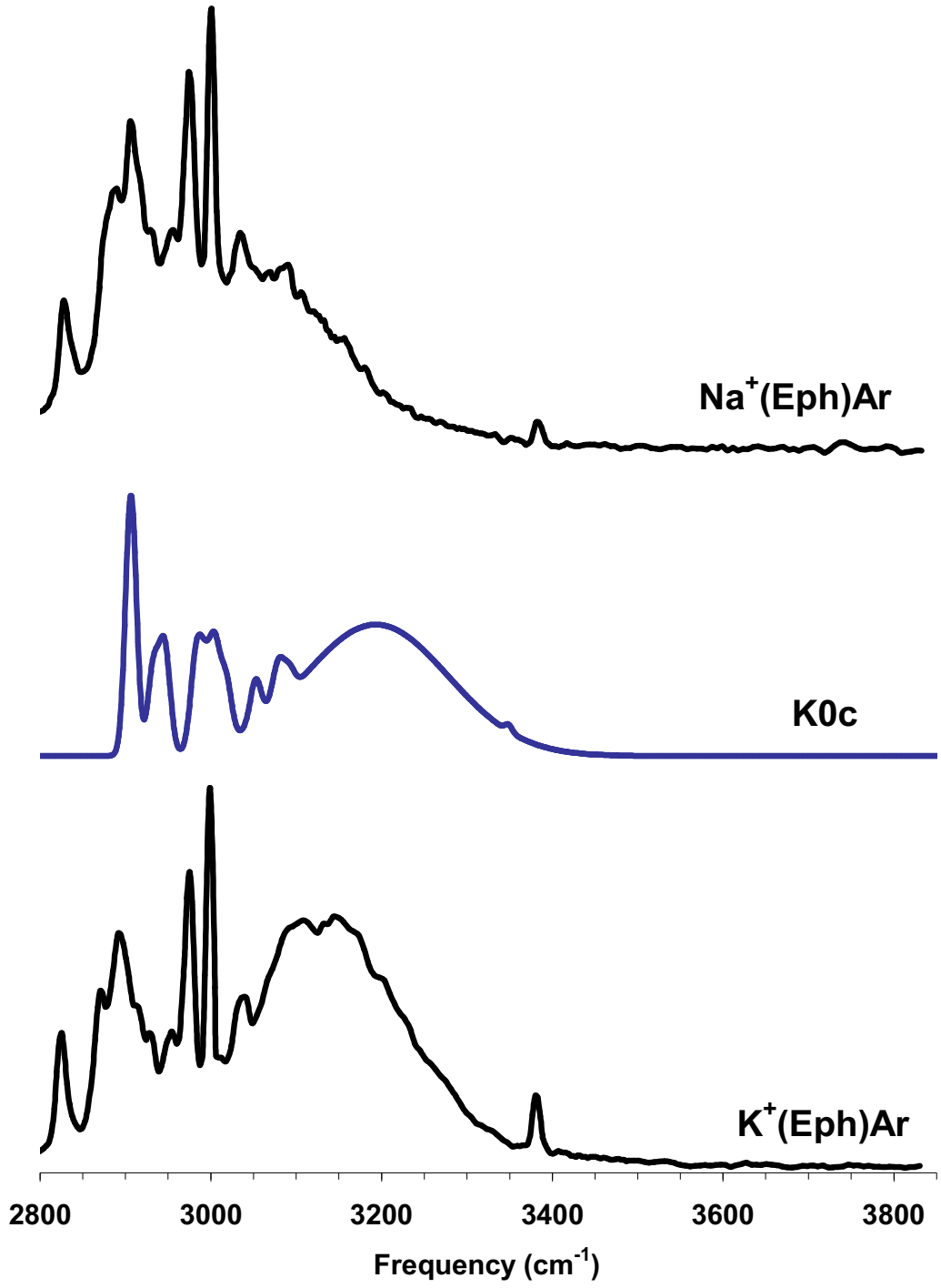

Figure 5.1: Experimental spectra of K^+(Eph)Ar (bottom) and Na^+(Eph)Ar (top), along with the calculated spectrum of isomer K0c

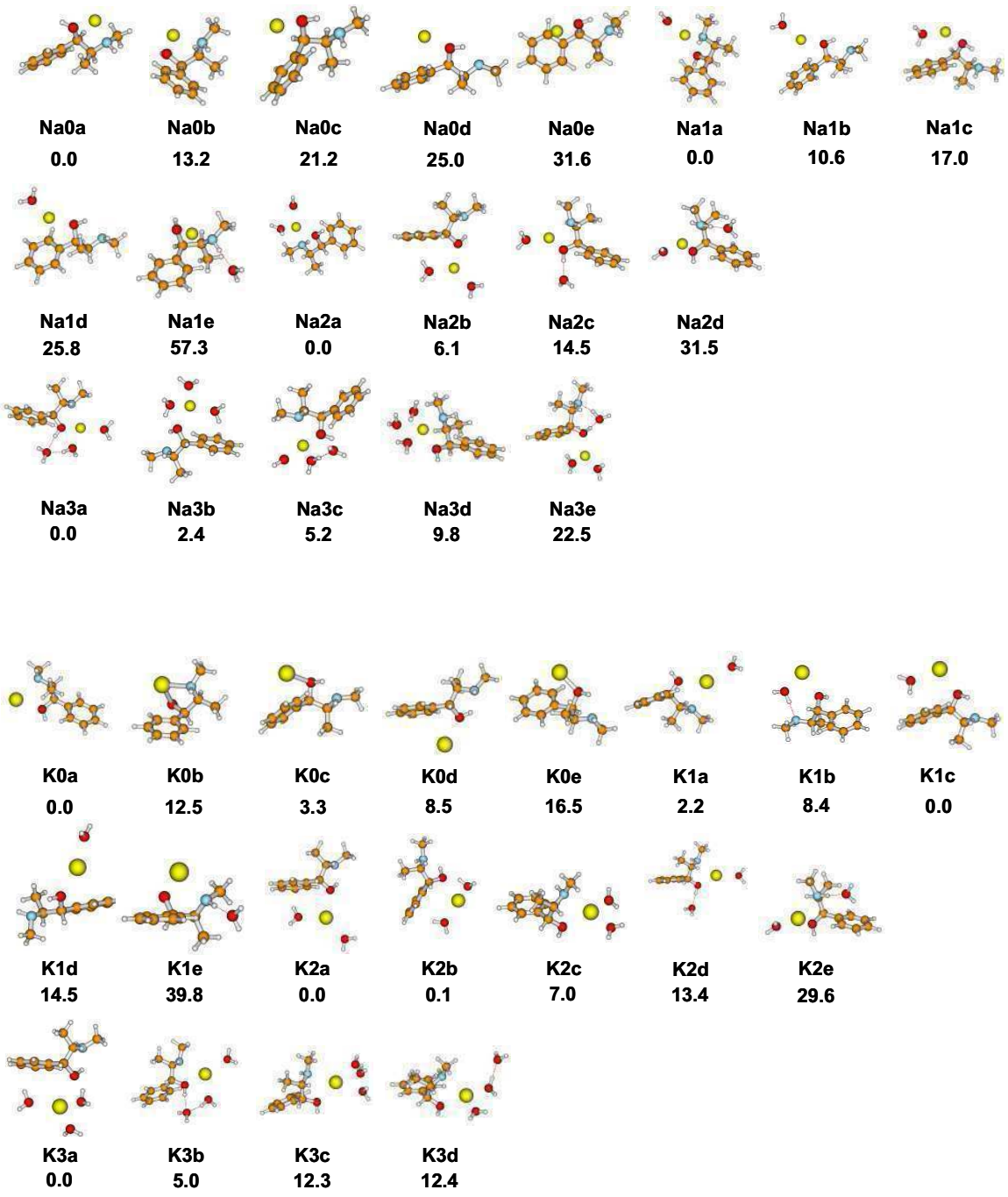

Figure 5.2: Low-energy isomers of $M^+(Eph)(H_2O)_{n=0-3}$ identified for both M = Na and K.

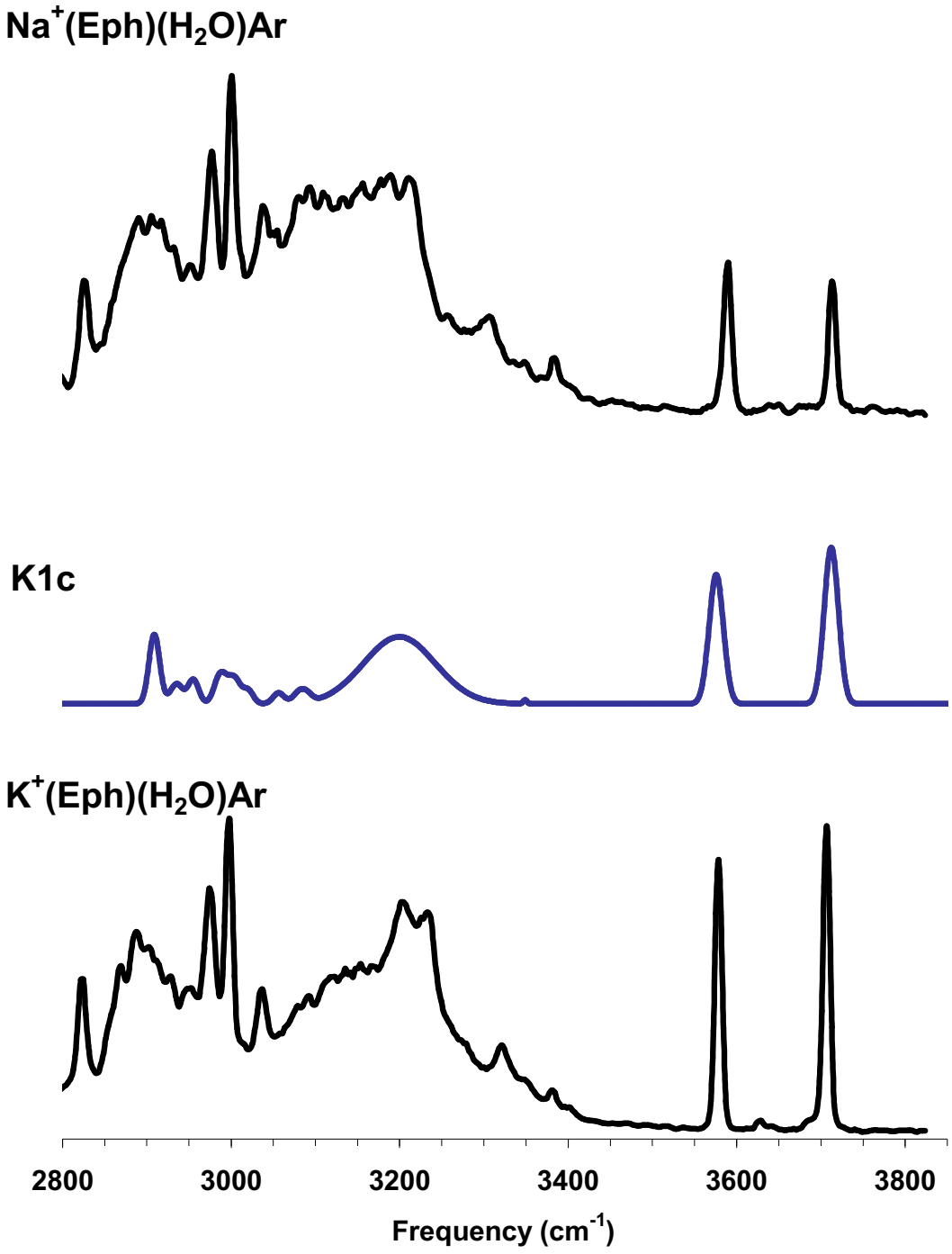

Figure 5.3: Experimental spectra of $K^+(Eph)(H_2O)Ar$ (bottom) and $Na^+(Eph)(H_2O)Ar$ (top), along with the calculated spectrum of isomer K1c

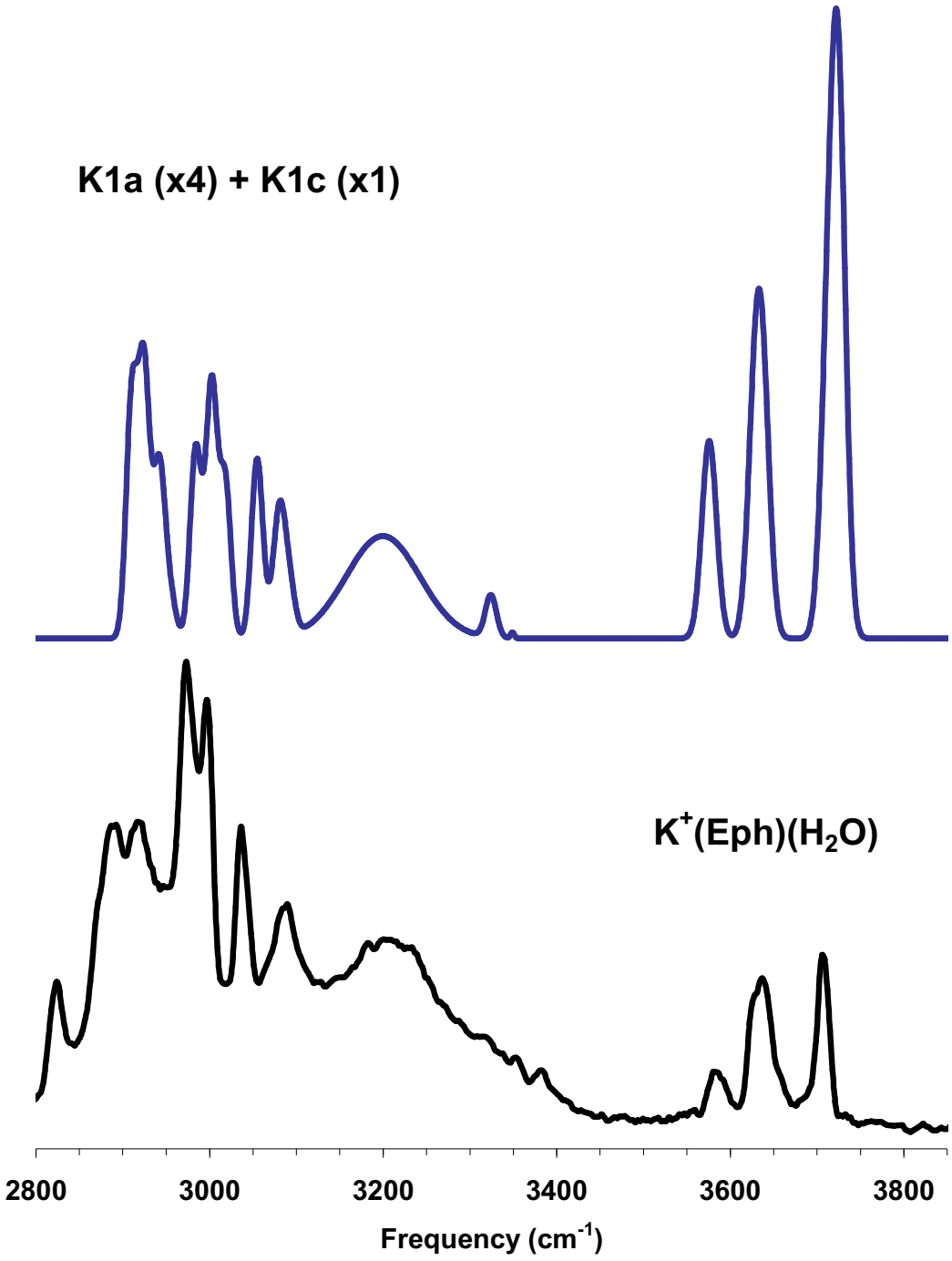

Figure 5.4: Experimental spectrum of $K^+(Eph)(H_2O)$ (bottom), along with a simulated spectrum generated by combining the calculated spectra of isomers K1a and K1c in a 4:1 ratio

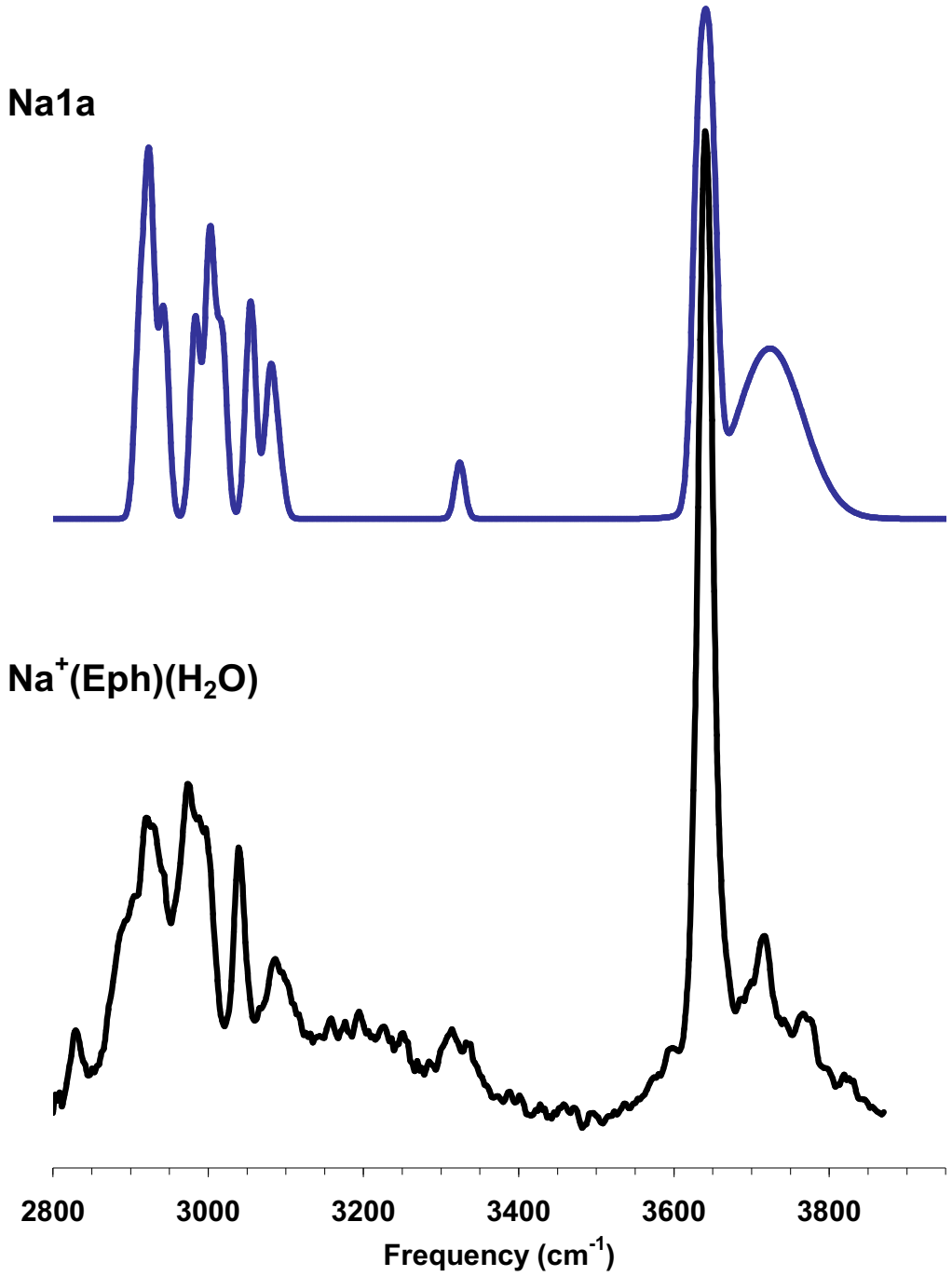

Figure 5.5: Experimental spectrum of $Na^+(Eph)(H_2O)$ (bottom), along with the calculated spectrum of isomer Na1a

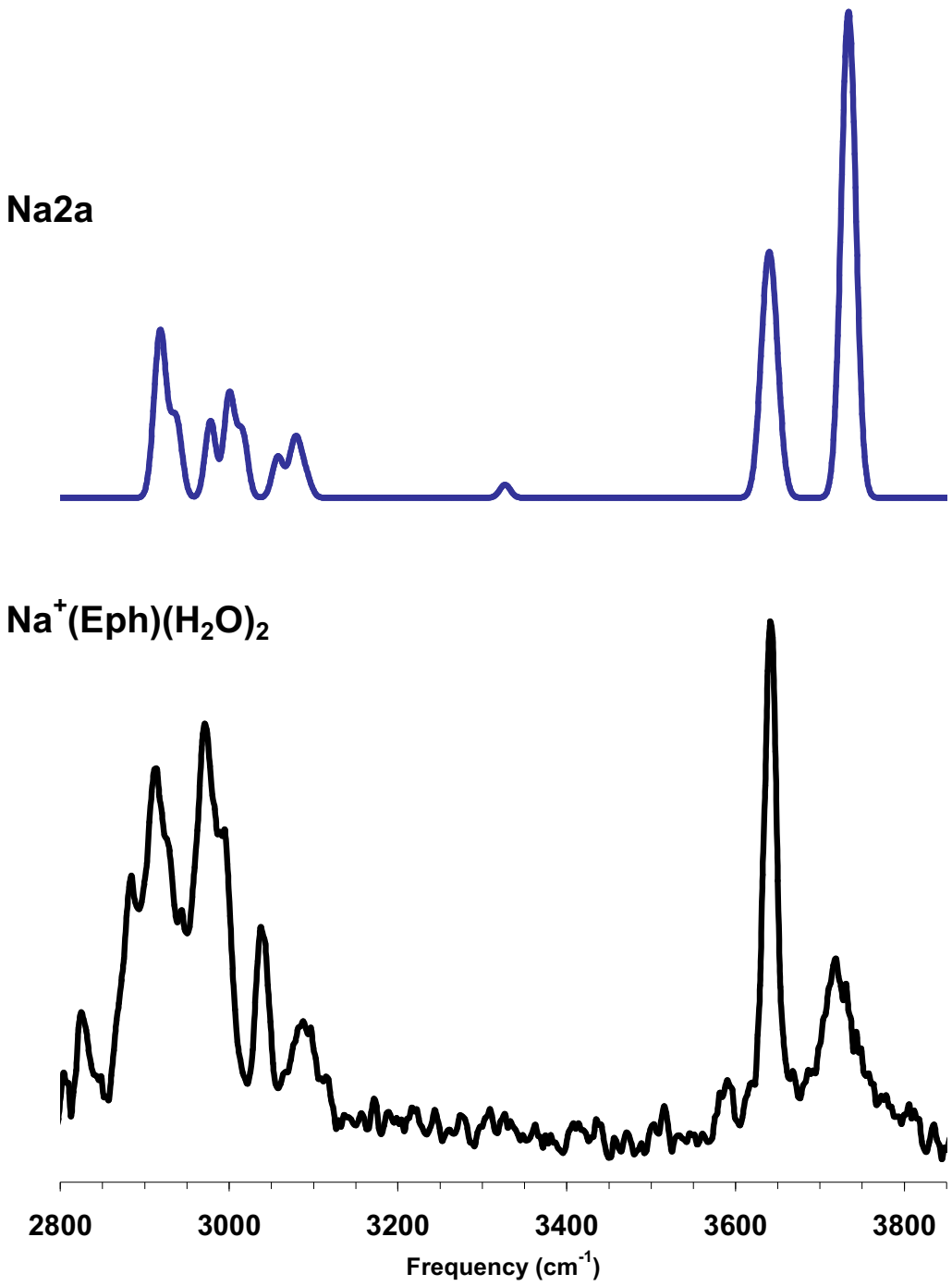

Figure 5.6: Experimental spectrum of $Na^+(Eph)(H_2O)_2$ (bottom), along with the calculated spectrum of isomer Na2a

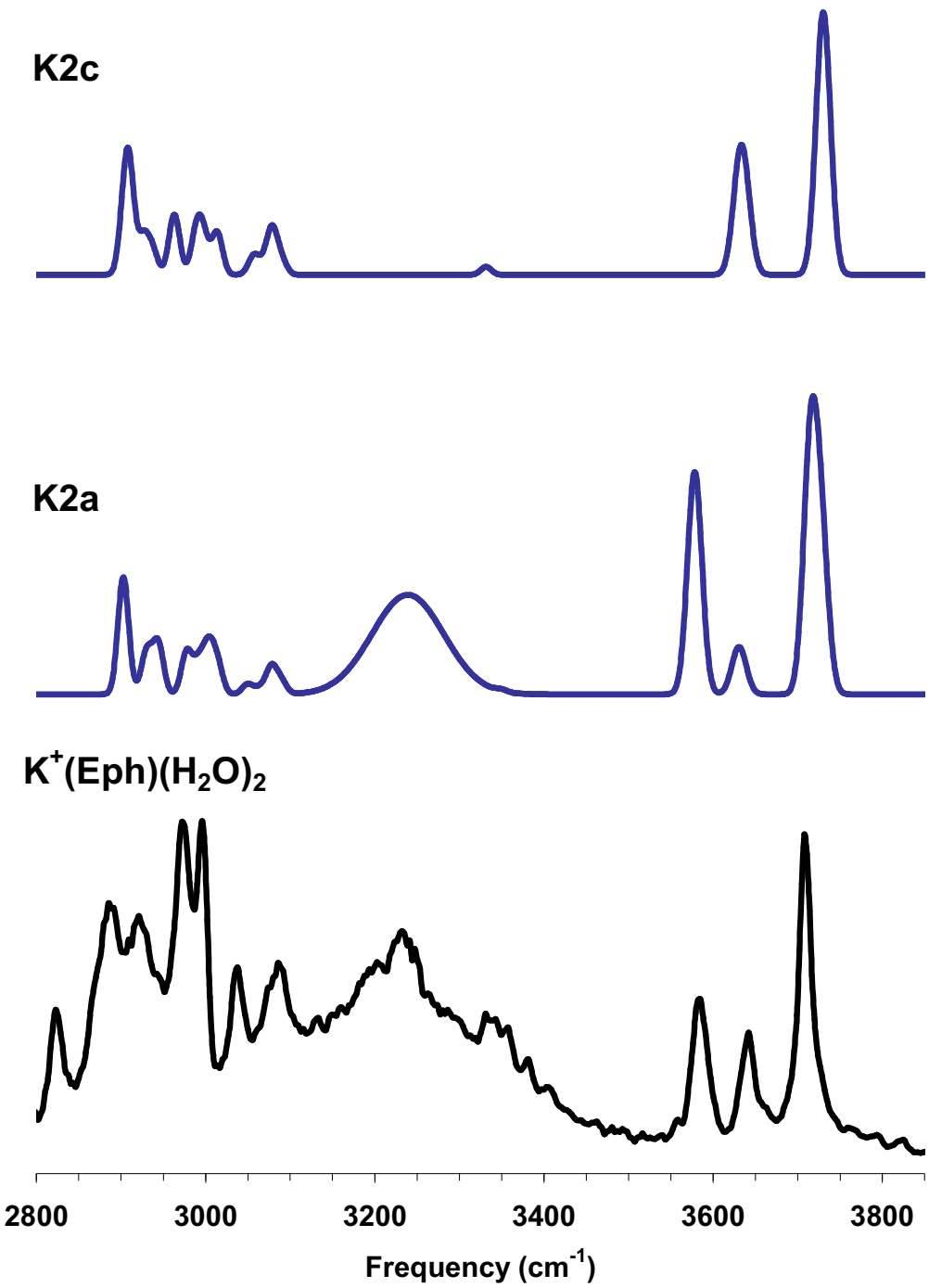

Figure 5.7: Experimental spectrum of $K^+(Eph)(H_2O)_2$ (bottom), along with the calculated spectra of isomers K2a and K2c

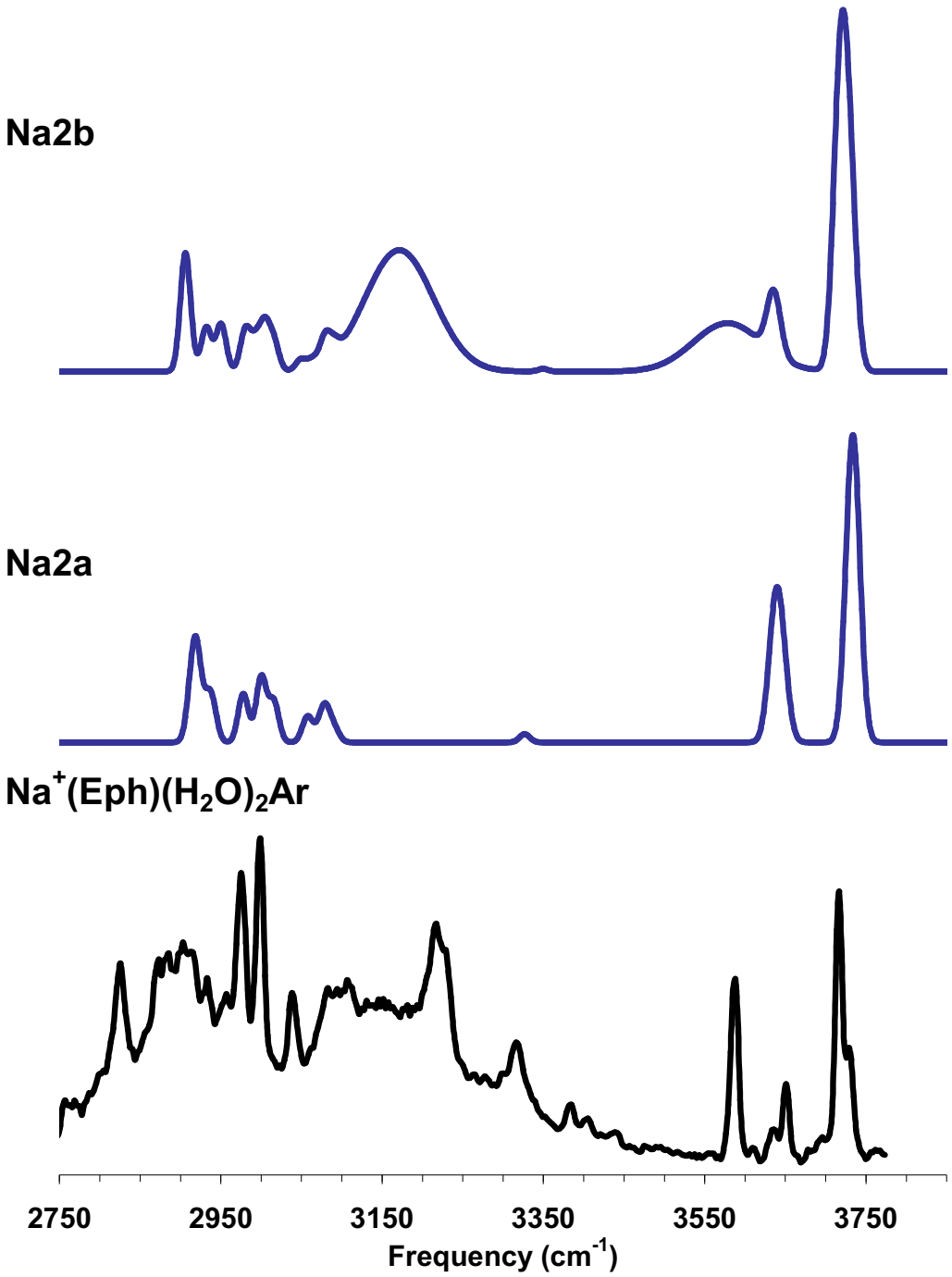

Figure 5.8: Experimental spectrum of $Na^+(Eph)(H_2O)_2Ar$ (bottom), along with the calculated spectra of isomers Na2a and Na2b

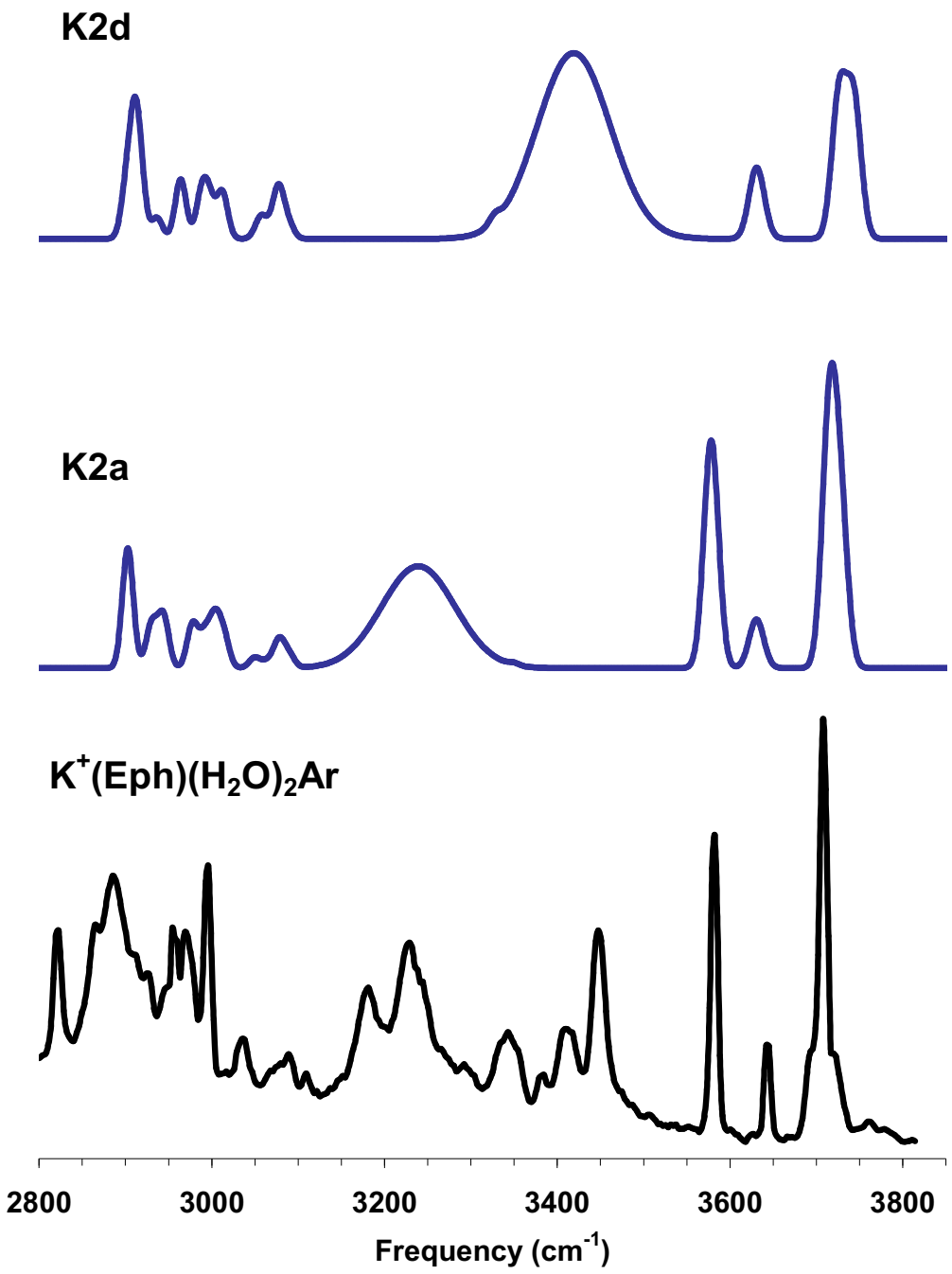

Figure 5.9: Experimental spectrum of $K^+(Eph)(H_2O)_2Ar$ (bottom), along with the calculated spectra of isomers K2a and K2d

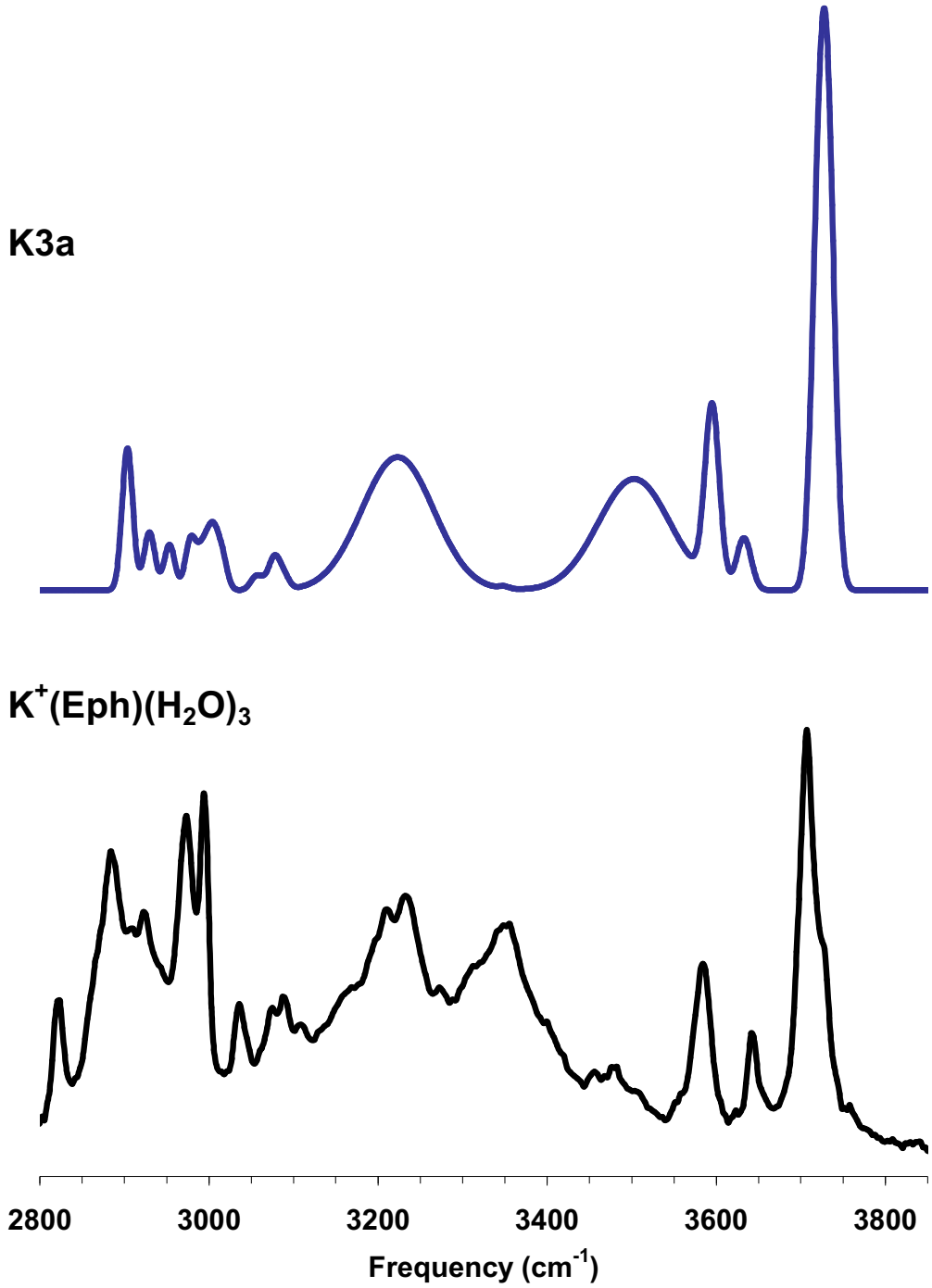

Figure 5.10: Experimental spectrum of $K^+(Eph)(H_2O)_3$ (bottom), along with the calculated spectrum of isomer K3a

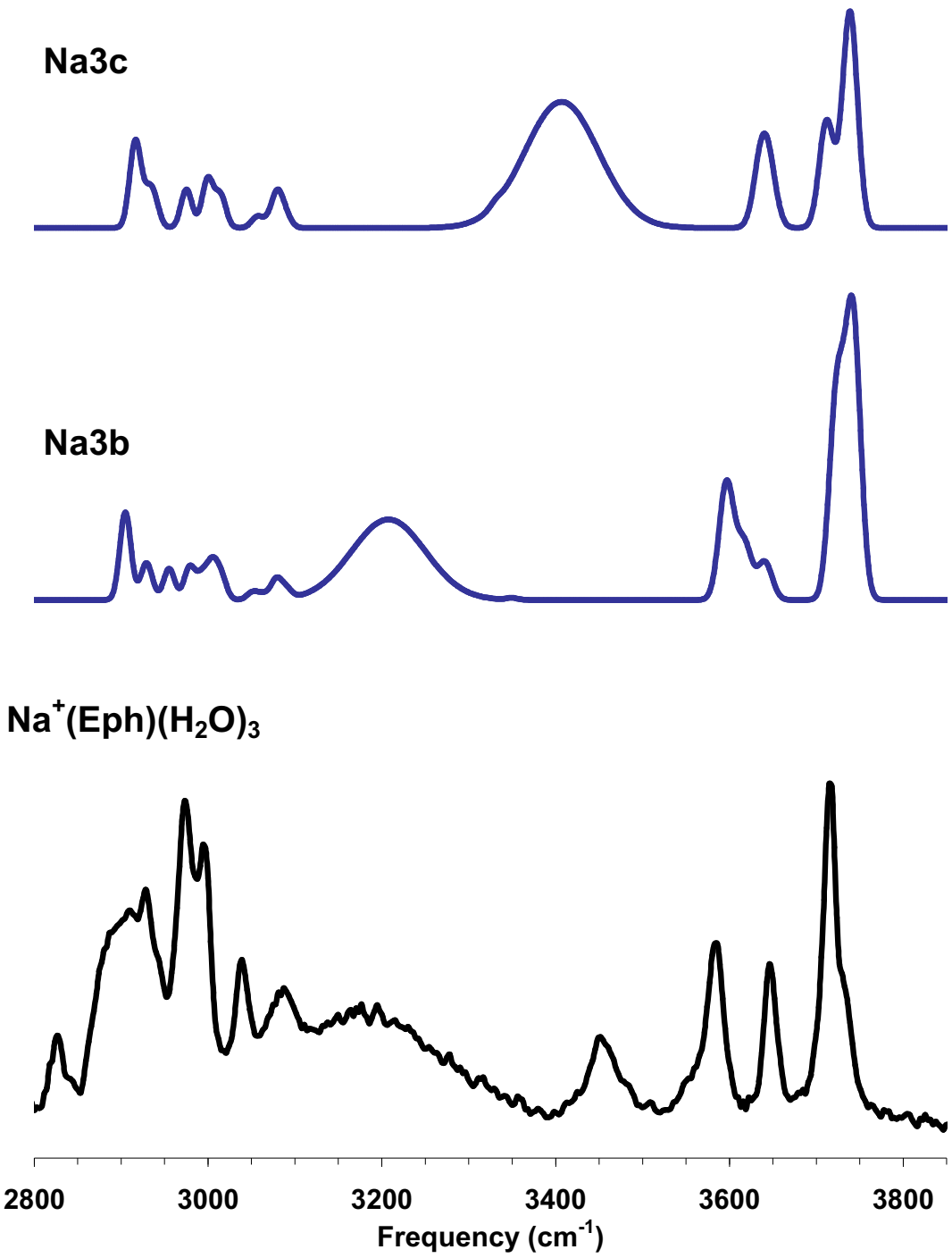

Figure 5.11: Experimental spectrum of $Na^+(Eph)(H_2O)_3$ (bottom), along with the calculated spectra of isomers Na3b and Na3c

References

1. Drew, C. D. M.; Knight, G. T.; Hughes, D. T. D.; Bush, M., Br. J. Clin. Pharmacol. 1978, 6, (3), 221.
2. Vansal, S. S.; Feller, D. R., Biochem. Pharmacol. 1999, 58, (5), 807.
3. Chervenkov, S.; Wang, P. Q.; Braun, J. E.; Neusser, H. J., J. Chem. Phys. 2004, 121, (15), 7169.
4. Alonso, J. L.; Sanz, M. E.; Lopez, J. C.; Cortijo, V., J. Am. Chem. Soc. 2009, 131, (12), 4320.
5. Butz, P.; Kroemer, R. T.; Macleod, N. A.; Simons, J. P., J. Phys. Chem. A 2001, 105, (3), 544.
6. Simons, J. P., Comptes Rendus Chimie 2003, 6, (1), 17.
7. Baker, C. M.; Grant, G. H., J. Phys. Chem. B 2007, 111, (33), 9940.
8. Graham, R. J.; Kroemer, R. T.; Mons, M.; Robertson, E. G.; Snoek, L. C.; Simons, J. P., J. Phys. Chem. A 1999, 103, (48), 9706.
9. Macleod, N. A.; Robertson, E. G.; Simons, J. P., Mol. Phys. 2003, 101, (14), 2199.
10. Miller III, T. F.; Clary, D. C., J. Phys. Chem. B 2004, 108, (7), 2484.
11. Butz, P.; Kroemer, R. T.; Macleod, N. A.; Simons, J. P., Phys. Chem. Chem. Phys. 2002, 4, (15), 3566.
12. Nicely, A. L.; Lisy, J. M., in preparation (Tryp).
13. Nicely, A. L.; Miller, D. J.; Lisy, J. M., J. Am. Chem. Soc. 2009, 131, (18), 6314.
14. Nicely, A., In preparation (APE).
15. Nicely, A. L.; Miller, D. J.; Lisy, J. M., J. Mol. Spectrosc. 2009, 257, (2), 157.
16. Miller, D. J.; Lisy, J. M., J. Am. Chem. Soc. 2008, 130, (46), 15393-15404.
17. Miller, D. J.; Lisy, J. M., J. Am. Chem. Soc. 2008, 130, (46), 15381-15392.
18. Vaden, T. D.; Forinash, B.; Lisy, J. M., J. Chem. Phys. 2002, 117, (10), 4628.
19. Vaden, T. D.; Weinheimer, C. J.; Lisy, J. M., J. Chem. Phys. 2004, 121, (7), 3102.

Chapter 6: Monte Carlo and Molecular Dynamics Simulations

Introduction

For the experimental systems discussed in the previous chapters, the preliminary geometries were generated using SPARTAN but relied on the intuition of the researcher or previous theoretical work. Because of this, important structures which may contribute to the experimental spectra may be neglected. A better approach to generating the initial geometries should be systematic and depend solely on the interactions between the components in the system. For the following discussion, the term "components" will refer to any ions, atoms or molecules in the cluster ions. Several approaches were used to systematically sample the potential energy surface, as described in the following sections.

Monte Carlo Simulations

An Ion Cluster Structure Generator (ICSG)[1] has been written and developed in-house following the Monte Carlo Metropolis algorithm[2]. This program, written in the C++ programming language, began by randomly positioning the components of the system in a box. The total energy of the system was computed by summing over all possible pairwise interactions using potentials published in the literature to incorporate M^+-Ar[3], M^+-H_2O[4], H_2O-H_2O[5] and H_2O-Ar[6] interactions. For each "step", a random component was selected and a small perturbation applied to its x, y and z coordinates. Water molecules were treated as rigid objects which translated and rotated as a unit when they were selected for a move. Once a move was completed, the new energy of the system was calculated. If the move resulted in a decrease in energy, it was accepted automatically. If the move resulted in an increase in energy, it was

evaluated further to determine whether it would be accepted. The probability that an increased energy would be accepted depends on a Boltzmann factor, as shown in Equation (1):

$$P(\Delta E) = \exp(-\Delta E / k_B T) \quad (1)$$

A random number between 0 and 1 was generated and compared with P(ΔE). The move was accepted if P(ΔE) was greater than the random number and rejected (and the components returned to their previous state) if P(ΔE) was less than or equal to the random number. This process of making and evaluating moves was repeated for a set number of iterations.

Several additional features were added to the code to help maximize the number of configurations sampled and to identify those configurations for further geometry optimization. First, it became necessary to periodically introduce large perturbations to the system so that it did not become stuck in a local (or absolute) minimum. This was accomplished by performing "wormhole" moves in which two components were randomly selected and swapped. This shifted the system out of an equilibrium state and allowed it to sample different configurations as it returned to its preferred structure.

Since each full run involved tens to hundreds of thousands of steps, it would be impractical to go through each one of them in order to identify unique structures. Instead, "snapshots" were taken periodically (as defined by the user) in which the coordinates of all of the components were saved and then later subjected to geometry optimization. In this manner, one simulation could generate anywhere from one to several hundred configurations, many of which ultimately collapsed into the same preferred structures.

Application to $Na^+(H_2O)_4$

Three low-energy isomers of $Na^+(H_2O)_4$ cluster ions were identified using the standard method of generating structures using SPARTAN and optimizing the geometries using Gaussian.[7] As a test of the algorithms, the ICSG was also used to generate isomers of $Na^+(H_2O)_4$, with the goal to have the program identify, at a minimum, the same three isomers which had already been identified with the traditional method. The ICSG was run at temperatures ranging from 50-350 K (in increments of 50 K), with a total of 2.5 million steps at each temperature. Wormhole moles were performed every 250,000 steps, and snapshots were taken 1500 steps after each wormhole move. The maximum step size was 0.18 Angstroms, and the maximum water rotation was 15°. The resulting isomers included the three which had been previously identified, plus two additional isomers. All five isomers are shown in Figure 6.1, along with their relative energies in kJ/mol. Although the new isomers were significantly higher in energy, the ICSG was still successful in identifying a full collection of potential isomers. As discussed in the previous chapters, our experiments are often able to trap high-energy isomers during cluster ion formation, so it is important to have a complete picture of the potential structural isomers which may contribute to each experiment.

Graphical User Interface

A graphical user interface (GUI) written in Java was added to the ICSG to make the program more user-friendly. The initial version of the program was entirely text-based and required the user to have some familiarity with the conventions of the input files. The GUI was a significant improvement because it had built-in documentation to walk the user through the simulation setup process. The GUI included five tabs, four of which were used for program

input such as the number of steps for the simulation or the components to include in the clusters. The five tabs are shown in Figures 6.2-6.6.

Figure 6.2 depicts the "About" tab, which includes basic information about the program and briefly describes the content of the other tabs. The "Components" tab is shown in Figure 6.3. This is the section in which the user selects which ion (if any) and ligands to include in the simulation. In addition, the source of the initial geometries (random or read from an input file) can be selected. The user can also specify a minimum ion-ligand distance for the starting geometry. Figure 6.4 shows the "Step Settings" panel, which includes all of the parameters related to the temperature of the simulation; minimum and maximum step sizes and angles of rotation; number of total steps, frequency of wormhole moves and frequency of saving data; and parameters for saving geometry data. Figure 6.5 shows the "Constants" panel. The parameters on this tab are already included, and in general, the user should not need to make any changes to these values. Finally, Figure 6.6 shows the "Output" panel, which allows the user to specify the location for the output files to be saved.

To run a simulation, the user simply needs to execute a script. The GUI will open, and the program will wait for all of the input to be entered. When the user closes the GUI, the script will automatically transfer all the input to the ICSG code, run the simulation and submit the appropriate geometries for optimization.

Aminoethanol

In an effort to expand the functionality of the ICSG, an additional ligand – aminoethanol - was added. Aminoethanol was selected since it was a relatively simple organic molecule, and it incorporated both an amino group and an alcohol group. This was an important characteristic

since the actual experiments in the lab included ligands such as tryptamine and ephedrine that included these two functional groups.

Addition of a new ligand to the program would require M^+-ligand, water-ligand and argon-ligand potentials (and a ligand-ligand potential if a simulation involving a cluster ion with more than one ligand was desired). Although the pairwise potentials for a specific ligand may not be available, there are force fields which can be used to create a potential for the desired ligand. Such a force field was used to generate the M^+-aminoethanol and water-aminoethanol potentials.[8] Unfortunately, the parameters for argon were not included in this force field, so simulations involving aminoethanol could not also include argon atoms.

Molecular Dynamics Simulations

Although possible, the inclusion of additional ligands was a time-consuming process. At this point it became clear that a home-built simulation program would not be able to keep up with the diversity of the actual experiments being performed in the lab. Fortunately, there are other programs available that are capable of performing similar types of simulations.

The program selected for use in our lab was NAMD,[9] a free molecular dynamics code specifically designed for large biomolecular systems. The initial tests were run with 2-amino-1-phenylethanol (APE) in a water sphere. Although parameter files are readily available for a wide variety of molecules, we were unable to locate parameters for APE. Instead, modifications were made to the parameters for ethanolamine – one hydrogen was replaced by a benzene ring and one proton was removed altogether – using molecules with similar functional groups as a guide.

$Na^+(APE)(H_2O)_n$ simulations

The output from the previous simulation was an optimized APE molecule surrounded by a sphere of water molecules. The minimized geometry included a network of water molecules inserted between the OH and NH groups, consistent with the structure of small $APE(H_2O)_n$ clusters.[10, 11] One of the outer water molecules was then replaced by a Na^+ in order to monitor the impact of the cation on the preferred APE structure. The $APE(H_2O)_n$ cluster was subjected to an energy minimization of 1000 steps followed by 500,000 equilibration steps, where each step corresponds to 2 fs. Thus, the equilibrations lasted for a total of 1 ns. Simulations were run at several different temperatures (50, 200 and 310 K).

The simulation output files were examined using the Visual Molecular Dynamics (VMD) program.[12] VMD was developed by the Theoretical and Computational Biophysics Group in the Beckman Institute for Advanced Science and Technology at the University of Illinois at Urbana-Champaign. For each simulation, the trajectory was viewed and analyzed. At 50 K, the water sphere appeared to be more or less frozen, and no significant interactions between the sodium cation and the APE molecule were observed. At both 200 and 310 K, the sodium cation approached the APE molecule, but then drifted away as the simulation progressed.

Figures

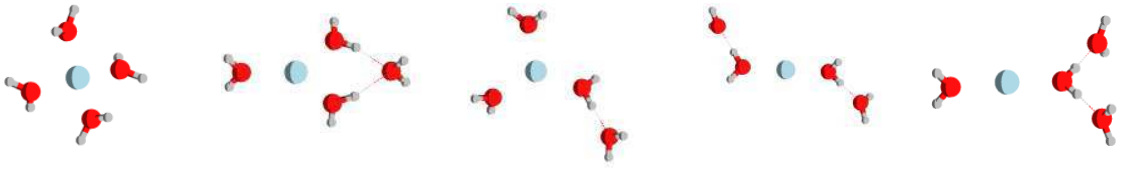

Figure 6.1: $Na^+(H_2O)_4$ isomers identified using the ICSG. Relative energies are given in kJ/mol. The three lowest-energy isomers were also identified using traditional methods, while the two higher-energy isomers had not been previously considered as possible contributors to the $Na^+(H_2O)_4$ IRPD spectrum.

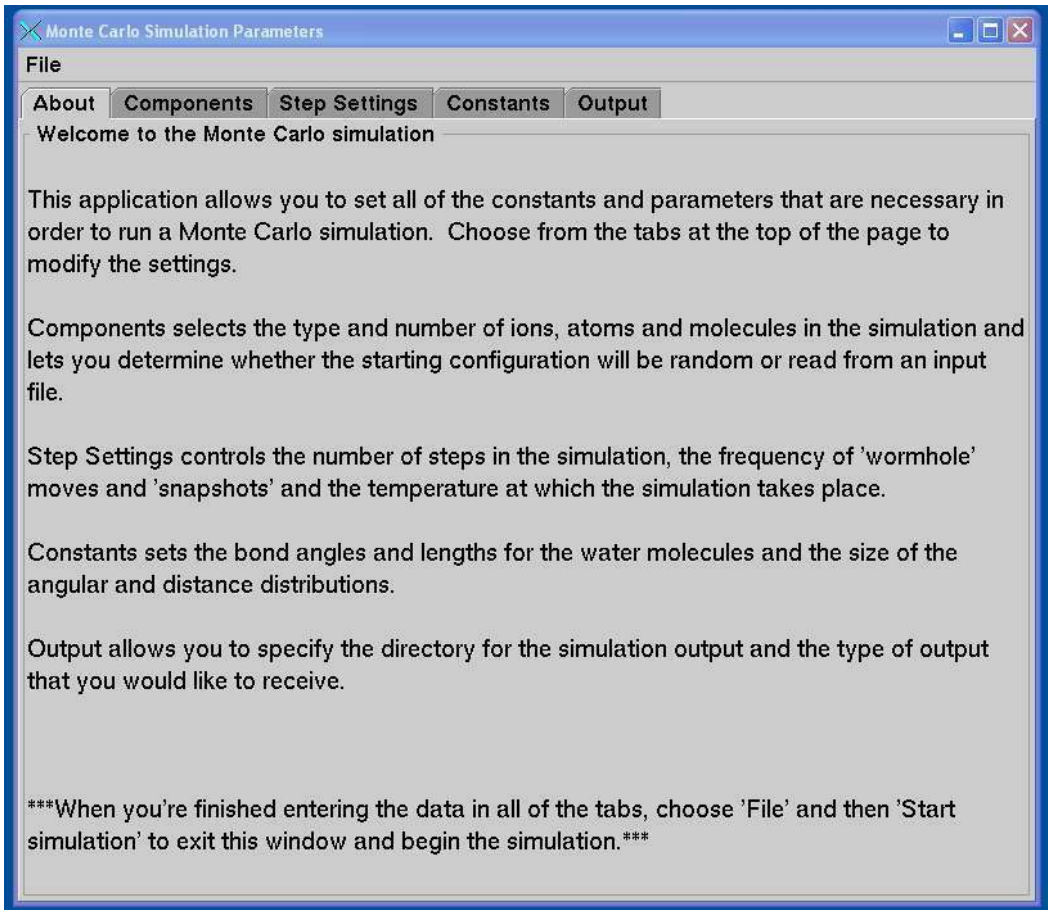

Figure 6.2: Screenshot of the "About" tab in the GUI designed for use with the ICSG simulation program

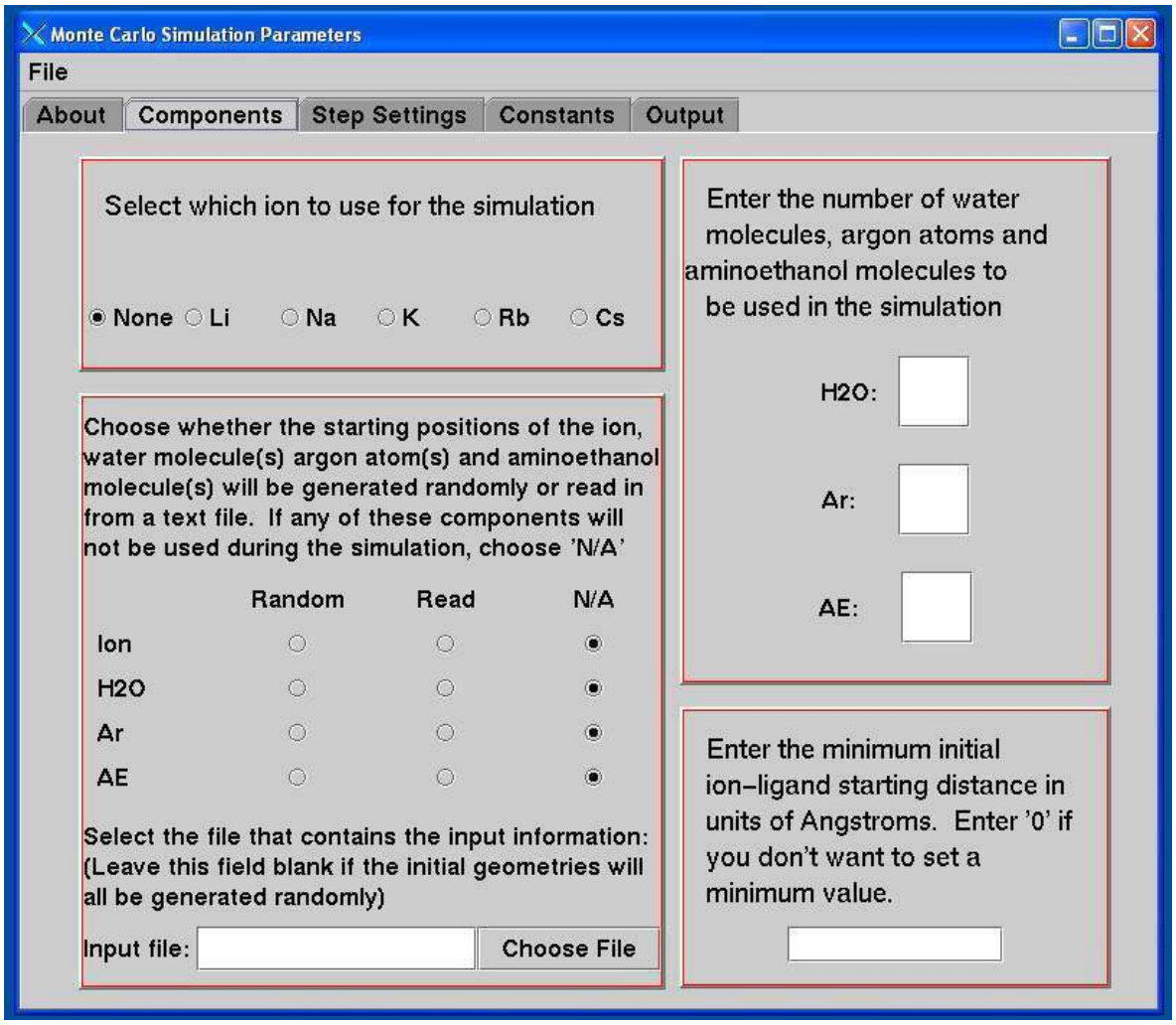

Figure 6.3: Screenshot of the "Components" tab in the GUI designed for use with the ICSG simulation program

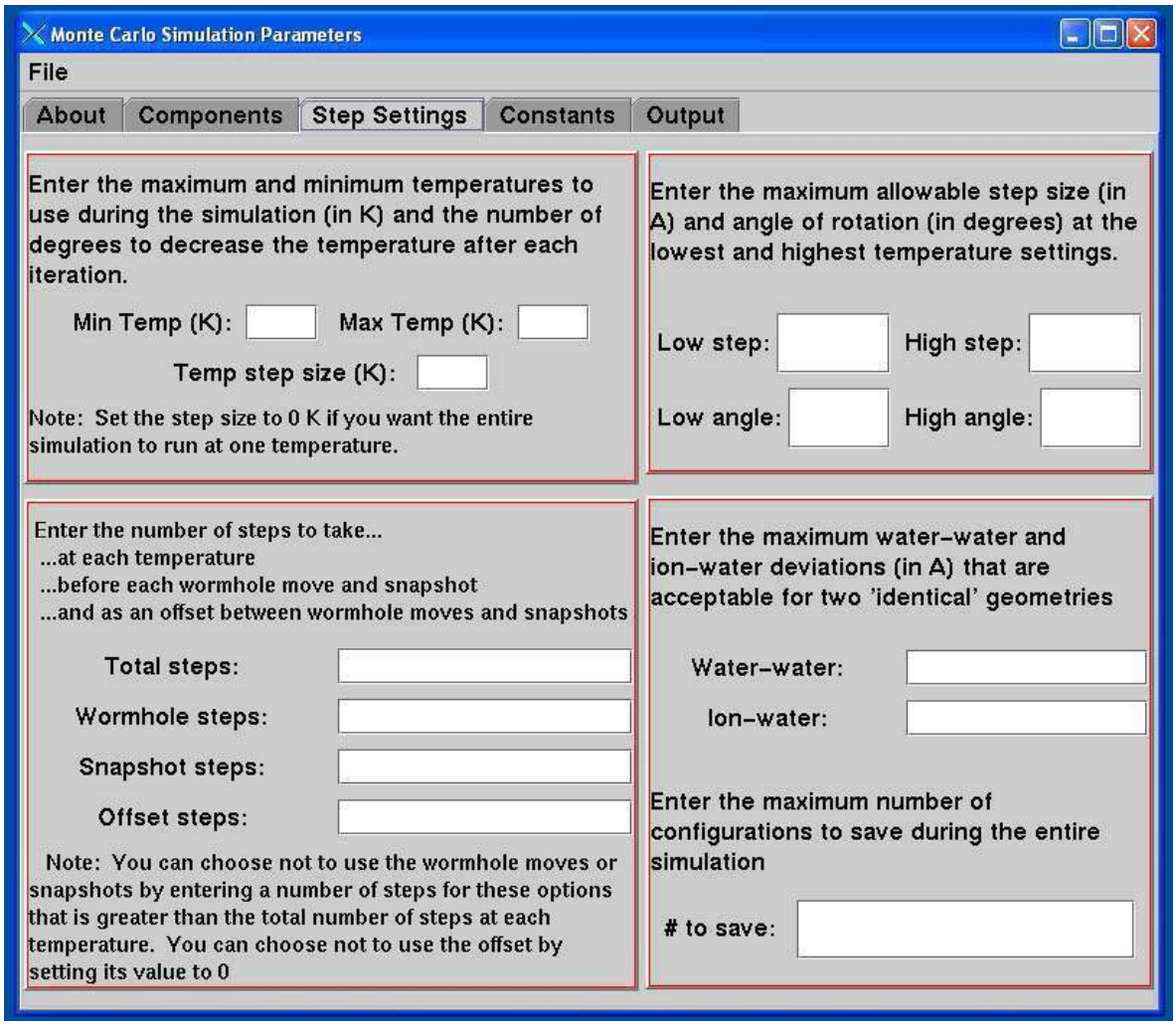

Figure 6.4: Screenshot of the "Step Settings" tab in the GUI designed for use with the ICSG simulation program

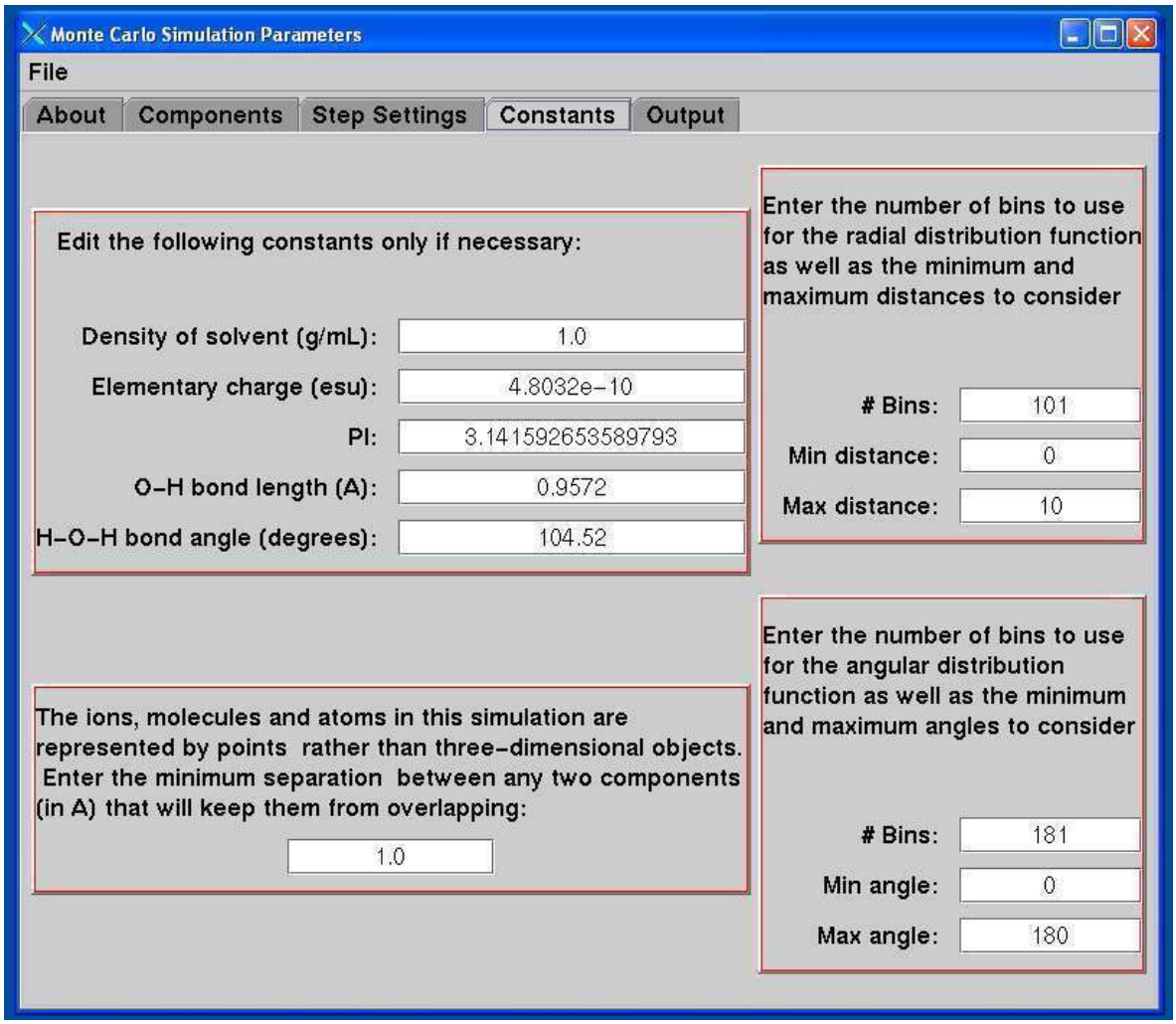

Figure 6.5: Screenshot of the "Constants" tab in the GUI designed for use with the ICSG simulation program

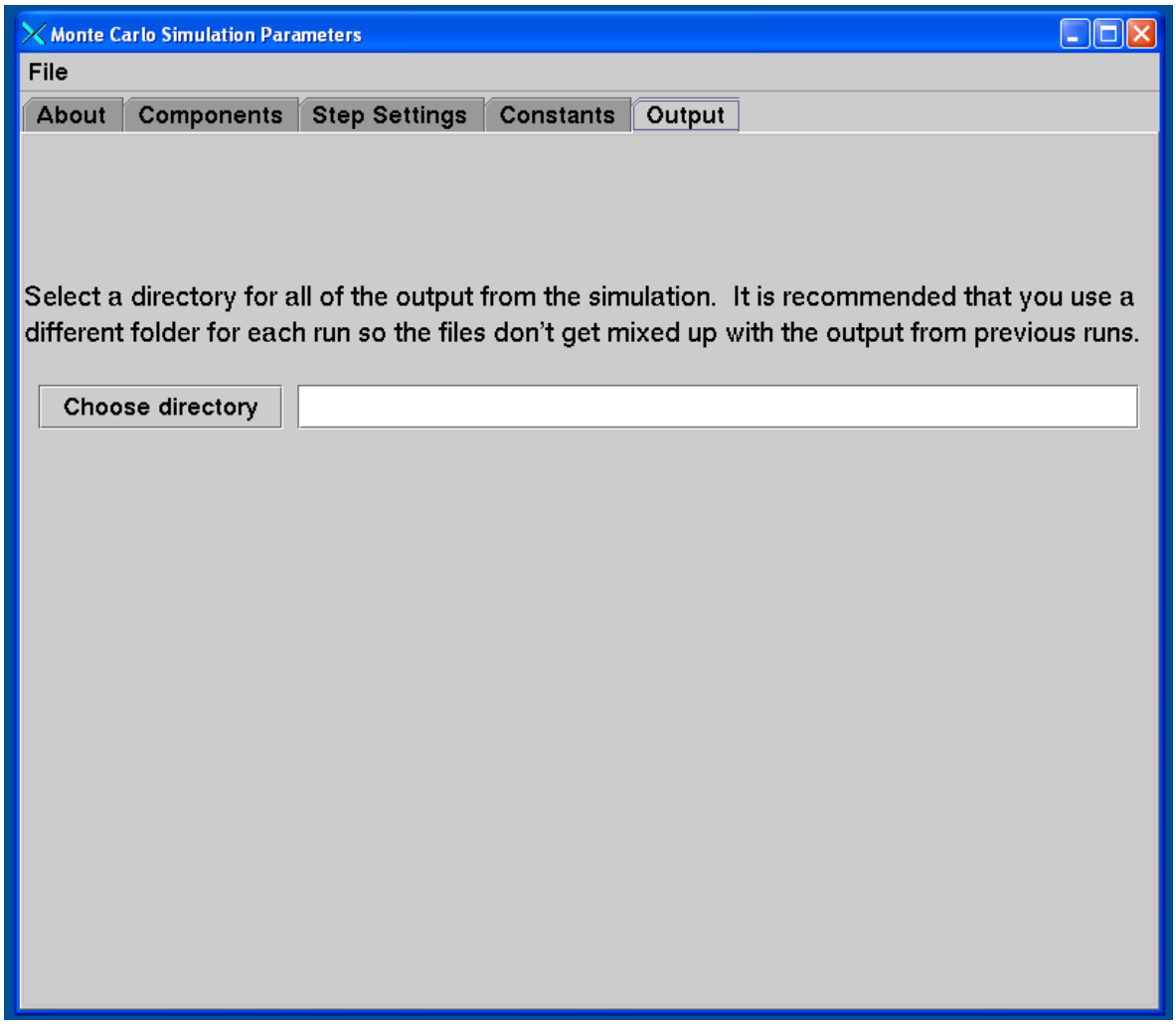

Figure 6.6: Screenshot of the "Output" tab in the GUI designed for use with the ICSG simulation program

References

1. Nicely, A. Ion Cluster Structure Generator 06, Department of Chemistry, University of Illinois: Urbana, IL, 2007.
2. Metropolis, N.; Rosenbluth, A. W.; Rosenbluth, M. N.; Teller, A. H.; Teller, E., J. Chem. Phys. 1953, 21, (6), 1087-1092.
3. Koutselos, A. D.; Mason, E. A.; Viehland, L. A., J. Chem. Phys. 1990, 93, (10), 7125-7136.
4. Lee, S. H.; Rasaiah, J. C., J. Chem. Phys. 1994, 101, (8), 6964-6974.
5. Jorgensen, W. L.; Chandrasekhar, J.; Madura, J. D.; Impey, R. W.; Klein, M. L., J. Chem. Phys. 1983, 79, (2), 926-935.
6. Anderson, B. J.; Tester, J. W.; Trout, B. L., J. Phys. Chem. B 2004, 108, (48), 18705-18715.
7. Miller, D. J.; Lisy, J. M., J. Am. Chem. Soc. 2008, 130, (46), 15393-15404.
8. Cornell, W. D.; Cieplak, P.; Bayly, C. I.; Gould, I. R.; Merz, K. M.; Ferguson, D. M.; Spellmeyer, D. C.; Fox, T.; Caldwell, J. W.; Kollman, P. A., J. Am. Chem. Soc. 1995, 117, (19), 5179.
9. Phillips, J. C.; Braun, R.; Wang, W.; Gumbart, J.; Tajkhorshid, E.; Villa, E.; Chipot, C.; Skeel, R. D.; Kalé, L.; Schulten, K., J. Comput. Chem. 2005, 26, (16), 1781-1802.
10. Graham, R. J.; Kroemer, R. T.; Mons, M.; Robertson, E. G.; Snoek, L. C.; Simons, J. P., J. Phys. Chem. A 1999, 103, (48), 9706.
11. Macleod, N. A.; Robertson, E. G.; Simons, J. P., Mol. Phys. 2003, 101, (14), 2199.
12. Humphrey, W.; Dalke, A.; Schulten, K., J. Molecular Graphics 1996, 14, 33-38.

Chapter 7: Conclusions

The chapters of this dissertation have explored the role of charge and temperature on the gas-phase structure of various hydrated cluster ions. As discussed in Chapter 2, the formation and relative abundance of $Rb^+(H_2O)_n$ and $Rb^+(H_2O)_nAr$ isomers are heavily dependent on the temperature of the cluster ions. For n=3, for example, the dominant isomer of $Rb^+(H_2O)_3Ar$ has a water molecule in the second solvent shell secured by two bent hydrogen bonds from the remaining waters in the first shell, while the warmer $Rb^+(H_2O)_3$ favored a structure with no hydrogen bonds that maximized water-ion interactions. For n=4, the dominant configurations for both the warm and cold cluster ions exhibit hydrogen bonding. The cold cluster ions had multiple hydrogen bonds, with bent and cyclic structures, while the warm cluster ions are dominated by a single linear hydrogen bond.

Rubidium tends to bridge the difference in behavior between potassium and cesium, as seen in Figures 2.6, 2.9 and 2.13. For the argonated cluster ions, the rubidium spectra resemble the potassium spectra for the n=3 and n=4 cases but resembles cesium for n=5. In the warmer experiments, the rubidium spectra reflect a combination of both the potassium and cesium spectra at each cluster size.

In Chapter 3, the spectra of M^+(Tryp)Ar, M^+(Tryp)(H_2O) and M^+(Tryp)(H_2O)Ar spectra were shown to not be particularly ion-dependent. The isomers assigned to the sodium spectra were all identical to those assigned to the potassium spectra. Except for K^+(Tryp)Ar and K^+(Tryp)(H_2O), the potassiated cluster ions displayed evidence of "sandwiched" water molecules. In contrast, these water sandwiches were only observed

for the sodiated cluster ions containing argon. The warmer $Na^+(Tryp)(H_2O)_{1\text{-}3}$ spectra were assigned to isomers containing mostly free or π-hydrogen-bonded water molecules.

For $K^+(Tryp)(H_2O)_{2,3,}$ the spectra were assigned to contributions from a greater number of isomers compared to the corresponding sodium-containing cluster ions. It appears that the stronger electrostatic interactions between sodium and water leads to a preference for one or two structural isomers in any given cluster ion. In contrast, the potassium-water electrostatic interactions are weaker and must compete with water-Tryp and water-water interactions of comparable strength, which leads to population of multiple low-energy isomers.

The spectra of hydrated APE cluster ions, discussed in Chapter 4, demonstrate a strong dependence on both the identity of M^+ and the evaporative cooling pathway. Cluster ions stabilized through the loss of argon are able to trap high-energy conformers, while cluster ions stabilized through the loss of water tend to reach thermodynamic equilibrium.

The cold n=0 and n=1 spectra were similar for both ions, although the features in the $Na^+(APE)Ar$ and $Na^+(APE)(H_2O)Ar$ spectra were shifted lower in frequency compared to the $K^+(APE)Ar$ and $K^+(APE)(H_2O)Ar$ due to the stronger electrostatic forces of the sodium ion. For all of the other spectra (with the exception of $M^+(APE)(H_2O)_3Ar$), the potassium spectra were more complex, and were assigned to contributions from multiple isomers. Also, almost every potassium spectrum contained features from isomers with an APE intramolecular hydrogen bond as well as those in which the potassium ion interrupted the internal hydrogen bond. The low-energy structures for sodium-containing isomers consistently indicated a strong preference for the sodium ion

to interrupt the APE internal hydrogen bond, while low-energy potassium-containing isomers were identified both with and without the internal hydrogen bond.

In the last of the experimental studies, Chapter 5 examined the role of charge and temperature on the structure of hydrated ephedrine cluster ions. It was clear that the warmer species are able to populate the energetically-preferred isomers, while the colder species often exhibit evidence of higher-energy, trapped configurations. This is a result of the argon evaporation process, where the removal of internal energy from the cluster prevents rearrangement to the lower-energy conformers.

The observed $M^+(Eph)(H_2O)_nAr_{0,1}$ spectra are almost all ion-dependent. While evidence of the ephedrine intramolecular hydrogen bond was present in all of the potassium-containing spectra, it was not observed in the warm sodium-containing spectra until the addition of a third water molecule. In addition, there are significant differences, mainly in the hydrogen-bonding region, between every sodium-containing spectrum and its potassium-containing counterpart except for the $M^+(Eph)Ar$ and $M^+(Eph)(H_2O)Ar$ spectra.

Finally, Chapter 6 presented an overview of the simulations used to help explore the potential energy surface of the various hydrated cluster ions. First, an Ion Cluster Structure Generator (ICSG) was written and developed to model $M^+(H_2O)_n$ cluster ions using pairwise interaction potentials. A combination of the Metropolis algorithm and "wormhole" moves ensured that the simulation sampled a variety of configurations. Argon atoms and ethanolamine molecules were also incorporated into the program to add extra versatility to the types of cluster ions which could be modeled.

As the scope of the experimental research quickly moved beyond the capabilities of the ICSG, the use of a molecular dynamics program was employed to run more sophisticated simulations. A parameter file was developed for 2-amino-1-phenylethanol (APE) and then used in APE$(H_2O)_n$ and Na^+(APE)$(H_2O)_n$ simulations at various temperatures.

A delicate balance of noncovalent interactions (including electrostatic and hydrogen bonding) directs the structures of hydrated cluster ions. As shown throughout this dissertation, the identity of the metal ion as well as the temperature (internal energy) of the cluster are important aspects in determining which way the balance will shift.